THE ROLE OF MATERNAL OBESITY AND CONSUMPTION OF A WESTERN-STYLE DIET ON OFFSPRING BRAIN DEVELOPMENT AND BEHAVIOR VIA AN INFLAMMATORY MECHANISM

by

GEOFFREY A. DUNN

A DISSERTATION

Presented to the Department of Human Physiology
and the Division of Graduate Studies of the University of
Oregon in partial fulfillment of the requirements
for the degree of
Doctor of Philosophy

March 2023

DISSERTATION APPROVAL PAGE

Student: Geoffrey A. Dunn

Title: The Role of Maternal Obesity and Consumption of a Western-Style Diet on Offspring Brain Development and Behavior via an Inflammatory Mechanism

This dissertation has been accepted and approved in partial fulfillment of the requirements for the Doctor of Philosophy degree in the Department of Human Physiology by:

Elinor L. Sullivan	Chairperson/Advisor
Adrianne G. Huxtable	Core Member
Carrie E. McCurdy	Core Member
Judith S. Eisen	Institutional Representative

and

Krista Chronister	Vice Provost for Graduate Studies

Original approval signatures are on file with the University of Oregon Division of Graduate Studies.

Degree awarded March 2023

DISSERTATION ABSTRACT

Geoffrey A. Dunn

Doctor of Philosophy

Department of Human Physiology

March 2023

Title: The Role of Maternal Obesity and Consumption of a Western-Style Diet on Offspring Brain Development and Behavior via an Inflammatory Mechanism

Currently almost 1 in every 3 women of childbearing age in the US are classified as obese. Consumption of a diet high in fats and sugars, such as the average American diet, is one of the largest predictors of increased levels of adiposity in an individual. Further, obesity is characterized in part by a low-grade chronic inflammatory state in peripheral circulation. Maternal obesity is a known risk factor for lasting impacts on neurobehavioral development in offspring. We therefore hypothesized that maternal consumption of a Western-Style diet and obesity-induced inflammation disrupts neurodevelopment of the serotonin system in the amygdala, increasing anxiety behaviors in non-human primate offspring. Indeed, our analyses suggest that maternal adiposity levels were associated with decreased offspring serotonin innervation in the amygdala which were associated with increased anxiety behaviors. Further, the number TPH2+ cells in the raphe nuclei, the site of serotonergic neuron cell bodies, were reduced in maternal WSD offspring. These finding suggested that maternal WSD and adiposity were associated with increased anxiety behavior in offspring through disrupting the development of the central serotonergic system during perinatal development.

Further examinations of the mechanisms by which maternal WSD and obesity influence offspring neurobehavioral development suggest that obesity-induced inflammation is driving the observed perturbations in the serotonergic system. As the primary immune cell of the central nervous system, microglia play an integral role throughout perinatal neurodevelopment. Quantifying microglial number and morphology in the offspring amygdala suggested that maternal WSD and adiposity levels influenced microglia function throughout both pre and postnatal development. Specifically, maternal WSD appeared to elicit persistent effects on offspring microglia number while levels of adiposity appeared to have a more transient effect in prenatal development. These findings suggest that maternal WSD and obesity may elicit their effects on offspring neurobehavioral development through modulation of microglia during perinatal development.

This dissertation includes previously published and co-authored material.

ACKNOWLEDGMENTS

I would like to acknowledge and thank all the incredible people who have helped support me throughout the process to complete this dissertation. First, I would like to thank my mentor Dr. Elinor Sullivan, for her unwavering support and guidance. It has been an incredibly rewarding journey. Thank you for your trust and allowing me the opportunity to develop as a researcher and scientist under your care.

I would like to thank all my committee members, Dr. Adrianne Huxtable, Dr. Carrie McCurdy and Dr. Judith Eisen, for the guidance and mentorship you have provided over the years. Thank you for giving your time and energy to help me navigate through this dissertation.

None of this work would be possible without the incredible efforts by the staff and researchers at the Oregon National Primate Research Center. I am deeply grateful for all the care and maintenance they provide for the animals every day.

Thank you to all my friends and lab mates who have been welcome distractions during the good times and the tough. To family, my mom, dad, and sister who have been so supportive of my curiosity from before I even knew I wanted to become a researcher. And finally, I would like to acknowledge and thank my wonderful girlfriend Maddie, who has been by my side throughout this whole process, listening to all my “fun facts” and rants over the many years.

TABLE OF CONTENTS

LIST OF FIGURES

LIST OF TABLES

I. INTRODUCTION

1.1 Fetal programming

The phenomenon termed fetal/early life programming describes how environmental factors such as events, stressors, nutrient availability experienced by the developing offspring either during gestation or neonatal life can alter the offspring's normal course of development. This allows the developing fetus to "prepare" for the predicted future environment in a way that often persists into adulthood. It is suggested to be an evolutionary mechanism that allows offspring to be the best prepared for the future environment it will be surviving in by altering cellular processes. However, this mechanism, to attempt to prepare the offspring for the future environment, can become maladaptive, especially when postnatal situations differ from the prenatal environment. The hypothesis that environmental influences can impact early life and even fetal development in possibly maladaptive ways originated from observing and following children born to mothers who experienced the Dutch famine of 1944 (1). They found that mothers exposed to starvation while pregnant gave birth to children that were more likely to develop metabolic disorders such as obesity, diabetes and cardiovascular disease when consuming an adequate diet postnatally (2). In this instance, undernutrition during gestation "programmed" the offspring metabolism to expect a nutrient deficient environment, and therefore, conserve energy and calories whenever possible. Importantly, this phenotypic shift was stable, extended into adulthood, and was not "corrected" during postnatal life.

This initial observation led to the study of many other types of environmental influences (e.g., maternal overnutrition, psychological stress, or infection) and how they impact fetal development. This field of study is now referred to as the Developmental Origins of Health and Disease (DOHaD). While fetal programming may impact many different systems in the body, the scope of this dissertation will focus on programming of the central nervous system. This field is one of the most rapidly growing arms of this line of research. There is extensive and continued work on maternal stressors and offspring neural outcomes (3, 4). Further, many of the different environmental influencers a mother may experience (e.g. infection, stress, diet) share a common aspect; the influence of the immune system, both maternal and fetal, on the neurodevelopment of the offspring. This is highlighted in studies of maternal infection during development. A large epidemiologic example is the examination of the neurodevelopmental outcomes of offspring

born to mothers exposed to the Influenza virus during pregnancy. In this study children that were born to mothers exposed to the influenza epidemic during the 2nd and 3rd trimesters had increased risk for developing schizophrenia in adulthood (5).

The current state of the field of fetal programming is focused on teasing out mechanisms by which adverse maternal environments interact with the development of the organ systems of the offspring. Researchers are investigating many different mechanisms such as inflammatory signals (e.g. cytokines/chemokines), oxidative stress, hormones, and epigenetics. It is very likely that many of these mechanisms are acting simultaneously and in varying degrees depending on the specific environmental stressors that the pregnant person and fetus are experiencing. This dissertation will focus on the environmental stressors of diet and accumulation of adiposity during gestation.

1.2 Obesity

Obesity is a metabolic disorder that results, in part, from overnutrition and is characterized by an accumulation of excess body fat or adiposity and the development of metabolic syndrome. Currently the most widely used metric for body fat is Body Mass Index (BMI) where in the US a BMI of 18.5-24.9 is considered normal weight, 25-29.9 is considered overweight, and 30+ is considered obese (6). It is important to note that while BMI is a useful tool that is easily measured it is also flawed and its use may over or under assess a person's actual metabolic health. Obesity has become an epidemic with almost 40% of all adults in the US classified as obese (6). Further, there doesn't appear to be any indication that rates will slow down anytime soon with projected data suggesting that in 2030, 51% of the American population will be classified as obese (7). While excess body fat itself is not deadly, obesity is highly correlated with much more serious health disparities such as type II diabetes, coronary heart disease, and many cancers (8-11). In addition to decreases in longevity and quality of life for obese individuals, these health outcomes create a massive economic burden on these patients, their families, and their community. Estimates indicate that obesity and its related comorbidities cost approximately $215 billion annually (12) with this burden predicted to increase by $48-66 billion/year by 2030 (13). In addition to the serious health and economic threats to already obese individuals, there is concern about how an obese society will impact future generations as a majority of women of child-bearing age are overweight or obese (14). Many epidemiologic studies link increased maternal BMI with an increased risk for adverse health outcomes in their

children such as obesity, coronary heart disease, type II diabetes, stroke, asthma (15, 16). More specifically, maternal obesity has been linked with increased risk of neuropsychiatric disorders, such as Attention Deficit Hyperactivity Disorder, Autism Spectrum Disorder, and impaired cognitive function, in the offspring (17-20). Development of neuropsychiatric disorders also results in considerable deficits in quality of life and economic burdens. Some estimates suggest that 13-20% of children living in the US (1 out of 5 children) experience a neurodevelopmental disorder in a given year, resulting in $247 billion in medical costs to treat these children (CDC). Both obesity and childhood behavioral disorders are considerable public health concerns that require comprehensive study to improve understanding and hopefully develop strategies and interventions that can reduce the prevalence of these disorders. This project will focus specifically on behavioral disorders experienced in children.

1.3 Western-Style Diet

One of the main factors believed to contribute to the development of obesity is the consumption of a Western-style diet (WSD). The WSD is considered to be the average diet of people living in the United States and, more recently, Western Europe. This diet is calorically dense, with large amounts of calories from fat, and high levels of simple sugars, from beverages, as a source of carbohydrates. Additionally, it is noteworthy that a WSD tends to contain higher quantities of saturated and trans fatty acids as much of the fat content is derived from animal fats versus plant-based lipids (21). Results from both clinical and preclinical studies suggest consumption of this dietary pattern can result in serious metabolic impairments, such as obesity, and glucose and insulin homeostasis (22, 23). Consumption of a WSD alone, without metabolic complications, may impact placental function and influence fetal nutrient availability and neurodevelopment (24). Similar to the association between maternal obesity and neuropsychiatric disorders, specific nutrient compositions in the WSD diet has been associated with adverse psychiatric outcomes in offspring (25). It is important to note that, while many studies have utilized preclinical maternal WSD models, most of the long-term effects on offspring neurodevelopment observed in these studies coincide with a maternally obese phenotype. Additionally, there is large variability in the specific quantities of macronutrients used in various animal models of maternal WSD, with some diets including 36% kilocalories from fat and others including up to 60% kilocalories from fats. This results in limited evidence of effects specific to diet or obesity independently. Recently, more advanced statistical

methodology and larger study design has begun to parse out unique effects of the these heavily cooccurring environmental influences. When studying dietary effects on neurodevelopment in humans it is inherently difficult to control for the vast amounts of confounding factors that may impact the developing child. Therefore, use of animal models is vital for targeted focus of specific environmental perturbations during pregnancy. In non-human primates, our group demonstrated that perinatal WSD and maternal obesity differentially impacted offspring anxiety behavior at 1 years old, with WSD being specifically associated with increased anxiety behavior and maternal obesity associated with increases in disruptive, high-energy behavioral outbursts (26). Other evidence of maternal diet induced effects on offspring behavior come from acute diet exposure models mostly in rodents. Evidence from these models suggest offspring born to dams consuming a WSD during pregnancy and through lactation display impairments of risk assessment and avoidance as well as increases in behavioral inhibition (27-30). Mechanistically, offspring born to dams consuming the WSD displayed dendritic atrophy and spine instability in the amygdala, hippocampus, and pre-frontal cortex (31-33). Interestingly, these alterations in dendritic and spine stability have been associated with neuropsychiatric disorders such as ASD, Schizophrenia, and Alzheimer's disease (34). However, the precise mechanisms underpinning the effects of consuming a WSD and experiencing obesity during pregnancy have not been fully fleshed out and remain largely unknown. It is the focus of ongoing research, including this dissertation, to provide comprehensive evidence of the specific factors underlying dietary and metabolic influences on the developing offspring.

1.4 Mechanisms Underlying WSD and Obesity's Influence on Offspring Development

1.4.1 Inflammation

Inflammation has historically been a general term that is used to describe an organism's response to infection, injury, or stress. However, as research into the field of inflammation has expanded, it has become clear that inflammatory signaling is a highly regulated, critical and dynamic form of communication that goes beyond just a response to damage or infection. In the most general form, inflammation is a result of the actions of immune cells, such as monocytes/macrophages, and the signaling molecules they release (e.g. cytokines/chemokines). Importantly, it is necessary for the immune system to communicate with the CNS in order for a proper coordinated response. This cross talk can occur in a variety of mechanisms including the passage of cytokines/chemokines across the blood brain barrier (35), signaling through the

endothelium and pericytes that make up the blood brain barrier (36, 37), signaling via the vagus nerve (38), or even peripheral leukocyte infiltration (39). Additionally, the magnitude and timescale of inflammatory response varies substantially in response to different stimuli. For example, inflammation because of microbial infection is characterized by large increases in circulating immune cells and the inflammatory factors they release over a relatively acute timescale of a few days to weeks (40). This response is notably different from the inflammatory state that develops due to obesity and metabolic syndrome, which is characterized by low-grade and chronic levels of circulating inflammatory factors that may be present for years (41).

1.4.2 Inflammation and development

Over the last two decades it has become clear that inflammatory signals and the cells that produce and respond to them are critical for proper development, especially neurodevelopment. Some well supported roles that inflammatory signals play in neurodevelopment are: a) neuronal migration (42), b) fate switching and differentiation of neurons, astrocytes and oligodendrocytes (43, 44), c) neurogenesis (45), as well as d) modulation of Wnt and sonic hedgehog signaling (46, 47). In addition to the signaling molecules themselves, another way inflammation influences neurodevelopment is through interaction and modulation of the resident immune cell of the CNS, microglia. Microglia are embryonic yolk-sac progenitors that invade the CNS very early during development, as early as embryonic day 8 in mice (48) and gestational week 5 in humans (49), where they are critically involved in guiding proper brain development. These cells perform a wide range of functions from regulating neural precursor cell number (50) and neuronal migration (51), to neural progenitor cell differentiation (52), and synaptic pruning (53, 54). Additionally, studies that inhibit microglia function, through either genetic knock-out of the neuronally expressed chemokine fractalkine *Cx3cr1* or pharmacological drugs (e.g., minocycline), during gestation demonstrate considerable neurodevelopmental abnormalities. Examples of these abnormalities include alterations in social and repetitive behavior (55), dysregulated neuron cell populations (50), and evidence for a lack of synaptic pruning (54). The diverse and critical roles that inflammatory signals and microglia play during development, suggest that perturbation of this system during gestation would have large effects on neurodevelopmental outcomes in offspring. Indeed, this is evident from studies of maternal immune activation, where typical inflammatory signaling has been altered and this results in profound impacts on brain development manifesting as increased rates of neurodevelopmental

disorders such as autism and schizophrenia (56). This is further supported at a neural level with work done by Stolp et al. 2011, which demonstrates that maternal immune activation via models of viral or bacterial infection in mice caused a short-term reduction in the number of mitotic cells in the ventricular proliferative zone of the dorsal cortex, and this transient insult led to long-term alterations in cortical neuron populations (45). It is most likely that many stressors during pregnancy contribute and culminate to produce the overall "inflammatory environment" that a developing fetus will experience throughout gestation. This project will focus on the inflammatory contributions from maternal obesity and consuming a WSD.

1.4.3 Inflammation from Obesity

Inflammation and obesity are intimately connected. Research indicates that circulating inflammatory factors are increased in obese individuals. The most well supported work suggests that this increased circulating inflammation is a result of increased macrophage accumulation in adipose tissue (57). With increased adiposity, the prevailing hypothesis suggests that adipocytes are enlarged through hypertrophy to an extent that results in massively increased rates of adipocyte cell death (58). The increase in adipocyte cell death in obese individuals leads to increased numbers of macrophages recruited to the tissue (58) where they develop a metabolically active phenotype and release pro-inflammatory cytokines (59). Interestingly, the location of the adipose tissue deposition appears to play a large role in how obesity propagates inflammation. In work done by Verboven et al. 2018, adipose tissue from visceral sources in obese individuals had increased mean adipocyte size, CD45+ leukocytes and M1 macrophage compared to their lean counterparts (60). In contrast, adipose tissue collected from subcutaneous sources in obese individuals showed no difference in immune cell populations, despite similar cellular hypertrophy (60). However, there is intriguing evidence that inflammation due to obesity may also require disturbance of the interaction between gut microbiota and the intestine (61). This increase in inflammation, however, is chronic and low-grade which differs from a situation in which the immune system is actively fighting an infection where circulating factors are acutely increased at much higher levels (62).

1.4.4 Inflammation from WSD

In addition to inflammatory outcomes due to obesity, specific nutrients consumed in the WSD may either directly or indirectly initiate inflammatory cascades in various tissues throughout the body (63). Some of these nutrients, include saturated fatty acids, essential fatty acids, and certain simple sugars such as fructose (64). As mentioned earlier, the WSD contains higher levels of saturated fatty acids than nutritional recommendations. In human studies, increased consumption of saturated fatty acids is associated with increased tissue and serum cytokine levels (65-67). Specifically, there is growing evidence that saturated fatty acids trigger inflammatory responses via Toll-like receptor 4 (TLR4) activation (68, 69).

In addition to saturated fatty acids, polyunsaturated fatty acids (PUFAs) are also highly involved in inflammatory signaling (70) as well as neuronal signaling (71). It is well established that n-3 PUFAs consumption elicit anti-inflammatory effects (72, 73). These fatty acids are key structural components of the lipid membranes of neurons and are necessary for proper function (74). For example, one subtype of PUFAs know as omega-3 (n-3) PUFAs have been shown to influence the functionality of receptors in dopaminergic neurons (75). Additionally, glial cell functionality, such as microglial phagocytosis (76, 77), and astrocyte differentiation (78), are influenced by levels of n-3 PUFAs. Notably, microglia are the main cell type responsible for detecting and responding to inflammatory signal and evidence suggests these cells express several receptors sensitive to lipids (79). In line with known anti-inflammatory actions, n-3 PUFAs have been shown to inhibit microglia activation and expression of proinflammatory cytokines, such as TNF-a and IL-6 (80). Further, maternal consumption of n-3 PUFAs is sufficient to modulate the lipid content in microglia in offspring (81).

Consumption of the WSD has also been associated with development of hypercholesterolemia and atherosclerosis, due to increases in circulating levels of low-density lipoproteins (LDL) (82). This promotes cholesterol accumulation and localized inflammatory responses in the artery wall (83). Further, LDLs have been shown to function as ligands for TLR, directly triggering inflammatory signaling pathways (84). Additionally, macrophages can engulf LDLs leading to amplified TLR signaling due to cellular cholesterol accumulation (84, 85).

In addition to the direct inflammatory effect of specific nutrients found in the WSD, these nutrients may also indirectly influence the inflammatory state of an individual through the

interaction with the gut microbiota. While research in this field is rapidly growing and critical for understanding the comprehensive relationship between diet and offspring development, it would go beyond the scope of this project to dive relatively deep here. Briefly, recent evidence suggests that consumption of a WSD disrupts colonization of diverse gut bacteria that are required for a healthy and balanced microbiome (86). Interestingly, disruption of this healthy balance was associated with low-grade inflammation and insulin resistance (86), which are well-known common comorbidities of consuming a WSD and obesity.

Regardless of the source of inflammation during development, the connection of this mechanism to the disruptions in neural development that result in offspring behavioral deficits remains relatively unknown. This dissertation will focus on one neurotransmitter system, serotonin, that might explain some of the observed behavior alterations.

1.5 Central 5-HT system development

The development of the mammalian central nervous system is a highly complex and strictly regulated process. The field is still rapidly growing in an attempt to comprehensively understand the processes and mechanisms by which the central nervous system is finely tuned during gestation and postnatal development. For this project we will focus on the development of the central serotonin (5-HT) system. Serotonin-containing neurons are among the earliest generated neurons, appearing at E9.5-E12 in rats and 5-7 gestational weeks in humans, which alone would suggest this neurotransmitter system is key for development (87). Indeed, this system is critical for proper development of the CNS, as 5-HT acts as a neurotrophic signal with functions such as neuronal migration, neural precursor proliferation and survival, as well as circuit formation (88). Interestingly, even though 5-HT neurons are present in the brain stem at E10 in rodents, they have not yet projected to their eventual final destinations of innervation in the cerebral cortex and subcortical structures until E17 at the earliest. Therefore, before E17, these telencephalic regions receive 5-HT signals from sources that are exogenous to the fetal CNS. Seminal work by Bonnin and colleagues demonstrated that the main source of this exogenous 5-HT is synthesized by the placenta from a maternal tryptophan precursor (89, 90). This implies that if placental 5-HT sources are altered during pregnancy this could drastically influence early cues needed for proper neurodevelopment in the offspring before fetal endogenous sources of 5-HT have been established. In fact, a rapidly growing body of literature

would suggest that inflammatory signals influence 5-HT synthesis and metabolism in maternal circulation as well as in the placenta (91, 92).

1.6 Negative Affect and Related Brain Regions

It would go beyond the scope of this dissertation to discuss all behaviors and the brain regions associated with them. Here, we will focus on behaviors related to negative affect including anxiety-like behaviors. Negative affect is classified under the behavior classes of mood, emotion, and affect. It refers to the subjective experience of a group of negative emotional states such as anxiety, depression, stress, sadness, worry, guilt, and anger (93). Previous work performed in our lab suggests that non-human primates born to obese mothers consuming a WSD display increased rates of anxiety behaviors, as well as aggression (94, 95). The current dissertation will focus on anxiety behaviors in offspring. The observation of these behavioral abnormalities suggests that specific brain regions are impacted by maternal obesity and WSD, namely the prefrontal cortex (PFC) and the amygdala. These two regions are intimately linked and allow for the perception, integration, and response to various external sensory inputs. Briefly, the amygdala is a part of the limbic system of the brain, which is associated with feelings of emotion, and mainly receives sensory inputs from the PFC and subsequently integrates and transmits the information to other brain regions that are able to elicit response behaviors, like the brainstem or striatum (96). Additionally, work done by David Amaral and colleagues demonstrated that when bilateral lesions to the amygdala were performed in non-human primates, there was a striking decrease or complete lack of behaviors such as fear responses and aggression (97). Within the amygdala itself there is a complex interplay between principle glutamatergic neurons, GABAergic inhibitory neurons, and innervating serotonergic (5-HT) axonal projections (98). Together, the amygdala appears to be a critical site in the production of proper emotional responses to various external stimuli.

In addition to the anatomical structure of the amygdala, there are very important neurotransmitter systems that regulate the activity of this region. One of the most important is the central 5-HT system. This system is almost ubiquitous throughout the central nervous system. Serotonergic cell bodies originate in the raphe nuclei in the brainstem and their axons project to almost every cortical and some sub-cortical structures in the brain and spinal cord. Importantly, the amygdala receives a dense innervation of 5-HT projections that regulate excitability of the different neuron populations located within the amygdala (99-101). Under normal conditions the

amygdala is under high inhibitory control (102) and the 5-HT system contributes to maintaining that inhibitory tone (103). In situations when the 5-HT system is perturbed, such as a reduction in brain 5-HT through dietary depletion of tryptophan, behaviors such as anxiety and depressive-like behaviors are increased (104).

1.7 Overarching Hypotheses

The overall hypothesis of this dissertation is that maternal WSD and obesity-induced inflammation disrupts neurodevelopment of the serotonin system in the amygdala, increasing anxiety behaviors in offspring. This dissertation will provide evidence for maternal metabolic and inflammatory state shaping inflammatory outcomes in offspring at fetal, juvenile (105), and adolescent times points. Additionally, this dissertation will present evidence that maternal and postweaning diet impact central serotonergic neurons in the raphe nuclei of offspring (106). Finally, this dissertation will suggest that maternal diet and metabolic state reduces the amount of serotonergic axonal innervation of amygdala which impacts behavioral outcomes in adolescent offspring.

II. MATERNAL METABOLIC AND INFLAMMATORY STATE SHAPE OFFSPRING CENTRAL AND PERIPHERAL INFLAMMATORY OUTCOMES IN JUVENILE NON-HUMAN PRIMATES

From: Dunn GA, Mitchell AJ, Selby M, Fair DA, Gustafsson HC, Sullivan EL (2022): Maternal diet and obesity shape offspring central and peripheral inflammatory outcomes in juvenile non-human primates. *Brain Behav Immun*. 102:224-236.

2.1 Introduction

Obesity is a rapidly growing epidemic that currently impacts 40% of adults living in the US. This public health crisis is largely driven by the consumption of a highly palatable and calorically dense diet, termed the Western-style diet (WSD). This diet is composed of higher percentages of saturated fats and simple sugars compared to other diets such as the Mediterranean diet. Chronic consumption of a WSD, and the corresponding obesity, results in public health consequences ranging from increased risk of developing insulin resistance and diabetes to hypertension and cardiometabolic disease (107). The impact of this epidemic on future generations is concerning as increasing numbers of women are classified as obese before becoming pregnant. In 2019, 30% of women were classified as obese prior to pregnancy, an 11% increase from 2016 (14). Many adverse birth outcomes have been associated with maternal obesity ranging from increased risk of preterm birth, preeclampsia, and increased gestational weight gain during pregnancy (108). A well-established body of research shows maternal consumption of a WSD and an obese metabolic state during pregnancy have long-lasting adverse impacts on offspring health. Preclinical models utilizing non-human primates (NHP) suggest these consequences include fetal exposure to increased circulating inflammatory factors (109), impaired placental function and inflammation (110), increased pancreatic inflammation (111), and even an increase in the number of microglia in the hypothalamus (112).

Maternal consumption of an obesogenic diet in both pre-clinical (25, 26, 94) and clinical populations (20, 113, 114) is associated with behavioral alterations in offspring. Clinical studies have associated maternal WSD overconsumption with increased risk of offspring neuropsychiatric disorders such as Attention-deficit/hyperactivity disorder (115) or autism spectrum disorder (ASD) (116). Results from preclinical studies using animal models support the trends observed in clinical studies. Work in both rodents and NHPs suggests maternal

consumption of a WSD increases offspring anxiety and depressive-like behaviors later in life (17, 26, 95). A common overlap shared amongst the clinical disorders is disrupted emotional control.

We postulate that these behavioral changes induced by maternal WSD consumption are due to alterations in fetal brain development. Previous work using our model has demonstrated offspring brain development is impacted by maternal diet. These findings include increased microglial staining in the fetal hypothalamus (112) as well as perturbations to the serotonin and dopamine systems throughout the brain (94, 95, 117). Here we expanded this hypothesis, by examining microglial alterations in the amygdala. The amygdala is a brain region of interest because of the integral role it plays in emotional control a behavioral domain that has been shown to be impacted by maternal diet in preclinical and epidemiologic studies. Also, its development has been reported to be altered by exposure to maternal obesity and WSD in both rodents (118) and NHP models (119). The primate amygdala complex has extensive connections with the neocortex as well as the hypothalamus, brain stem, basal forebrain, hippocampus, and striatum (120). The amygdala complex contains distinct subnuclei that are associated with various facets of emotional control (121). In this study, we examined how consumption of a WSD impacts both specific subnuclei as well as the amygdala as a whole.

Microglia are the main immunocompetent cells of the brain. In response to various stimuli, microglia alter their functional state by proliferation, migration to the site of interests, alteration of their morphology, and activation of cell signaling cascades related to inflammation. During development, aside from their main function fighting infection and responding to damage, microglia play a crucial role in guiding proper neurodevelopment by performing functions such as synaptic pruning (54), phagocytosis of neural progenitor cells (50), and refining network connectivity(122). Due to their integral role in development, many hypotheses implicate microglia in neurodevelopmental disorders (123, 124).

Maternal diet, adiposity, and peripheral inflammation have all been proposed as potential mechanisms underlying changes in offspring brains and behavior (125). However, differentiation of the unique programming effects of these early environmental factors on offspring inflammatory outcomes has remained largely unaddressed. While it is believed the main source of inflammatory burden in obese individuals is due to increased production of inflammatory

factors due to increased adipose tissue mass, dietary studies indicate specific nutrients such as saturated fatty acids, simple carbohydrates, and polyunsaturated fatty acids are capable of pro-/anti-inflammatory signaling capabilities. In the present study, we aim to differentiate the unique effects of maternal adiposity, inflammation, or diet on offspring outcomes.

In this study, we utilized a NHP model of diet-induced maternal obesity, where animals consumed a diet modeled after the WSD including higher percentages of fat, especially saturated fats, and sugars. We examined animals at 13-months in an effort to increase translatability to clinical populations in humans. This timepoint in NHPs correspond to approximately 3-4 years in humans (126, 127), which are some of the earliest timepoints neurodevelopmental disorders (e.g. ASD, ADHD) can be diagnosed (128, 129). The goal of this study was to characterize the complex relations among maternal diet, metabolic, and inflammatory states during pregnancy and to examine how these factors impact offspring inflammatory outcomes. We hypothesized that baseline central and peripheral inflammation in offspring is programmed via metabolically induced inflammation in the mother during gestation. This NHP model is uniquely situated to tease out the independent effects of the various maternal factors on offspring inflammatory outcomes. To our knowledge, this is the first NHP study to examine the direct and indirect effects of chronic WSD consumption, maternal metabolic state, and gestational inflammatory environment on offspring central and peripheral inflammation.

2.2 Methods

2.2.1 Animal Group Formation/Demographics

2.2.1.1 Non-human Primate Model

All animal procedures were in accordance with National Institutes of Health guidelines on the ethical use of animals and were approved by the Oregon National Primate Research Center (ONPRC) Institutional Animal Care and Use Committee.

The present study utilized an established preclinical NHP model (M*acaca fuscata*) of maternal overnutrition to investigate the impact of maternal consumption of a WSD diet on offspring central and peripheral inflammatory outcomes compared to controls. The macaque develops the full spectrum of metabolic disease associated with human consumption of WSD (130) and has similar gestational and neurodevelopmental trajectories (131). The high-fat diet

utilized in this model is designed to calorically reflect the typical WSD both prior to and during pregnancy, increasing the translatability and relevance to human maternal overnutrition (130).

Maternal metabolic variables were measured prior to conception and during the third trimester to determine the role that maternal metabolic state plays in influencing offspring inflammatory outcomes. Given the association between maternal overnutrition and inflammatory burden and the role of maternal inflammatory factors in fetal programming, maternal systemic cytokine levels were also examined during pregnancy.

Adult female Japanese macaques (*Macaca fuscata*) were housed in indoor/outdoor pens in groups of 4-12 individuals (male/female ratio 1-2/3-10). All animals were given *ad libitum* access to water and one of two experimental diets: control diet (CTR; 14.7% kcal fat; Monkey Diet no. 5000, Purina Mills) or WSD (36.6% kcal fat; TAD Primate Diet no. 5LOP, Test Diet, Purina Mills). Breakdown of macronutrients in each diet has been previously reported in *Thompson et al. 2017* (94). Females received the majority of their caloric intake exclusively from their experimental diets; the diets were supplemented by daily enrichment of fruits or vegetables. Additionally, once a day WSD females were provided a calorically dense treat (35.7% kcal fat, 56.2 % kcal carbohydrate, 8.1% kcal protein).

Females were allowed to breed with intact males. Each measure included is unique to a singleton pregnancy. Adult females consumed their respective diet for at least 1 year prior to pregnancy with any offspring included in this study. Offspring were born naturally and maintained with their mothers until approximately 8 months of age (**Figure 2.1**).

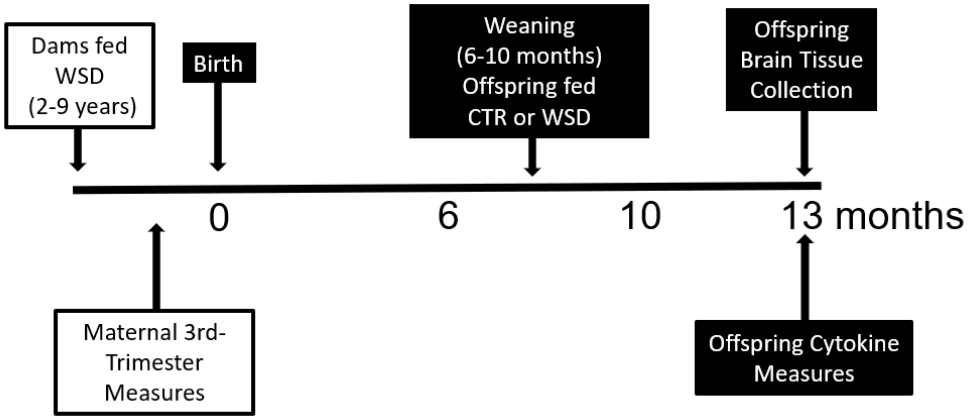

Figure 2.1. Schematic of experimental paradigm

2.2.1.2 Measurement of Maternal Adiposity

Prior to pregnancy, 122 female animals underwent dual-energy X-ray absorptiometry scans to determine body composition. A Hologic QDR Discovery scanner (Hologic, Bedford, MA, USA) in "Adult Whole Body" scan mode and Hologic QDR Software version 12.6.1 was used to calculate percent body fat. The mean ± standard error of pre-pregnancy adiposity for each diet group is as follows: CTR = 19.96 ± 1.15% body fat; WSD = 27.51 ± 1.42% body fat (**Table 2.1**).

Table 2.1. Animal Numbers for Maternal Procedures

Maternal Measures	N (per diet group)	Average Measures, mean ± SE		Maternal Age (years), mean ± SE	
		CTR	WSD	CTR	WSD
Prepregnancy adiposity	122 (CTR = 61, WSD = 61)	19.96% ± 1.15	27.51% ± 1.42	10.20 ± .35	9.01 ± .30
Third-trimester Inflammatory markers	117 (CTR = 52, WSD = 65)	See Table S2.1		9.94 ± .39	8.97 ± .27

Note: CTR control Diet; WSD Western-style Diet.

2.2.1.3 Plasma cytokine measure collection

Plasma samples were collected from 117 adult females in the third trimester and 93 juvenile offspring at 13-months (**Tables 2.1 & 2.2**). Prior to pregnancy, plasma supernatant was aliquoted and stored at −80°C until the time of assay. Plasma concentrations of inflammatory marker levels were determined using a monkey 29-plex cytokine panel (ThermoFisher Scientific, Waltham, MA, USA) following the manufacturer's instructions. Three plates were used to complete this analysis, originating from the same lot (#1833398A). Concentrations of each cytokine were calculated from a standard control curve. Samples were analyzed on a Milliplex Analyzer (EMD Millipore, Billerica, MA, USA) bead sorter with XPonent Software version 3.1 (Luminex, Austin, TX, USA). Data were calculated using Milliplex Analyst software version 5.1 (EMD Millipore). The inter-assay CV and lower limit of quantification (LLOQ) for each assay are listed in Table S1. Growth factors were not considered for this analysis.

Table 2.2. Animal Numbers for Juvenile Procedures

Juvenile Measures	N (per diet group)	N (per sex)
Immunohistochemistry	24 (CTR/CTR = 8, WSD/WSD = 8, WSD/CTR = 8)	F = 12, M = 12
13-month Inflammatory markers	93 (CTR/CTR = 28, WSD/CTR = 36, CTR/WSD = 11, WSD/WSD = 18)	F = 42, M = 51

Note: CTR control Diet; WSD Western-style Diet.

2.2.2 Immunohistochemistry Methodology

A fluorescent immunohistochemistry (IHC) experiment was performed to quantify microglial cell density in the right amygdala of 13-month juvenile animals. Tissue was obtained from the Obese Resource tissue bank. At 13.25 ± 0.71 months juveniles were euthanized and brain tissue was collected. Euthanasia was performed by ONPRC Necropsy staff and adhered to American Veterinary Medical Association Guidelines on Euthanasia in Animals and ONPRC standard operating procedures and guidelines. Briefly, animals were sedated with ketamine HCl (15-25 mg/kg i.m.) transported to the necropsy suite and deeply anesthetized with a surgical dose

of sodium pentobarbital (25–35 mg/kg i.v.). After sufficient anesthetic depth was reached, animals were exsanguinated from the aorta while cerebral perfusion was performed via the carotid artery. Perfusion consisted of an initial flush of 0.5-1 liter of 0.9% heparinized saline followed by 1–2 liters of 4% paraformaldehyde buffered with sodium phosphate (NaPO4, pH 7.4) to fix tissue. After perfusion, the brain was removed, sectioned into regional blocks, and placed in 4% paraformaldehyde for 24 hours at 4°C to complete fixation. Brain tissue blocks were then transferred to 10% glycerol buffered with NaPO4 for 24 hours and finally transferred to 20% glycerol solution for 72 hours. Tissue blocks were frozen in −50°C 2-methylbutane and then stored at −80°C until sectioning. Coronal sections (35 μm) of the temporal lobe were collected in 1:24 series using a freezing microtome and stored in cryoprotectant at -20°C until immunohistochemistry was performed.

Twenty-four animals balanced for maternal measures such as age and offspring sex (12 females) were included in this study. Diet manipulation involved long-term maternal consumption of a control or WSD which was maintained for offspring post-weaning until tissue collection (WSD/WSD and CTR/CTR). One group of offspring received a diet intervention at weaning when they were transitioned from WSD to the control diet (WSD/CTR). Standard IHC methodology was used. Briefly, 35 μm thick tissue sections containing the amygdala were bath washed in a KPBS solution. Sections were then blocked for 1 hour in 2% Normal Donkey Serum (NDS; Jackson ImmunoResearch Cat #017-000-121), 0.4% Triton-X100 (Fischer Bioreagents Cat# BP151-500) KPBS solution. Following blocking, sections were transferred to a primary antibody solution (2% NDS in KPBS) containing 1:1500 rabbit anti-IBA-1 (Wako FujiFilm Cat# 019-19471 Lot# PTE0555) and 1:100 mouse anti-Acetylcholinesterase (Abcam Cat# ab2803 Lot# GR3242309-4). Sections were incubated at room temperature for 2 hours before being transferred to 4°C where they remained for 22 hours.

After primary incubation, sections were removed from 4°C and washed in KPBS. Tissue was then transferred to secondary antibody solution (2% NDS in KPBS) containing 1:1000 donkey anti-rabbit Alexa 488 (ThermoFisher Cat# A21206) and 1:1000 donkey anti-mouse Alexa 555 (ThermoFisher Cat# A31570). Sections were incubated for 2 hours at room temperature. After secondary incubation, sections were again washed in KPBS. Next, tissue sections were mounted onto gelatin-subbed slides, coverslipped using Prolong Gold Antifade (ThermoFisher Cat# P36930) and stored at 4°C until imaging.

2.2.3 Automated Cell Counting

2.2.3.1 Acquisition

Z-stacks of the right amygdala were acquired using a Leica SPE point scanning confocal with an HC Fluotar L 25x magnification 0.95 NA W VISIR objective. Each stack was 293.91 μm by 293.91 μm, with 45 frames separated by 0.57 μm to acquire information through the entire volume of each region of interest. Seven sections, representing the whole rostral to caudal aspect of the right amygdala, from each animal were analyzed. To examine specific subregions of the amygdala, boundaries of each region were determined using an AChE stain with a 5x objective (**Figure 1**), referencing an adolescent non-human primate atlas (132). To have a representative count for each subregion, three images were acquired and averaged for each subregion per section. Once images were collected, 20 Z-stacks were selected at random and assessed for the presence of signal. As frames 3 through 43 contained signal for all Z-stacks this range was selected for analysis to ensure all images represented the same volume of tissue. A custom FIJI macro was recorded and used to generate max projections.

2.2.3.2 Analysis

A selection of representative images, balanced for diet, sex, and subregion, were used to make a microglia identification guide. In brief, microglia were defined by an observable circular cell body, brighter on the boundaries and dimmer in the center. To be counted as a microglia, a cell needed to have at least a single process present with positive staining for IBA-1. Cell bodies were also roughly similar in size (around 40 μm^2), so any potential microglia that appeared noticeably larger or smaller than other cells in the image were rejected. Masses of processes without an associated cell body or otherwise-identifiable microglia touching the edge of the image were rejected. Following training, two experimenters counted microglia in 35 images selected at random to use as a “gold standard” to compare to automated counts.

A FIJI macro was written to allow fast identical application of the methodology to every image (133). In brief, to reduce background noise a Gaussian blur (sigma=60) was applied to the image, and an Otsu local threshold (radius=15) was used to separate any IBA1+ signal from the background. The FIJI function "Analyze Particles" was used to count microglia cell bodies. Cell bodies were distinguished from processes or small patches of autofluorescence using a size filter of 40 μm^2. The circularity filter was set to 0.05-1.00; this range excluded individual thin processes without excluding microglia of a diversity of morphologies. Fiji then generated an output image, which contains a table of object counts (cells and any false positives that passed the filters) as well as an image showing outlines of the objects counted. This automated method was accepted when it captured at least 85% of the manually counted cells per image in the 35-image test set. Each outlined object was then assessed by the experimenter for false positives, and any images that failed the automated method due to poor staining were recorded and excluded from analysis.

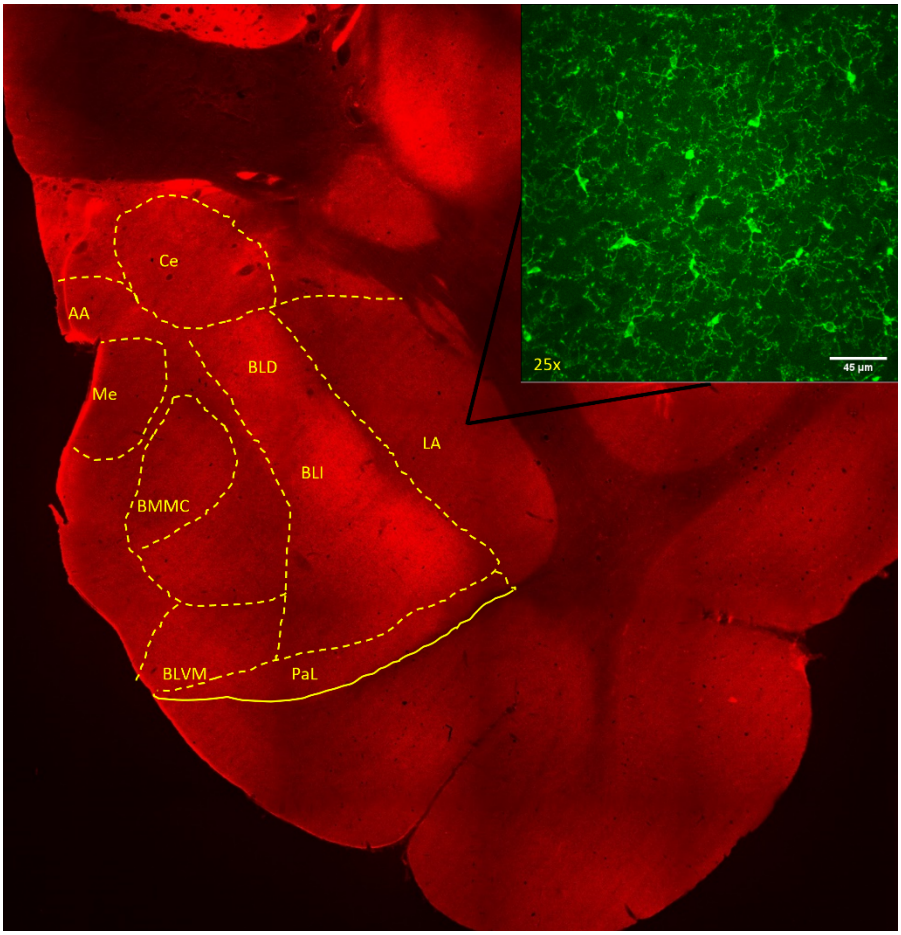

Figure 2.2. Representative image of AChE stain in the right amygdala at 4x magnification. Dashed lines indicate approximate locations of subregions based on reference of the non-human primate atlas (Paxinos et al., 2009). The inlet provides a representative image of IBA-1 positive cells at 25x magnification that were used in analysis of microglia counts. AA=anterior, BLD=basolateral dorsal, BLI=basolateral intermediate, BLVM=basolateral ventromedial, BMMC=basomedial magnocellular, Ce=central, LA=lateral, Me=medial, PAL=paralaminar.

Our analysis focused on subregions that had representation from 90% of animals and section. These regions included the basolateral dorsal (BLD), basolateral intermediate (BLI), basolateral ventromedial (BLVM), basomedial magnocellular (BMMC), lateral (LA), and paralaminar (PAL) amygdala nucleus. Two animals needed to be removed from analysis due to poor staining as a result of imperfect fixing of the brain tissue at necropsy.

2.2.4 Data analysis/Statistics

Data were analyzed using a structural equation modeling (SEM) framework (134) using Mplus 7.4 (135). The robust maximum likelihood estimator was used for models considering continuous outcome variables and the weighted least squares means estimator was used for models that considered categorical outcome variables. These estimators accommodate non-normally distributed data by adjusting standard errors using the Huber-White sandwich estimator. Model fit was assessed using standard fit indices, the Comparative Fit Index (CFI), the Tucker-Lewis Index (TLI), and the root mean square error of the approximation (RMSEA). CFI and TLI values above .90 and RMSEA values below .08 indicate adequate model fit (136, 137). Non-independence of observations (i.e., the nesting of offspring with the same mothers) was handled using the Mplus Cluster command. Missing data was handled using full information maximum likelihood (138).

2.2.4.1 Data Cleaning Process

Inflammatory marker data were processed prior to analysis. This method was applied to more accurately capture variability in inflammatory marker concentrations that may be lost when large numbers of concentration values fall below the lower limit of quantification (LLOQ). Briefly, inflammatory marker concentrations below the LLOQ were replaced with values equal to LLOQ/2 (139). The number of subjects that had values below the LLOQ for each inflammatory marker were noted. Next, a log2 transformation was performed on the inflammatory marker values. Base 2 transformations are more physiologically relevant and usually provide more normal distributions. Outliers 5 standard deviations above the mean were removed. In both maternal and juvenile inflammatory marker measures, no values were removed as outliers. After outliers were screened, mean and SD were recalculated. Next, values 3 SD above the mean were Winsorized (140). Inflammatory markers that produced more than 55% of the values below the LLOQ were discarded and not considered in analysis. The inflammatory

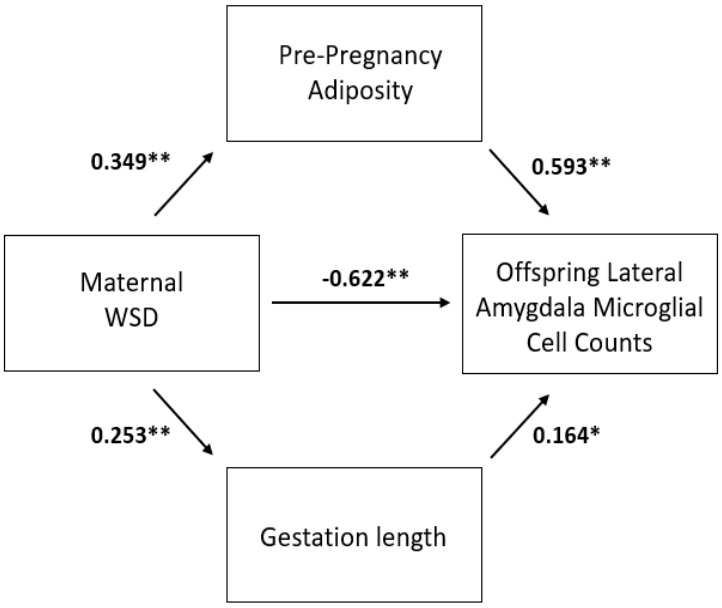

Figure 2.3. Path analysis model including maternal metabolic state measures and 13-month offspring Lateral amygdala microglial cell counts. Indirect mediated pathways through pre-pregnant adiposity significantly predict juvenile offspring microglial cell counts in the Lateral subregion of the right amygdala. Black lines indicate significant direct effects (* = $p<0.05$, ** = $p<0.01$) and are labeled with a beta value.

markers that were removed at this step were FGF-Basic, GMCSF, IL-4, IL-5, IL-10, and MIG. Inflammatory markers where 11.5%-55% of concentration values were below the LLOQ were transformed into categorical variables with bins of equal amounts, where the first category is comprised of the values below the LLOQ and the remaining values are placed into equal sized bins (e.g., for juvenile IL-17, 0 = all values below the LLOQ (20), 1 = 19 values, 2 = 18 values, 3 = 18 values, 4 = 18 values). Summary of the inflammatory markers that were excluded or transformed into categorical variables are summarized in Table S2.1 (Appendix A).

2.2.4.2 Data Reduction

Confirmatory factor analysis (CFA) was used to reduce the high dimensionality of the cytokine data. Based on widely accepted categorizations of inflammatory signaling molecules, we created four latent variables that captured unique aspects of inflammatory signaling: maternal pro-inflammatory cytokines, maternal chemokines, offspring cytokines, and offspring chemokines. Maternal and offspring chemokine latent variables were indicated by MCP-1, Eotaxin, RANTES, ITAC, MDC, and IP10. The maternal pro-inflammatory cytokine variable was indicated by IL-12, MIF, TNFα, IFNγ, and IL-1b. The offspring cytokine variable was indicated by MIF, TNFα, IFNγ, IL-1b, IL-2, IL-6, IL-15, IL-17, and IL-1RA (Table S2.2) (Appendix A).

2.2.4.3 Hypothesis Testing

After determining which latent variables to include in analysis we used SEM to investigate the relative effects of maternal diet, maternal metabolic state, and maternal inflammation on offspring central and peripheral inflammatory outcomes. This statistical modeling technique has the advantage of being able to simultaneously estimate complex relationships between maternal metabolic and inflammatory factors and offspring outcome measures, including both direct (e.g., WSD→offspring inflammation) and indirect (e.g., WSD→adiposity→inflammation) effects. Model estimation proceeded as follows. First, we examined the influence of WSD and adiposity on offspring central and peripheral inflammation. Specifically, the offspring inflammation measure was regressed on maternal adiposity and maternal WSD. Additionally, maternal adiposity was regressed on WSD. Offspring central and peripheral inflammatory variables were considered in separate models. Second, maternal inflammation was added to this model as a mediator of the effect of WSD and adiposity on offspring inflammation. Specifically, maternal inflammation was regressed on WSD and maternal adiposity. Additionally, offspring inflammation was regressed on maternal inflammation. Maternal cytokines and chemokines were assessed in separate models. The statistical significance of indirect effects were tested using the model indirect command.

2.3 Results

Our group has previously characterized the metabolic changes experienced by dams consuming a WSD compared to a control diet in our NHP model (22, 94). Briefly, pregnant dams consuming a WSD have increased body fat percentage, and impaired insulin sensitivity and glucose metabolism. However, in our NHP model we do not observe a significant difference in gestational weight gain between diet groups during pregnancy (94).

2.3.1 Confirmatory Factor Analysis Model Fit

Prior to hypothesis testing, four confirmatory factor analyses were used to create latent variables (described above) to model various inflammatory profiles. All latent variables, including maternal chemokines [$\chi 2$ (4) = 4.088, p = 0.394, CFI = 0.999, TLI = 0.997, RMSEA = 0.014], maternal pro-inflammatory cytokines, [$\chi 2$ (3) = 4.073, p = 0.254, CFI = 0.989, TLI = 0.965, RMSEA = 0.055] offspring chemokines [$\chi 2$ (9) = 7.69, p = 0.57, CFI = 1.000, TLI = 1.033, RMSEA = 0.000], and offspring cytokines [$\chi 2$ (22) = 26.622, p = 0.226, CFI = 0.972, TLI

= 0.954, RMSEA = 0.048], fit the data adequately. All factor loadings were statistically significant ($p<.05$), and the variances of the latent variables were significant (Table S2.1) (Appendix A). Together, these results suggest that these latent variables represent a statistically sound and appropriate way to consider these cytokine data.

2.3.2 Offspring microglial counts in specific amygdala subregions were associated with maternal diet and adiposity but not circulating inflammatory factors.

Results from the model used to test the influence of maternal diet, adiposity, and gestation length during pregnancy on offspring microglial counts in the lateral amygdala are presented in Figure 2.3. Previous work has suggested that length of gestation can have profound and lasting effects on neurodevelopment (141, 142), so we included this measure in our models for this study. This model fit the data well (CFI = 0.981, TLI = 0.885, RMSEA = 0.063). Maternal WSD was significantly associated with decreased offspring microglial counts ($\beta_{\text{Diet} \rightarrow \text{offspring microglia counts}} = -0.622$, SE = .195, $p<0.01$), when accounting for adiposity and gestational length. We also found evidence that WSD indirectly affected microglial counts via WSD's effects on pre-pregnant adiposity ($\beta_{\text{indirect WSD} \rightarrow \text{pre-pregnant adiposity} \rightarrow \text{offspring microglia counts}} = 0.207$, SE = .093, $p<0.05$). Specifically, maternal WSD was associated with increased adiposity prior to pregnancy ($\beta = 0.349$, SE = .087, $p<0.05$) compared to CTR animals, which in turn was associated with greater microglial cell counts ($\beta = 0.593$, SE = .180, $p<0.01$). Finally, we found that length of gestation significantly influenced microglial counts when accounting for maternal diet and adiposity ($\beta_{\text{gestation length} \rightarrow \text{offspring microglia counts}} = 0.164$, SE = .214, $p<0.05$) where increases in gestation time were associated with increased microglia number. In sensitivity analyses aimed at determining if this effect was specific to a particular subregion of the amygdala, this model was re-run 6 times, one model for each of the 6 subregions described in the "automated cell counting analysis" methods above. In these models, the total microglial count in each of the subregions considered in place of our primary analysis variable. In these supplemental analyses, maternal variables were only associated with the BLD and BLI subregions. These subregions followed a similar pattern and directionality of association as observed between maternal variables and the lateral amygdala (Table S2.3) (Appendix A). Previous studies indicate that microglia are highly responsive to local cues in the parenchyma (143) and perform crosstalk events with the periphery (144). To account for the possibility that offspring circulating inflammatory factors were driving the changes we see in microglia counts in the amygdala we

tested if offspring cytokines or chemokines were associated with microglia counts in the amygdala and found that there was no association (β =0.360, SE = .324, p=0.266, and β =0.243, SE = .266, p=0.362 respectively). Additionally, to account for offspring diet consumed post-weaning, we ran sensitivity analyses including offspring diet as an indicator regressed onto microglial cell counts and found no significant effects in any subregion (data not shown).

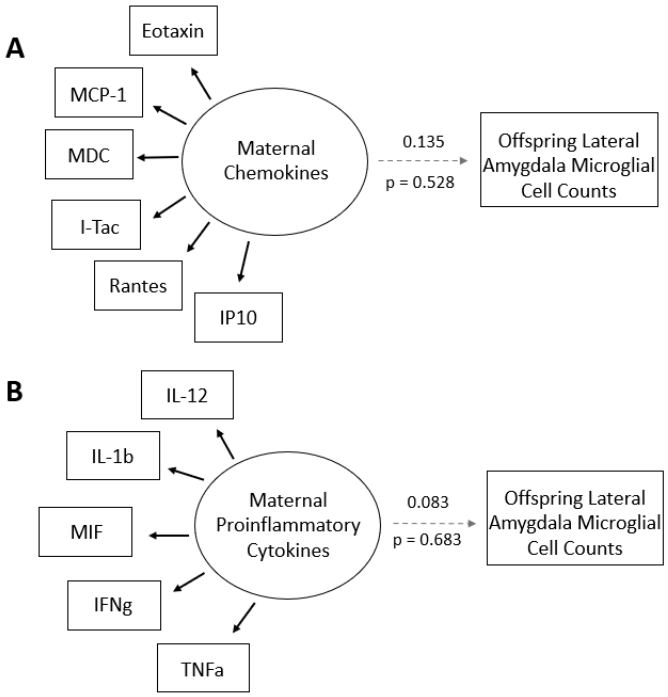

Figure 2.4. Maternal third trimester inflammatory markers do not significantly predict offspring microglial cell counts. Models of maternal chemokine and proinflammatory cytokine latent variables are presented with constituent cytokine protein markers. Corresponding standardized factor loadings are listed in Table S1. Both maternal A) Chemokines and B) pro-inflammatory cytokines do not significantly predict microglia number in the lateral amygdala at 13 months. Grey dashed lines indicate measurements that were estimated but were non-significant ($p<0.05$) and are labeled with a beta value and specific p-value.

To test if maternal circulating inflammatory factors had a direct effect on the number of microglia in the amygdala of offspring, SEM was used to examine the association between maternal chemokines and the number of microglia counted in the lateral amygdala of offspring (Figure 2.4A). This model fit the data fit adequately (χ^2 (9) = 9.906, p=0.358, CFI = 0.994, TLI = 0.985, RMSEA = 0.029). Maternal chemokines did not significantly predict microglial counts in offspring lateral amygdala (β = 0.135, SE = .214, p=0.528). Maternal pro-inflammatory cytokines followed a similar trend of results as maternal chemokines (Figure 2.4B). Additionally, all other amygdala subregions did not show significant association with maternal circulating inflammatory factors (data not shown).

2.3.3 Offspring peripheral inflammatory factors were associated with maternal adipose-derived decrease in circulating chemokines.

Previous work by our group has suggested that maternal WSD influences circulating maternal chemokine levels via its effects on maternal adiposity (26). Here, we confirm our previous findings and take a further step by suggesting that maternal adiposity-derived third trimester chemokines are associated with offspring cytokines and chemokines at 13-months. Figure 2.5A presents the results from the SEM used to examine the association between the maternal diet, adiposity and chemokines and offspring cytokines latent variables. This model fit the data adequately (χ^2 (107) = 117.63, p = 0.227, CFI = 0.961, TLI = 0.950, RMSEA = 0.026). We found higher levels of maternal chemokines were associated with lower levels of offspring cytokines (β = -0.389, SE = .117, p<0.01). We also found a significant

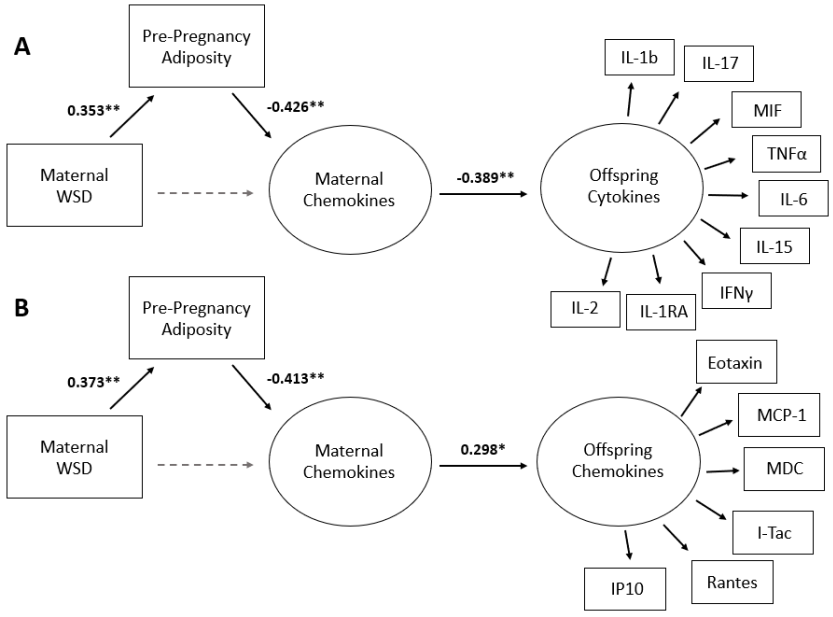

Figure 2.5. Maternal adiposity-induced chemokines influence offspring peripheral inflammatory outcomes. Models of maternal chemokine and offspring chemokine and cytokine latent variables are presented with constituent cytokine protein markers. Corresponding standardized factor loadings are listed in Table S1. A) Indicates the path analysis model including maternal diet, adiposity, and chemokine latent variables influence on offspring cytokine latent variable. Model fit statistics suggest adequate model fit with RMSEA = 0.026, CFI= 0.961, and TLI = 0.95. B) Indicates the path analysis model including maternal diet, adiposity, and chemokine latent variables influence on offspring chemokine latent variable. Model fit statistics suggest adequate model fit with RMSEA = 0.039, CFI= 0.942, and TLI = 0.919. Black lines indicate significant direct effects (* = p<0.05, ** = p<0.01) and are labeled with a beta value. Grey dashed lines indicate measurements that were estimated but were non-significant.

indirect effect of maternal WSD on offspring cytokine levels via maternal adiposity-induced increases in maternal chemokine levels ($\beta_{\text{indirect WSD} \rightarrow \text{pre-pregnancy adiposity} \rightarrow \text{maternal chemokines} \rightarrow \text{offspring cytokines}} = 0.058$, SE = .238, $p<0.05$). Specifically, maternal WSD was associated with increased adiposity ($\beta = 0.353$, SE = .088, $p<0.01$) compared to controls, which in turn was associated with decreased maternal chemokines ($\beta = -0.426$, SE = .133, $p<0.01$), which resulted in decreased offspring circulating cytokines at 13-months ($\beta = -0.389$, SE = .117, $p<0.01$). Figure 2.5B presents the results from SEM used to examine the association between the maternal chemokines and offspring chemokines latent variables. The data fit this model adequately (χ^2 (65) = 79.27, p = 0.110, CFI = 0.942, TLI = 0.919, RMSEA = 0.039). We found maternal chemokine levels were positively associated with offspring chemokine levels ($\beta = 0.298$, SE = .149, $p<0.05$). Similar to Figure 2.5A, we found maternal WSD was associated with increased maternal adiposity ($\beta = 0.373$, SE = .084, $p<0.01$), which in turn was associated with decreased maternal chemokines ($\beta = -0.413$, SE = .112, $p<0.01$), which were then associated with a decrease in offspring chemokines ($\beta = 0.298$, SE = .149, $p<0.05$). We also ran models examining the influence of a maternal proinflammatory cytokine latent variable on offspring peripheral measures, however no significant effects were found (data not shown). Figure 2.6A presents results from the model used to test the impact of maternal diet and adiposity on offspring circulating cytokines. This model fit the data adequately (χ^2 (38) = 46.08, p = 0.173, CFI = 0.952, TLI = 0.931, RMSEA = 0.040). Maternal diet was not significantly associated with offspring peripheral circulating inflammatory factors ($\beta_{\text{WSD} \rightarrow \text{offspring cytokines}} = -0.099$, p=0.488). Similarly, pre-pregnant adiposity ($\beta_{\text{pre-pregnancy adiposity} \rightarrow \text{offspring cytokines}} = 0.114$, p = 0.425) was not significantly associated with offspring cytokines. The same trend of results held true for the model that included offspring chemokines in place of offspring cytokines (Figure 2.6B). Additionally, we performed regression analyses examining the relationships between maternal obesity, maternal and offspring diet and their effects on individual cytokine levels (Table S4) (Appendix A).

2.4 Discussion

We hypothesized that maternal consumption of an obesogenic WSD during pregnancy would impact juvenile offspring inflammatory outcomes via obesity-induced maternal inflammation. The current study provides a novel examination of the unique effects of several maternal factors on the developing offspring through the use of structural equation modeling. For the first time, we found that the number of microglia in the basolateral amygdala of juvenile NHP offspring were associated with maternal diet and adiposity, but not maternal circulating inflammatory factors. We also found that juvenile NHP offspring peripheral inflammatory outcomes in the form of basal circulating cytokine and chemokines levels were associated with maternal obesity-induced circulating chemokine levels during the third trimester of gestation. These results suggest that maternal diet, adiposity, and inflammation differentially influence various offspring inflammatory outcomes.

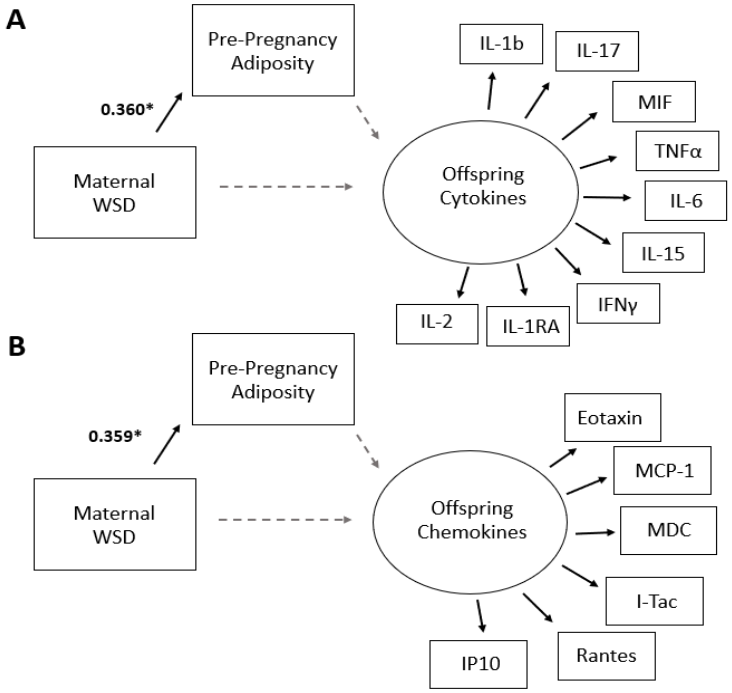

Figure 2.6. Maternal metabolic state does not directly influence offspring peripheral inflammatory markers. Models of offspring chemokine and cytokine latent variables are presented with constituent cytokine protein markers. Corresponding standardized factor loadings are listed in Table S1. A) Path analysis model includes maternal diet and adiposity measures and 13-month offspring cytokine latent variable. Model fit statistics suggest adequate model fit with RMSEA = 0.040, CFI= 0.952, and TLI = 0.931. B) Path analysis model includes maternal metabolic state measures and 13-month offspring chemokine latent variable. Model fit statistics suggest adequate model fit with RMSEA = 0.015, CFI= 0.993, and TLI = 0.990. Black arrows indicate significant direct effects and are labeled with β value. Dashed grey arrows indicate non-significant estimations. WSD, Western-style diet. * = $p<0.05$.

The precise mechanisms by which maternal WSD and adiposity during gestation influence microglia number or circulating inflammatory markers in offspring are not fully elucidated. The findings of this research informs several possible mechanisms that warrant exploration in future

work. First, we originally hypothesized that increases in maternal adiposity influences the developing offspring through an inflammatory mechanism. Increases in adiposity are associated with alterations in circulating inflammatory markers, such as increases in proinflammatory cytokines and decreases in chemokines (26, 145). This obesity derived inflammatory state is then able to either directly or indirectly impact the developing fetus (Figure 2.7). This hypothesis appears to be true when considering offspring peripheral circulating inflammatory marker outcomes as we saw that decreases in maternal circulating chemokines influenced offspring chemokine and cytokine levels.

2.4.1 Mechanisms by which Maternal Diet and Obesity-Induced Inflammation Impacts Fetal Development

Adipose tissue is hormonally active and maintains dynamic communication with the immune system through cytokine release and macrophage recruitment (146). Obesogenic diets alone can stimulate cytokine release through adipocyte Toll-like receptor 4 (TLR-4) activation (147). The increased adipose tissue mass associated with obesity exacerbates inflammation and contributes to constitutive cytokine expression (148, 149). Adipose tissue hypertrophy is associated with large, fragile adipocytes (150) and increased tissue hypoxia and reactive oxygen species generation (151). This contributes to non-apoptotic adipocyte death, a pro-inflammatory process that leads to macrophage recruitment, proliferation, and cytokine release from adipose tissue (58). The overall effect of obesity and WSD consumption is termed “meta-inflammation,” a chronic condition of low-level elevated inflammation and immune activation (152). These changes in maternal immune and inflammatory profile during pregnancy may impact fetal development to produce the alterations in basal levels of inflammatory markers we observed in juvenile offspring.

The immune response during a healthy pregnancy is a complicated, less understood process that requires a delicate balance between pro and anti-inflammatory responses to provide protection from external pathogens while simultaneously preventing the rejection of the developing fetus by the mother's body. Longitudinal studies in humans suggest that there is a reduction in pro-inflammatory cytokine production coinciding with a progressively increasing expression of anti-inflammatory biomarkers (153). However, there are conflicting results across both human and animal models that are likely due to variations in study design, such as species, specific biomarkers examined, and the possible lack of inclusion of underrepresented populations (154, 155).

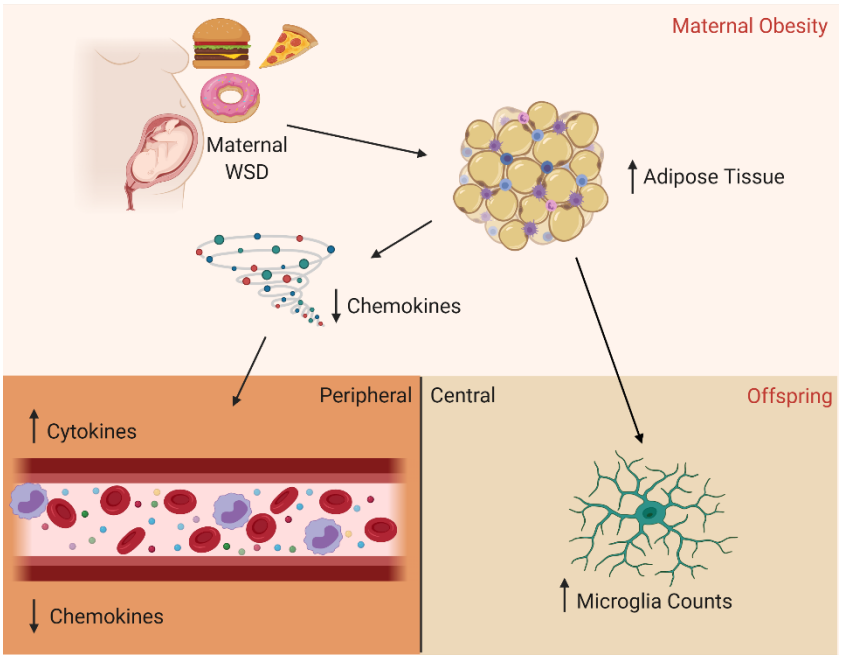

Figure 2.7. Conceptual figure describing the results observed in this study. Consuming a WSD leads to increased adiposity, this increased adiposity can affect central and peripheral inflammatory outcomes in juvenile offspring. Peripherally, adiposity tissue leads to decreased maternal circulating chemokines which in turn increases cytokines and decreases chemokines in circulation of juvenile offspring. Centrally, increased maternal adiposity leads to increased microglial counts in juvenile offspring. Created with BioRender.com.

Despite conflicting results in what is considered "typical" progression of the inflammatory response during pregnancy, disruptions to this finely tuned process are proposed to impact fetal brain development. This has been consistently shown in epidemiological studies of maternal immune activation, where children born to mothers who experienced an infection display increased risk for behavioral outcomes associated with schizophrenia and autism spectrum disorder (156). Interestingly, these same associated risks for neuropsychiatric disorders overlap strongly with outcomes of animal models where offspring are exposed to maternal consumption of a WSD (157).

In addition to obesity-induced inflammatory changes, specific nutrients that are consumed in excess when eating a WSD (saturated fat, simple carbohydrates) have been shown to have inflammatory signaling capabilities, but the precise mechanisms are not fully elucidated. The route by which saturated fatty acids (SFAs) enact inflammatory effects is heavily debated. Some evidence suggests SFAs such as palmitate can stimulate TLR4 receptors (68). However, other studies claim that SFAs do not directly stimulate TLR4 receptors, but instead enact their effects through obesity-induced increases in circulating LPS which reprograms macrophage metabolism to be more sensitive to subsequent stimulation by SFAs and induces further inflammatory signaling (158, 159). Similarly, the inflammatory actions of simple carbohydrates may be indirect. It is postulated that chronic consumption of high amounts of sugar promotes lipogenesis in the liver eventually leading to lipotoxicity (160). This lipotoxicity is then suggested to be involved in inflammatory processes such as reactive oxygen species formation (161).

2.4.2 Offspring Microglia Influenced by Maternal Diet and Obesity but Not Maternal Circulating Inflammation

We found that microglia counts were specifically impacted by maternal diet, adipose tissue mass, and length of gestation, and not by maternal or offspring circulating inflammatory molecules. This finding contradicts the proposed mechanism of maternal obesity-derived inflammation directly programming microglia. We see in Figure 3 that maternal diet and adiposity have unique but opposing effects on microglial cells counts in the offspring. This finding may suggest a compensatory response by offspring to maternal WSD exposure on microglial number in the brain. Additionally, the unique effects of maternal diet and adiposity may result in alterations in other aspects of microglia such as morphology, which has not been captured in this current study. One possible mechanism by which increased adiposity may exert its effects on the number of microglia in the brain of offspring is through adipose tissue-derived hormones, such as leptin, which has been suggested to influence fetal brain development (Figure 2.8) (162). The roles of other adipokines such as, adipokine and neuregulin, have not been extensively studied in offspring brain development. Additionally, it has been shown that obesity during pregnancy affects sex steroid concentrations depending on fetal sex (163). This is important because microglia are known to be highly responsive to modulation by sex hormones

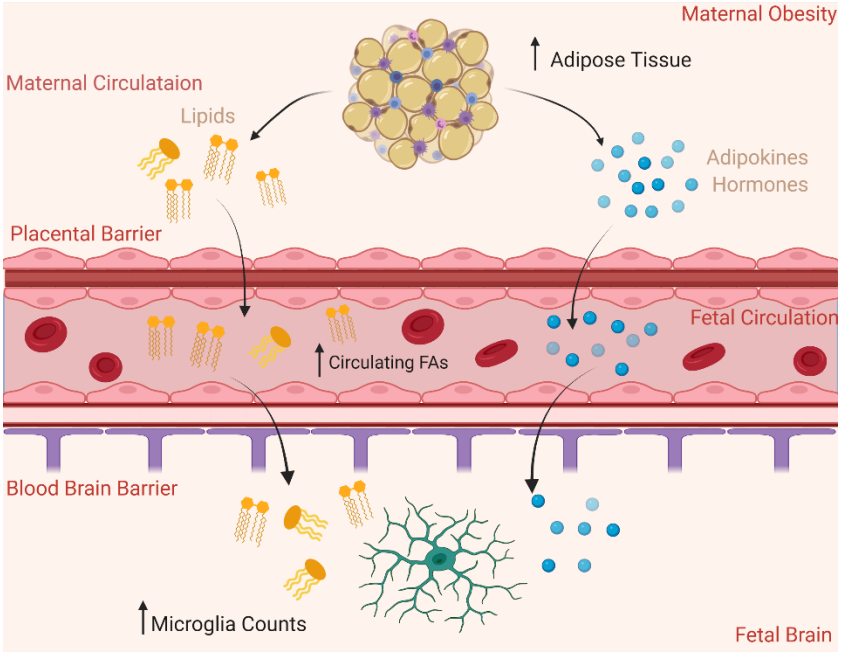

Figure 8. Conceptual figure illustrating potential mechanisms underlying adiposity's ability to increase microglia counts in the amygdala of juvenile offspring. The first mechanism shown here includes increased adipose mass leading to increased circulating fatty acids that can cross both the placental and blood-brain barriers to impact microglial membrane composition as well as function. Second, increased adipose tissue could release abnormal levels of adipose-derived hormones such as adiponectin, leptin, neuregulin, as well as impact steroid hormones such as estrogen and testosterone. These altered levels of hormones could impact microglial state and possibly lead to increased microglia counts in the amygdala. Created with BioRender.com.

during gestation (164). This mechanism is currently understudied but could provide much needed context for maternal adiposity's ability to influence offspring microglial number.

Excess fatty acids crossing the placenta into fetal circulation is a potential mechanism shared by maternal diet and adiposity for influencing offspring neural outcomes. Maternal obesity is known to reduce the efficiency of adipose tissue fatty acid turnover which results in increases in circulating fatty acids as well as ectopic fatty acid accumulation (165).

Additionally, maternal diet, outside the context of obesity, can modulate the levels of lipid content in fetal brains, as well as microglia membranes specifically (81, 166, 167). This is important given the role of membrane lipids in cellular signaling. Finally, under homeostatic conditions microglia express several lipid-sensitive receptors such as triggering receptor expressed on myeloid cells 2 (TREM2), cluster of differentiation 36 (CD36), and Toll-like receptors (TLRs) (79). These lipid-sensitive receptors also perform traditional inflammatory signaling. This overlap may provide a key connection between the increased microglial number in the amygdala and maternal overconsumption of fats in an obesogenic diet.

2.4.3 Offspring peripheral inflammatory state impacted by maternal obesity-induced circulating inflammation.

We found that offspring peripheral inflammatory outcomes were indirectly programmed by maternal adiposity's impact on circulating maternal chemokines during the third trimester. Previous work examining maternal circulating inflammatory factors have focused on single factors (e.g., IL-6, CRP, TNFα), but here, through the use of confirmatory factor analysis and the creation of latent variables, we are able to take a novel approach to examine how many related factors (i.e., chemokines and cytokines) exert their effects in concert as a measure of the overall inflammatory burden variable rather than individually. With that said, even though certain maternal inflammatory factors may load well onto a latent variable (indicating that they are capturing a shared underlying construct), it is possible that individual markers may exert specific effects on the developing offspring. It is important to explore this in future research as these specific effects could be targeted for therapeutic intervention in the future. The offspring immune system can be programmed by several different maternal factors such as psychosocial stress and nutrition (168), as well as maternal immune activation (169). Two major maternal-fetal immune transfer mechanism are the placenta prenatally and breast milk postnatally. Our group has previously reported that breast milk from WSD dams contained lower levels of eicosapentaenoic acid (EPA) and docosahexaenoic acid (DHA) as well as lower levels of total protein than CTR dams (170). It is plausible that the reduction in circulating chemokines of obese individuals in our study is perceived by the developing offspring's immune system at the placental interface during gestation or through breast milk postnatally.

2.4.4 Limitations

The current study contained a few limitations. In addition to alterations in number, microglia change other aspects of their phenotype to respond to various cues. This current study is limited by only measuring counts, but additional measures that should be considered in future work are morphology (ramified vs ameboid), gene expression, and the proteins downstream for various inflammatory signaling cascades. Collecting these additional measures provides a more comprehensive picture of the overall state of offspring microglia. Furthermore, in this study we examined microglia, which are only one of the cell types in the brain. This decision was guided by previous work performed by our group which suggested that microglia were impacted by

maternal WSD in the hypothalamus at a fetal 3rd trimester timepoint (112). However, there are other important glial cells, such as astrocytes, that may be impacted by maternal diet and adiposity during development that have the capacity to influence behavior outcomes. Additionally, the small sample size of offspring in the IHC experiment may have limited our ability to detect only large effects where we may not have been powered to detect small to intermediate effects sizes. Our models, like most statistical tests, capture linear associations among our study variables. We did not find evidence of non-linear associations among our focal variables; however future research should further explore this possibility. Finally, another limitation of this study is based on the translatability of the specific diet used here. The WSD utilized in this study was created to reflect the average American diet and may not reflect the actual dietary practice of any one individual.

2.4.5 Conclusion and Future Directions

While we did not examine the effects of maternal diet, adiposity and inflammatory state on offspring behavioral outcomes in this study, previous work by our group and others shows strong evidence that consuming a WSD and the resulting metabolic and inflammatory outcomes influence offspring behavior, such as increased anxiety and depressive behaviors (26, 95, 119). Thus, our findings may have implications for understanding offspring risk for mental health disorder. The precise mechanisms by which maternal factors influence offspring behavior remain to be fully elucidated but studies suggest that modulation of maternal and offspring inflammatory systems may play a role (26, 115). Additionally, findings from this study that implicate alterations in microglia in the juvenile amygdala indicate a possible mechanism for the behavioral alterations observed previously in the offspring as the amygdala is known to be involved with emotional regulation. While the amygdala is a key brain region involved in behavior, future studies should examine other brain regions involved in modulating behavior such as the pre-frontal cortex.

Interventions that target and modify the maternal immune system may be useful for ameliorating the programming effects on offspring circulating inflammatory factors as well as behavior. Currently, one of the more promising intervention routes in the context of maternal nutrition, is omega-3 (n-3) polyunsaturated fatty acid (PUFA) supplementation. N-3 PUFA consumption is generally reduced when individuals are consuming a WSD compared to other

diets such as a Mediterranean diet. Preclinical studies that examine n-3 PUFAs consumption during pregnancy suggest n-3 supplementation may protect against offspring behavioral risk associated with increased maternal adiposity (171) as well as modify microglial phagocytic capacity (76, 77). Further work to understand strategies that may be able to relieve adverse health outcomes in offspring born to obese mother is an important field of research.

III. PERINATAL WESTERN-STYLE DIET ALTERS SEROTONERGIC NERUONS IN MACAQUE RAPHE NUCLEI

From Dunn GA, Thompson JR, Mitchell AJ, Papadakis S, Selby M, Fair D, et al. (2022): Perinatal Western-style diet alters serotonergic neurons in the macaque raphe nuclei. *Front Neurosci*. 16:1067479

3.1 Introduction

Serotonin is critical for the healthy development of the central nervous system where it actively shapes neuronal networks and coordinates behavioral response and cognition (172, 173). Dysfunction in the central serotonergic system contributes to behavioral pathologies such as anxiety, major depressive disorder and obsessive-compulsive disorder (172, 174, 175). Considering its importance, a surprisingly small number of neurons are responsible for producing the serotonin transmitted throughout the brain. These neurons reside in the raphe nuclei of the midbrain and contain the enzyme tryptophan hydroxylase 2 (TPH2) which is responsible for synthesizing endogenous serotonin used to signal between neurons.

Previous work in our lab has shown that disruption of TPH2 synthesis in the raphe corresponds to decreased serotonin delivery in the cortex and behavioral dysregulation in developing nonhuman primates (26, 94). These outcomes resulted from developmental exposure to a Western-style diet (WSD) and the associated metabolic responses, part of a larger body of work demonstrating that maternal diet and metabolic state have long-lasting influences on offspring behavior and neurodevelopment (25, 176). Recent work in rodents has emphasized the susceptibility of the serotonin system to dietary influences during development (177). As such, identifying how and why serotonergic signaling is impaired during developmental insult is highly relevant to researchers and for public health.

The TPH2 populations that primarily supply the forebrain with serotonin are the dorsal raphe (DR), largely confined to the periaqueductal gray, and the more ventrally located median raphe. Modern research has highlighted the diversity of the raphe nuclei, relying heavily on rodent models (178). The DR is organized into smaller subnuclei arranged along the rostral-caudal axis of the hindbrain (179). These subnuclei are delineated by anatomical boundaries,

developmental lineage, co-receptor expression, morphological characteristics, and electrophysiological properties (180).

Recent advances in single cell characterization and projection tracing have revealed that the heterogenous phenotypes of these subnuclei correspond to populations of cells with distinct projection targets (181-184). One particular molecular marker, *vesicular glutamate transporter 3* (VGLUT3), has emerged as a particularly straightforward and informative indication of DR subnuclei. In humans and rodents, populations of TPH2 positive neurons in the raphe co-express VGLUT3 to varying degrees (87, 185, 186).

This heterogeneity is associated with behavioral regulation. VGLUT3+ DR projections concentrate in behaviorally-relevant brain regions like the medial prefrontal cortex and amygdala (182, 187-189). Loss of VGLUT3 impacts behavioral response, with one study showing VGLUT3 null mice exhibited increased anxiety-like behaviors during development and adulthood (187). Unfortunately, apart from one study establishing the presence of VGLUT3 in the human DR, all of the evidence implicating VGLUT3 with the behaviorally-relevant functions of the DR come from rodent models. To date there have been no studies examining the expression of VGLUT3 in the nonhuman primate DR.

In the current study, we labeled midbrain tissue sections with anti-TPH2 and anti-VGLUT3 antibodies to probe the diversity of the juvenile Japanese macaque (*Macaca fuscata*) raphe nuclei. Examining cells across the rostral-caudal extent of the raphe, we looked across anatomical boundaries at morphological characteristics such as cell area and shape, cell density, VGLUT3 identity, and TPH2 intensity to examine how serotonergic neuron diversity in the macaque relates to that reported in rodent literature. We hope that this study can be a resource for future studies of serotonergic development in primates. We simultaneously leveraged the WSD model established in our research group to investigate how perinatal WSD impacts serotonergic integrity across raphe subnuclei. We examined three diet groups: animals exposed to a single diet from gestation through post-weaning, either the control diet or WSD, and animals that were exposed to WSD during gestation and lactation but received a control diet intervention from post-weaning onwards. We hypothesized that perinatal WSD would decrease TPH2 availability across the raphe. Additionally, because of our groups previous *tph2* mRNA findings (94), we hypothesized that TPH2 protein in animals that were switched to a control (CTR) diet at weaning

would remain reduced. We predicted that compensatory changes in VGLUT3 expression may coincide with TPH2 disturbances.

3.2 Methods

3.2.1 Animals

All animal procedures were in accordance with National Institutes of Health guidelines on the ethical use of animals and were approved by the Oregon National Primate Research Center (ONPRC) Institutional Animal Care and Use Committee.

Japanese macaques (Macaca fuscata) used in this study were born naturally into social groups and kept with their mothers until weaning at 8.43 ± 0.90 months of age. After weaning, animals were housed in mixed-sex social groups with 4-7 other age-matched Japanese macaques and 1-2 unrelated adult females.

3.2.2 Diet Characterization

Two diets were administered to animals in this study: the Western-style diet (WSD) and a control diet (CTR). The WSD (TAD Primate Diet no. 5LOP, Test Diet, Purina Mills) provides approximately 36.6% of calories from fat, which is in line with the fat and saturated fat content of the typical Western-style, American diet. Alternatively, the CTR diet (Monkey Diet no. 5000; Purina Mills) provides approximately 14.7% of calories from fat. The carbohydrate sources differed between the two diets, with sugars (primarily sucrose and fructose) comprising 18.94% of the WSD but only 3.14% of the CTR diet. All animals fed the WSD were also given calorically dense treats once per day (94).

Animals were assigned to a diet group based on their source of nutrition in two life-stages: maternal (pre-weaning) diet and post-weaning diet. In the case of maternal WSD, pregnant adult females had consumed the WSD diet for at least 1 year before producing offspring considered in this study. In the case of the maternal CTR diet, adult females had been fed CTR chow for their entire lives. The offspring were exposed to the maternal diet in utero. Following birth, all animals maintained their same diet such that the offspring received continued nutrition from the maternal diet in the form of breastmilk. Most offspring began independently ingesting the maternal diet by 4 months of age and by 6 months of age this was their primary food source.

When animals were weaned, most juveniles continued their maternal diet post-weaning (CTR/CTR or WSD/WSD). Some maternal WSD animals received a diet intervention and switched to the CTR diet post-weaning (WSD/CTR). In this way we can examine the effect of nutrition during early development (maternal diet) or later development (post-weaning diet). A total of 24 animals were used in this study: 8 C/C (4 female), 8 W/C (4 female), 8 W/W (4 female).

3.2.3 Tissue Collection

Brain tissue was obtained from the Obese Resource tissue bank (P51 OD011092). Tissue utilized in this experiment were part of a larger more comprehensive study that examined many different tissue systems there may be impacted by maternal diet. At 13.25 ± 0.71 months of age the juveniles were euthanized and brain tissue was collected. Euthanasia was performed by ONPRC Necropsy staff and adhered to American Veterinary Medical Association Guidelines on Euthanasia in Animals and ONPRC standard operating procedures and guidelines. Animals were sedated with Ketamine HCl (15-25 mg/kg i.m.) for transport to necropsy suite and then deeply anesthetized with a surgical dose of sodium pentobarbital (25–35 mg/kg i.v.). Once sufficient anesthetic depth was reached, animals were exsanguinated from the aorta while cerebral perfusion was performed via the carotid artery. Perfusion consisted of an initial flush of 0.5-1 liter of 0.9% heparinized saline followed by 4% paraformaldehyde (PFA, approximately 1–2 liters) buffered with sodium phosphate ($NaPO_4$, pH 7.4) until tissue was fixed. The brain was then removed, regionally partitioned, and placed in 4% PFA for 24 hours at 4°C to complete fixation. Brain tissue blocks were then transferred to 10% glycerol buffered with $NaPO_4$ for 24 hours and finally transferred to 20% glycerol solution for 72 hours. Tissue blocks were frozen in −50°C 2-methylbutane and then stored at −80°C until sectioning. Coronal sections (25 μm) of the midbrain were collected in 1:24 series using a freezing microtome and stored in cryoprotectant at -20°C until immunohistochemistry was performed.

3.2.4 Tissue Selection

Detailed stereological assessment of the entire dorsal raphe was not possible to due to the use of some tissue sections from these animals in previous experiments. While our sections could not be used to quantitatively reconstruct the entire dorsal raphe, the sections used in this experiment for all animals spanned the rostro-caudal progression of the raphe.

Brain sections could be identified as corresponding to rostral, medial, and caudal raphe based on gross anatomical markers. The most informative anatomical markers were the size and shape of the periaqueductal gray (PAG) and cerebral aqueduct (aq)/fourth ventricle (iv vent), the presence and location of medial longitudinal fasciculus (mlf), and the presence of fibrous pontine tissue. This selection technique was refined in pilot experiments using a set of 6 additional juvenile brains that were not included in the experimental dataset. This pilot group consisted of 3 C/C (2 females), 1 W/C (0 females), and two W/W (1 female) whose brain sections represented the range of sectioning angles and section sizes present in the experimental group. Through these pilot studies we determined that classification of the floating tissue section along a custom 10-point rostral-caudal scale based on anatomical markers matched well with the actual classification of the section based on immunofluorescent staining of TPH2 populations. The full rostro-caudal extent of the raphe could be represented with 12-14 sections collected from the midbrain. The final number of sections included per animal in the experimental dataset was as follows: C/C= 8-14 sections per animal (median: 12), W/C= 9-14 sections per animal (median: 11), W/W= 10-14 sections per animal (median: 13). Example images illustrating the section heterogeneity across the raphe are presented in Figure 1.

3.2.5 Immunohistochemistry

Tissue sections were removed from cryoprotectant and transferred to PBS in netted wells in a 6-well plate. Unless otherwise stated, all steps occurred at room temperature. Sections underwent four 5-minute washes, using fresh PBS for each wash. Tissue was then blocked for one hour in 5% normal donkey serum (NDS; Millipore-Sigma Cat# S30-100ML), 0.4% Triton-X 100 (Fisher Bioreagents Cat# BP151-500) in PBS. Sections were then transferred to primary antibody solution (2% NDS in PBS) containing the following primary antibodies: 1:500 anti-TPH2 goat (Abcam Cat# 121103), 1:100 anti-VGLUT3 mouse (Abcam Cat# 134310). Sections were incubated at room temperature at 40 RPM for one hour and then transferred to 4°C where they were kept for 22 hours.

After primary incubation, sections were washed 3 times (5-minutes each at 40 RPM in fresh PBS). Tissue was then transferred to secondary antibody solution (2% NDS in PBS) containing: 1:300 donkey anti-goat TRITC (Abcam Cat# 6882), 1:500 donkey anti-mouse Alexa 647 (Abcam Cat# 150107). Secondary incubation occurred at 40 RPM for one hour, followed by

three more washes (5-minutes each at 40 RPM in fresh PBS). Nuclei were then labeled with DAPI (4',6-diamidino-2-phenylindole; 3uM in PBS; ThermoFisher Cat# D3571) for 3 minutes at 40 RPM before two final 5-minute washes in fresh PBS. Sections were then moved into fresh PBS before being mounted onto gelatin-subbed slides. Slides were finally coverslipped with 100uL Prolong Gold (ThermoFisher Cat# P36930) and 1mm coverslips (Thermo Scientific Cat# 6776215). Slides were left to cure overnight before they were sealed with nail polish and stored in 4°C until imaging.

3.2.6 Imaging

Images were taken using the Olympus VS110 slide-scanning microscope. Images were collected at 20x. Channel settings were as follows: DAPI exposure= 100ms, intensity=100%, dynamic range: 300-8000; FITC exposure= 250ms, intensity=100%, dynamic range: 750-6000; TRITC exposure= 200ms, intensity=100%, dynamic range: 1000-3000; Cy5 exposure= 500ms, intensity=90%, dynamic range: 500-1500.

The pilot studies referenced above also determined the imaging area bounding box, based on anatomical landmarks present in brightfield images. For rostral and medial sections, or any section clearly containing the cerebellar decussation (xcsp), a single DR image was collected (Figure 3.1A i-iii). The upper limit of the DR image area was slightly above the widest point of the PAG and always included a small portion of the cerebral aqueduct. The image area extended ventrally to the upper quarter or middle of the xcsp, which marked the lower limit. The width of the DR imaging area was defined by the far edges of the mlf. For caudal sections (Figure 1A iv), a single image was taken that contained both the DRc and the median raphe. The upper limit began at approximately half the height of the PAG and the lower limit was the upper boundary of the pons. The width was determined by the outer edge of the densest dorsal tegmental nuclei bundles (DTg). Focal spots were determined after image area selection, with approximately 6 evenly spaced focal spots selected in the PAG of rostral and medial sections, and only 2 in the PAG for caudal sections. Between 2-3 focal spots were placed in the interfascicular region, and the IV nerve bundles received 1 focal each. Once all focal spots were determined, imaging commenced with the Olympus system prompting the experimenter to manually focus (using the DAPI channel) at each of the determined focal spots. The entire image area was then collected by the scanning microscope (Figure 3.1B).

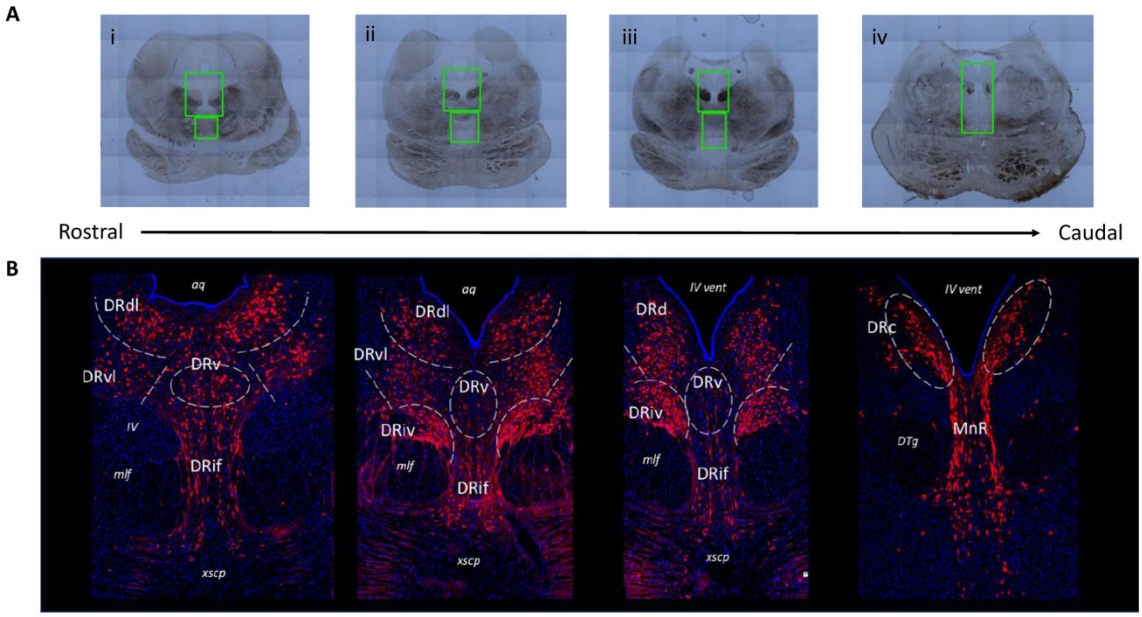

Figure 3.1. Representative images of various subnuclei distinctions across the rostral-caudal axis of the greater raphe nuclei. Distinctions were made based on gross anatomical makers such as the size and shape of the periaqueductal gray (PAG) and cerebral aqueduct (aq)/fourth ventricle (iv vent), the presence and location of medial longitudinal fasciculus (mlf), and the presence of fibrous pontine tissue. (A) Example overview images indicating slide scanner imaging areas. Green boxes indicate locations of 20× magnification images that were used in analysis. (B) Representative images of juvenile Japanese macaque midbrain sections indicating the subnuclei divisions used in subsequent analysis. Gray dashed lines indicate nuclei boundaries the experimenter identified and where rectangular bounding box was placed to produce separate images for each subnucleus. The lateral nuclei (DRdl and DRvl) and the DRiv were separated into left and right components, but only left components are labeled for visualization purposes. Blue: 4′,6-diamidino-2-phenylindole (DAPI), red: tryptophan hydroxylase 2 (TPH2). DRd, dorsal nucleus of the dorsal raphe; DRdl, dorsolateral nucleus of the dorsal raphe; DRv, ventral nucleus of the dorsal raphe; DRvl, ventrolateral nucleus of the dorsal raphe; DRiv, fourth nerve nucleus of the dorsal raphe; DRif, interfascicular nucleus of the dorsal raphe subnucleus; MnR, median raphe nucleus; xscp, cerebellar decussation; DTg, dorsal tegmental nucleus.

3.2.7 Subnuclei Division

Given the lack of serial sections, plus the variation in tissue size and sectioning angle, we opted to not perform true stereological quantification on the entire DR. Rather, we adopted a user-defined sampling method to isolate image regions for quantification. The criteria used to

define these quantification regions are derived from literature descriptions of the diverse subnuclei within the DR.

We found that the juvenile macaque raphe mapped consistently to the adult human DR (190) (Figure 1B). Based on the histological location and cell morphology outlined in Baker et al., 1990, we identified the dorsal DR (DRd), ventral DR (DRv), ventrolateral DR (DRvl), inferfascicular DR (DRif), caudal DR (DRc), a IV nerve, mlf subnucleus (DRiv), and median raphe (MnR) (191). We further segregated the rostral DRd as its own subnucleus, since we consistently saw 1) rostral DRd positions were more lateral and 2) rostral DRd exhibited distinct cells size and density patterns that medial DRd and DRc. Owing to its more wing-like population, we called this the dorsolateral DR (DRdl).

Within the CellSens program we used rectangular bounding boxes to isolate the TPH2 neurons that appeared in these stereotyped locations. We generated distinct images for each of the 8 subnuclei: DRdl, DRvl, DRv, DRd, DRc, DRif, DRiv, and MnR. The DRdl, DRvl, DRd, DRc, and DRiv all were present in bilaterally symmetric clusters, so two cropped images of each of these subnuclei were generated from each initial DR image.

3.2.8 Image Processing

FIJI (192) for ImageJ (193) software was used to develop an in-house macro to combine automated and manual TPH2 cell measurement. The macro steps are summarized here and are available from the authors upon request.

First, the macro performed a minimum filter (5 pixels) of the raw TPH2 image and then averaged the minimum filtered image with the original raw image. For all images except for DRc, the Triangle thresholding algorithm was then applied to the averaged image. Due to the proximity of the DRc to the tissue border of the fourth ventricle and the resulting increase in background for those images, the MaxEntropy thresholding algorithm was used for DRc images only. The subsequent processing steps were consistent for all images.

After thresholding, raw grayscale image was overlaid atop the resultant binary image such that the detail of the grayscale image was preserved but the thresholded portions of the image appeared faintly red. An experimenter (blind to all experimental conditions and tissue source) used these thresholding guides to manually count the TPH2 cells in the image.

Immediately after counting, experimenters were prompted to review the thresholded cell selection. The paint tool was used to ensure that each cell was properly segmented and considered separate from its neighbor. The final binary image was saved and imported into CellProfiler for quantification.

FIJI ImageJ software was also used to determine the threshold of VGLUT3 signal. Display minimum and maximum were set to fixed values for all raw images and the 16 color LUT was applied to visually identify the intensity range that reliably measured true positive signal with little background. This method indicated that a single intensity threshold could be applied to all images (absolute intensity 500).

All images were processed using the CellProfiler software (194). The processing pipeline is summarized here and is available from the authors upon request. Briefly, the pipeline first generated VGLUT3 objects from the VGLUT3 grayscale image using the pre-determined intensity threshold. Then the final thresholded, binary TPH2 image output from the FIJI macro was used to generate a single TPH2 object for each individual cell. The TPH2 and VGLUT3 images were re-matched to each other and the VGLUT3 objects were assigned to corresponding TPH2 objects based on overlapping area. Measurements were then performed to calculate the grayscale intensity of the full images and of the identified objects. The size and shape of TPH2 and VGLUT3 objects were determined. The area of VGLUT3 signal that lay within and outside of the TPH2 objects was also calculated. If greater than or equal to 20 pixels of a TPH2 cell were above the VGLUT3 threshold, that cell was classified as VGLUT3+. We found that there was a large proportion of VGLUT3+ cells with <50 pixels above the VGLUT3 threshold, and so we determined a second cutoff to identify highly VGLUT3+ TPH2+ cells where greater than or equal to 50 pixels were above the threshold.

3.2.9 Statistical Analysis

Statistical analysis of TPH2+ cell measures were performed using R (195, 196). This study utilized mixed effect/multi-level modeling (MLM) to investigate effects of maternal and post-weaning diet and sex on outcome measures of interest. Measurements were calculated per cell and then per-image averages were generated for each image. The MLM modeling framework was selected as it allows examination of parameters that vary at different levels and allows data to be organized in nested levels. In this study the multiple images collected from

each subregion were "nested" within every animal. Normality was assessed using skewness and kurtosis scores as well as the Shapiro-Wilkes test with a $p>0.05$ considered normally distributed. The following measures were found to be normally distributed after the indicated transformation was applied: TPH2+ cell density (square-root), TPH2+ cell area (square-root), TPH2+ mean intensity (square-root), and VGLUT3+ cell density (square-root). Additionally, Bonferroni corrections were performed whenever multiple comparisons were conducted.

Model creation for the final analysis included fixed effects of diet and sex, and random effects were introduced to the models to account for the random variability in the number of images collected from each animal and nucleus within that animal. As not every animal contributed an image for each subnucleus identified, the random effects of the model are considered partially crossed and not "intrinsically nested." To address the unequal representation of animals and subnuclei, we included a partially crossed random effect to control for the variation in the number of images derived from each. The model was run with the lmerTest package in R (197). The model formula that was selected for final analysis was:

TPH2 Cell Measure ~ Diet Group + Sex + (1|Offspring ID) + (1|Offspring ID : Nuclei)

In this model, TPH2 Cell Measure is the outcome variable, Diet Group and Sex are the fixed effects, and the components (1|Offspring ID) and (1|Offspring ID : Nuclei) indicate the random effects. In the model, the syntax "(1|effects)" indicates that the effects are allowed to have randomly varying intercepts at each level of the effect, while the slope is held constant. The syntax (Offspring ID: Nuclei) indicates these two random variables are partially crossed (i.e. not every animal contributed an image from every nuclei). Thus, this model framework is based on the expectation that the relationship between diet group, sex, and cell density remains constant (fixed slopes) while being able to account for the fact that some nuclei may be predisposed to having inherently different levels of cell density than other nuclei (random intercept). Similarly, including (1|Offspring ID) as a random variable allows for the model to account for individual differences that are unrelated to diet group or sex effects. Model building began with an intercept model and sequentially added fixed and random effects based on a priori hypotheses of how each factor would influence the data. The best fitting model was determined using a variety of model fit metrics including Psuedo-R2 values, Intra-class correlation coefficients (ICC), Bayesian

information criterion (BIC) and Akaike information criterion (AIC) with decreasing BIC and AIC values indicating better fit.

When creating models to examine differences between subnuclei, we included nuclei as a fixed effect with the same random effects as described previously for the intervention model. The final model used for this analysis was:

$$\text{TPH2 Cell Measure} \sim \text{Nuclei} + (1|\text{Offspring ID}) + (1|\text{Offspring ID} : \text{Nuclei})$$

VGLUT3 staining revealed punctate signal that may be indicative of the vesicles containing glutamate. Due to the binary nature in signal, we thresholded the VGLUT3 images and performed additional analyses on the area of VGLUT3 above this threshold (Materials and Methods). These measurements were nonparametric due to data being heavily skewed because of a significant number of images containing no VGLTU3 staining and were thus investigated through a two-step analysis. First, we converted these data to a binary dataset where an image either contained VGLUT3 staining or did not. This transformed data was analyzed utilizing logistic regression analysis within the MLM framework as described previously. We then analyzed VGLUT3 data in a second method where only images that contained VGLUT3 staining were included in analysis as this data was normally distributed, utilizing similar MLM methodology. The combination of these two methods allowed for the comprehensive assessment of the variance structure of this data set that was heavily inflated and skewed by zeros.

3.3 Results

3.3.1 TPH2 and VGLUT3 Characterizations

3.3.1.1 TPH2 Characterization

TPH2+ cell distribution and characteristics have been examined extensively in rodents, to our knowledge this study is the first to describe the characteristics of TPH2+ cells within subnuclei of the DR in a nonhuman primate model. While highly correlated, the DR subnuclei appear differently in rodents and direct equivalences have not been made (180, 183, 186, 198). Our detailed characterization will provide a valuable resource to research groups investigating the development of the DR in primates.

We compared TPH2+ cell density, size, and integrated intensity for 8 different subnuclei across the rostro-caudal extent of the serotonergic raphe nuclei. The 8 subnuclei were chosen from the 9 total bounding regions collected that had a high enough sampling rate to produce meaningful results (pontine raphe excluded). In addition to the qualitative distinctions described in the methods (Section 3.2.7), the subnuclei stratify on distinguishing features such as cell size and TPH2 cell density (data not shown).

Our morphological and TPH2 characterization support the distinction of 8 subnuclei (Figure 3.2). For example, although DRd appears to transition into the DRc as sections progress caudally, the two nuclei achieve TPH2 abundance in different ways. Whereas the DRd exhibits the most densely packed TPH2 cells ($p<.05$, Fig. 3.2a), what the DRc lacks in cell density, it makes up for in TPH2 signal intensity ($p<.05$, Fig. 3.2c).

Further, our designation of the rostral DRdl as a separate subnucleus from the DRd was supported by a stronger homogeneity between the two lateral wing nuclei than between the DRdl and DRd. The DRdl and the DRvl exhibited elevated mean TPH2 intensity and cell size with respect to their medial counterparts ($p<.05$, Fig. 3.2b-c). Nevertheless, the two lateral wings were more than just separated spatially; the DRdl TPH2 cells were significantly larger and less densely packed than DRvl TPH2 cells ($p<.05$, Fig. 3.2a-b).

The DRif, which is uniquely identified in primates but arguably is homologous to the larger DRv in rodents, did in fact possess similar cell size and TPH2 intensity as the DRv ($p>.05$, Fig. 3.2b-c). Nonetheless, the uniformly oriented fusiform cells of the DRif distinguish it from the more diverse and compact DRv ($p<.05$, Fig. 3.2a). The DRiv displayed similar characteristics to its most proximal subnuclei (DRv) but did show minor yet significantly increased cell density and mean TPH2 signal ($p<.05$, Fig. 3.2a,c).

Our data indicate that there is an unavoidable difference between the rostral and medial raphe and the caudal subnuclei – the DRc and MnR ($p<.05$, Fig. 3.2a-c). Finally, the MnR displayed the lowest mean intensity of the subregions yet it contained some of the largest sized cells, consistent with its distinct developmental origin ($p<.05$, Fig. 3.2c).

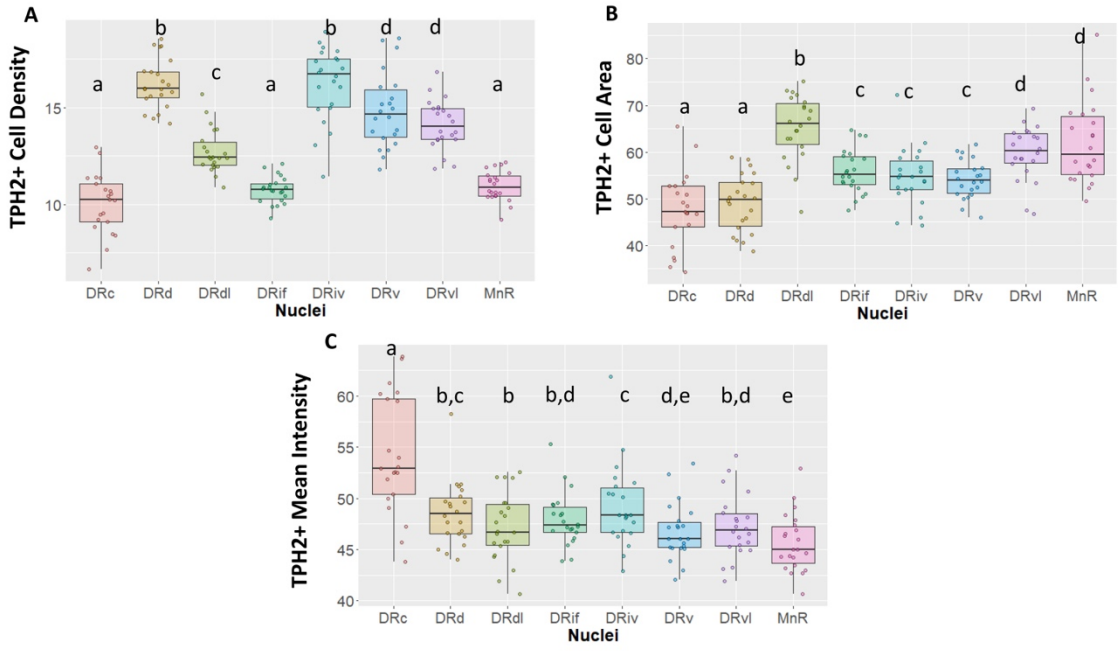

Figure 3.2. Tryptophan hydroxylase 2 (TPH2) cell measurements across subnuclei within the greater raphe nuclei. Data are expressed as box plots with boxes indicating the 1st–3rd quartile range and the median expressed as the horizontal bold line. Nuclei that share letters (e.g., "a") are not significantly different from each other, different letters indicate significant differences between subnuclei at $p < 0.05$. Bonferroni corrections were made when making multiple comparisons across all different subnuclei included. In instances denoted with multiple letters (e.g., "a, b") these groups are not significantly different from any groups that are also denoted with the same letter. (A) Number of TPH2+ cells in each subnuclei region. (B) Cell area in pixels of TPH2+ cells. (C) Mean intensity of TPH2 signal per image. DRd, dorsal nucleus of the dorsal raphe; DRdl, dorsolateral nucleus of the dorsal raphe; DRv, ventral nucleus of the dorsal raphe; DRvl, ventrolateral nucleus of the dorsal raphe; DRiv, fourth nerve nucleus of the dorsal raphe; DRif, interfascicular nucleus of the dorsal raphe subnucleus; MnR, median raphe nucleus.

3.3.1.2 VGLUT3 Characterization

To our knowledge, VGLUT3 abundance in the subnuclei of the DR has previously only been studied in rodent models and this is the first study to characterize VGLUT3 staining in subnuclei of the primate raphe. Here we examined four different measures of VGLUT3 staining in the 8 raphe subnuclei: 1) the number of cells that were dual stained for both VGLUT3 and TPH2 (VGLUT3+/TPH2+); 2) the proportion of all TPH2+ cells that contained VGLUT3 staining; and 3) the proportion of VGLUT3 signal located within the TPH2+ cells of an image versus outside of those cells but within the image boundary. An example of a TPH2+ cell that

does not contain VLGUT3 signal is denoted by blue asterisks in Figure 3.3D. An example of VGLUT3 signal occurring outside of a TPH2+ cell can be seen in Figure 3.3E denoted by white asterisks. We found that classifying cells as highly VGLUT3+ did not reveal any additional information not present in our standard VGLUT3 density measurement.

VGLUT3 signal is highly variable across different subnuclei in the raphe nuclei (Figure 3.3). Our data demonstrate that a large amount of variability in VGLUT3 measurements is yet unaccounted for. In spite of this, we uncovered striking differences between the DRiv and all other subnuclei. This region has the highest density of VGLUT3+/TPH2+ cells, the largest proportion of TPH2 cells that are VGLUT3+, and the most VGLUT3 signal localized within TPH2+ cells (Fig. 3.3A,B,C). Examples of this enrichment are clearly seen in Figure 3.3 D-E.

The VGLUT3 measurements reinforced the divide between the caudal subnuclei and the rest. The MnR has the lowest VGLUT3+ density and the fewest number of TPH2+ cells that are VGLUT3+, but nevertheless the VGLUT3 signal that is present is quite specific to the TPH2 neurons (Fig. 3.3C). This contrasts with the VGLUT3 localization in the DRc, which was significantly less than the other nuclei and below chance. The opposite is true in the DRd, which is often considered a more medial extension of the DRc. Despite the high TPH2 cell density in the DRd, the chances of finding a VGLUT3+/TPH2+ cell in the DRd was actually lower than in the DRc, a comparatively sparse region (Fig. 3.3B). Yet, the little VGLUT3 signal present in DRd images was more likely to be found within TPH2 cells than outside of them, still indicating a relative VGLUT3 enrichment in these cells (Fig. 3.3A).

Lastly, we found that the DRvl possessed more VGLUT3+/TPH2+ cells per unit area than the DRdl (Fig. 3.3A). However, the lack of difference in other VGLUT3 measures suggests that this may be an artifact of the overall increased TPH2 density in the DRvl.

3.3.2 Effect of Western-style diet on TPH2 and VGLUT3 Measures

For analyses examining the effects of WSD on TPH2 and VGLUT3 cell measurements, we focused our analysis on 5 subnuclei that the rodent literature most strongly associates with projection sites in the forebrain (182). These subnuclei include the DRd, DRdl, DRv, DRvl, and DRif. We also examined the MnR as our previous results found that post-weaning diet altered tph2 mRNA abundance in that region (94).

3.3.2.1 TPH2 Measures

3.3.2.1.1 TPH2+ Cell Count

Diet had an overall effect on TPH2+ cell density such that the TPH2+ population was least concentrated in the W/W group ($\beta = -1.09$ $p<0.05$) (Figure 3.4A), with the W/C group following a similar trend ($\beta = -0.72$ $p=0.19$). We did not observe an overall sex effect ($\beta = -0.31$ $p=0.43$) on TPH2+ cell density. Since density was highly variable between DR compartments, we examined the impact of WSD on the specific subnuclei. In this analysis we found that the pan-DR effect of W/W on TPH2 cell density was reflected in the DRv, DRdl, and DRvl, all of which were significantly decreased from C/C ($\beta = -1.35$, $p<.05$). The diet intervention (consumption of a CTR diet at weaning) did not correct TPH2 density impairments in the DRdl ($\beta = -1.23$ $p<0.05$). Intriguingly, the MnR was also sensitive to the effect of WSD on TPH2 cell density, with the TPH2 cell density of W/C ($\beta = -0.89$ $p<0.05$) and W/W ($\beta = -0.74$ $p<0.05$) groups decreased compared to the C/C group (Figure 3.4B).

Figure 3.3 (next page). Vesicular glutamate transporter 3 (VGLUT3) cell measurements across subnuclei within the greater raphe nuclei. Data are expressed as box plots with boxes indicating the 1st–3rd quartile range and the median expressed as the horizontal bold line. Nuclei that share letters (e.g., "a") are not significantly different from each other, different letters indicate significant differences between subnuclei at $p < 0.05$. Bonferroni corrections were made when making multiple comparisons across all different subnuclei included.
In instances denoted with multiple letters (e.g., "a, b") these groups are not significantly different from any groups that are also denoted with the same letter. (A) Cell density of tryptophan hydroxylase 2 (TPH2)/VGLUT3 dual positive cells in each subnuclei region. Dual positive cells were defined as TPH2+ cells that contained 20 or more pixels of VGLUT3 signal. (B) Percent of all TPH2+ cells that also have VGLUT3 signal. (C) Ratio of signal that is located either inside or outside of a TPH2+ cell. A ratio of 0.5 indicates VGLUT3 signal is equally likely as not to occur within a TPH2+ cell. Ratios above 0.5 indicate a high likelihood VGLUT3 signal will be located inside a TPH2+ cell. (D,E) Representative images of TPH2 and VGLUT3 signal localization. (E) Typical VGLUT3 signal in the DRdl. Blue asterisks indicate TPH2+ cells with a lack of VGLUT3 signal present. Example of intense VGLUT3 signal found in the DRiv. White asterisks indicate VGLUT3+ non-TPH2 cells. These cells additionally serve to demonstrate that although TPH2 signal and VGLUT3 signal are correlated, this is not the result of "bleed-through" between channels. DRd, dorsal nucleus of the dorsal raphe; DRdl, dorsolateral nucleus of the dorsal raphe; DRv, ventral nucleus of the dorsal raphe; DRvl, ventrolateral nucleus of the dorsal raphe; DRiv, fourth nerve nucleus of the dorsal raphe; DRif, interfascicular nucleus of the dorsal raphe subnucleus; MnR, median raphe nucleus.

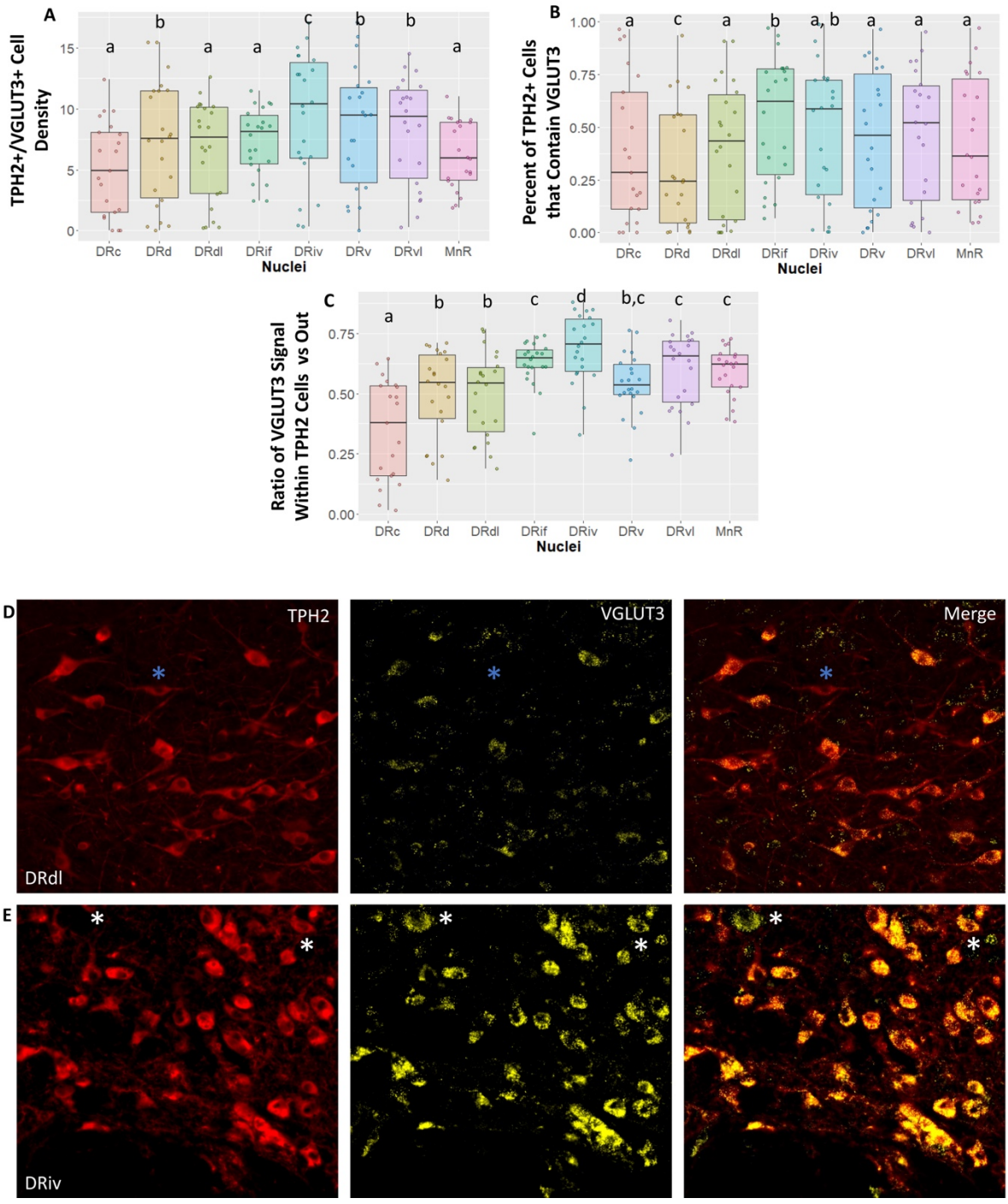
A
TPH2+/VGLUT3+ Cell Density
Nuclei
DRc
DRd
DRdl
DRif
DRiv
DRv
DRvl
MnR
B
Percent of TPH2+ Cells that Contain VGLUT3
C
Ratio of VGLUT3 Signal Within TPH2 Cells vs Out
D
TPH2
VGLUT3
Merge
DRdl
E
DRiv

Additionally, a sex effect was observed in the MnR, with male animals having reduced TPH2+ cell density compared to females ($\beta = -0.62$ $p<0.05$).

3.3.2.1.2 TPH2+ cell size

We found no overall effect of diet group on TPH2+ cell size in the raphe as a whole ($p>0.1$) (Figure 3.4C). Additionally, we did not observe an overall sex effect ($\beta = 1.71$ $p=0.44$) on TPH2+ cell size (Figure 3.4C). As we saw significant differences in cell density at the nuclei level, we asked whether diet elicited a subnuclei-specific effect on TPH2+ cell size. We found a significant increase in TPH2+ cell size in the DRd nuclei of the W/W ($\beta = 6.63$ $p<0.05$), but not the W/C group ($\beta = 3.76$ $p=0.25$) compared to controls (Figure 3.4D). We did not find significant differences in cell size for any other subnuclei.

3.3.2.1.3 TPH2 Mean Intensity

We found that diet did not have an overall effect on TPH2 mean intensity in the raphe as a whole ($p>0.5$) (Figure 3.4E). Similar to other measures, we observed large variability in mean intensity levels across subnuclei and probed whether diet impacted specific subnuclei. In this case, we found that diet did not account for variability in TPH2 intensity for any subnuclei (Figure 3.4F).

3.3.2.2 VGLUT3 Measures

The VGLUT3+ identity of TPH2+ cells were not impacted by perinatal diet for any measure examined. The probability of having an image with zero staining or some VGLUT3 was not significantly different for the W/C ($\beta = 0.07$ $p=0.48$), or W/W ($\beta = -0.06$ $p=0.53$) groups when compared to controls (Figure 3.5A). Additionally, when we analyzed only images that contained at least some VGLUT3+ staining we found no significant difference in cell number for W/C ($\beta = -0.11$ $p=0.95$), or W/W ($\beta = 0.64$ $p=0.73$) animals compared to control animals (Figure 3.5B). Further, we found that no specific nuclei were impacted by diet (Figure 3.5C). This pattern of results was found to be similarly nonsignificant for both the proportion of VGLUT3+ TPH2 cells and the quantity of highly VGLUT3 expressing cells (Supplemental Figures 3.1-3).

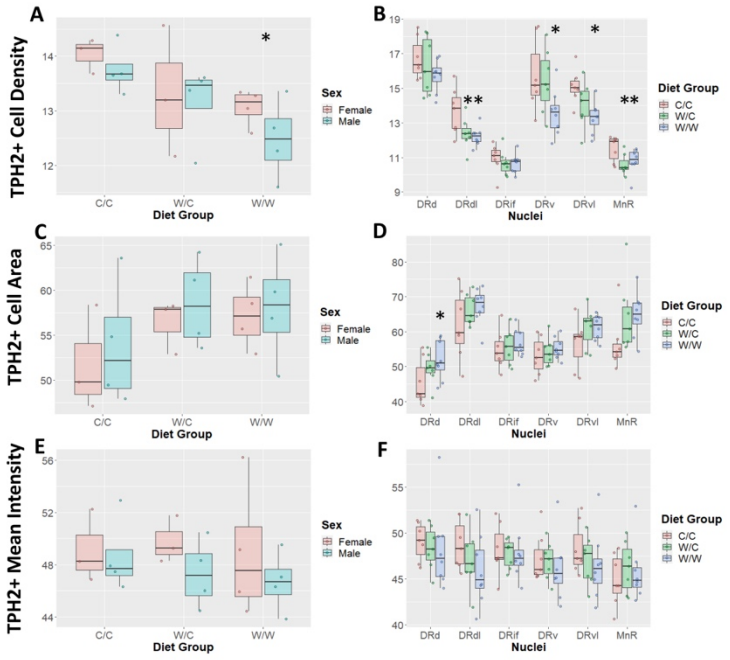

Figure 3.4. Western-style diet (WSD) influences raphe tryptophan hydroxylase 2+ (TPH2+) cell outcomes. Data are expressed as box plots with boxes indicating the 1st–3rd quartile range and the median expressed as the horizontal bold line. Asterisks indicate significant differences compared to C/C groups. (A) TPH2 cell count was decreased by perinatal exposure to WSD. The W/W group was decreased compared to the C/C and W/C groups. (B) TPH2 cell number in specific regions appear to be uniquely impacted by perinatal WSD. The DRd and DRif appears not to be impacted, while the DRdl and MnR subregions both the W/C ($p < 0.05$) and W/W ($p < 0.05$) groups were reduced compared to the C/C group. Additionally, in the DRv and DRvl subregions only the W/W was reduced compared to the C/C group ($p < 0.05$). While the W/C group was not significantly different from the C/C group, it did trend in the same direction as the W/W group. (C) TPH2 cell area was not found to be significantly different between diet groups. (D) TPH2 cell area was only significantly increased in the DRd subregion ($p < 0.05$). (E) TPH2 mean intensity per image was not found to be significantly different between diet groups. (F) TPH2 mean intensity per image was not found to be significantly different in any specific subregions. DRd, dorsal nucleus of the dorsal raphe; DRdl, dorsolateral nucleus of the dorsal raphe; DRv, ventral nucleus of the dorsal raphe; DRvl, ventrolateral nucleus of the dorsal raphe; MnR, median raphe nucleus.

3.4 Discussion

We investigated how TPH2 cell measurements varied throughout the subnuclei of the dorsal raphe of juvenile Japanese macaques. TPH2 is the rate-limiting enzyme for serotonin production, and the TPH2 neurons in the soma of DR neurons generate the vast majority of the

serotonin for the entire central nervous system. It is known that serotonergic anatomy is established in the early postnatal period in rodents (87, 179). This is the first study to systematically examine the DR anatomy in juvenile primates. We found that the anatomical distribution of TPH2 neurons in the DR of juvenile macaques was similar to that of adult Japanese macaques (191), rhesus and cynomolgus macaques (199, 200), and humans (190). Our analysis suggests that the anatomical and morphological properties of the adult DR are established before 13 months of age in Japanese macaques.

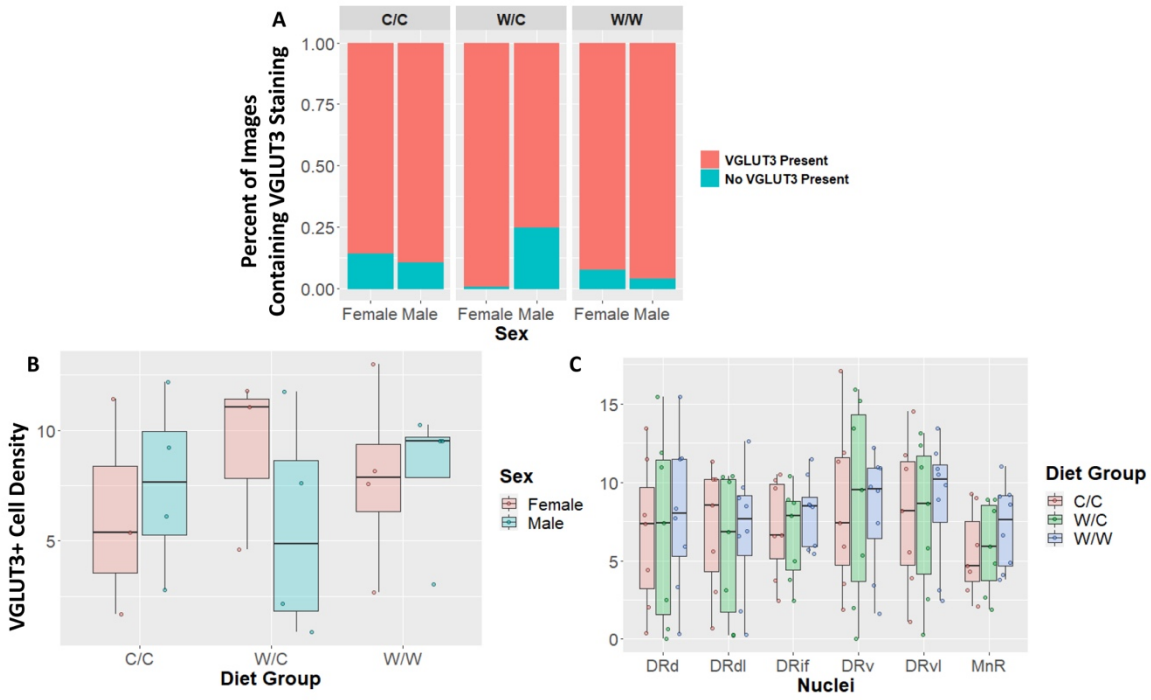

Figure 3.5. Vesicular glutamate transporter 3 (VGLUT3) cell density does not appear to be impacted by maternal Western-style diet (WSD). Data in panel (A) is expressed as percentages of images containing either some or no VGLUT3 staining. Data in panels (B/C) are expressed as box plots with boxes indicating the 1st–3rd quartile range and the median expressed as the horizontal bold line. (A) No significant diet or sex main effects were found when comparing the percentage of images that either contained some VGLUT3 staining or no staining at all. (B) VGLUT3 cell density was not significantly impacted by perinatal diet. (C) VGLUT3 cell density in specific subregions were not uniquely impacted by perinatal diet. DRd, dorsal nucleus of the dorsal raphe; DRdl, dorsolateral nucleus of the dorsal raphe; DRv, ventral nucleus of the dorsal raphe; DRvl, ventrolateral nucleus of the dorsal raphe; MnR, median raphe nucleus.

One of the major goals of this study was to reconcile the anatomical differences in TPH2 neuron clusters in the DR between rodents and primates. Much of the research into the functional

properties of the DR comes from rodent studies, particularly the determination of the targets of DR projections (reviewed in (201-203)). Translatability of these findings is obscured by some key differences in the anatomy of the rodent and primate DR. Rodents have a considerable serotonergic neuron population along the midline of the dorsal and ventral DR, while in primates the dorsal DR has clear clusters on the left and right hemispheres. In mice and rats, most dorsal serotonergic neurons are in the midline population and these cells are significantly smaller than the ventral population (180). In contrast, our analysis and previous studies have shown that the largest neurons in the primate DR are in the dorsolateral DR (190, 200). Importantly, it is unclear which primate DR subregion is homologous to the ventral DR in rodents.

To better direct translational research in the developing serotonergic system, we examined if VGLUT3 expression provided insight with which we can better compare the murine and primate DR subnuclei. This study is the first to detail VGLUT3 expression patterns in the primate DR. We found considerable VGLUT3 signal within (somatic) and outside of TPH2 neurons throughout the DR, consistent with the rodent literature (182, 186, 204).

The degree of overlap reported in TPH2 and VGLUT3 expressing neurons varies based on methodology and host species. We found that in the juvenile macaque DR, roughly 45% of TPH2 neurons were VGLUT3 positive. One study in adult rats estimated that about 30% of serotonergic neurons in the DR were VGLUT3+ (198). In spite of a lack of agreement on the proportion of VGLUT3+ serotonergic neurons in the DR, what remains clear is that different DR populations possess unique proportions of VGLUT3 and TPH2 colocalization (181, 186, 198, 205). Recently, one research group found that cortical regions are primarily targeted by VGLUT3+ serotonergic neurons, regardless of DR subnuclei (183). There is an additional degree of subnuclei specificity; as they reported that in the ventral DR roughly 60% of VGLUT3 neurons overlapped with TPH2 neurons, and that these populations have specific cortical targets (182).

We hypothesized that perinatal WSD would decrease TPH2 availability across the raphe. TPH2 availability is limited by the concentration of TPH2 in each cell (estimated by mean TPH2 signal intensity), the amount of TPH2 within each cell (estimated by TPH2+ cell size), and the number of TPH2-producing cells (evaluated with TPH2+ cell density). We found that the DR of animals that received nutrition from WSD *in utero* through to sample collection presented with

fewer TPH2 neurons. These results were driven by significant decreases in TPH2 cell density in the DRdl, DRvl, DRv, and MnR. Surprisingly, we did find that W/W increased TPH2 cell size in the DRd. Our findings indicate that perinatal WSD likely limits the serotonin production capacity of the DR.

Based on our previous findings that W/C and W/W decreased the percent area of *Tph2* mRNA in the DR (94), and the corroboration of those findings in the W/W in this study, we expected that diet intervention would not reverse the insult to TPH2 neuron size and density. However, we found that TPH2 cell density was less susceptible to WSD exposure when limited to the pre-weaning period, and that only the DRdl and the MnR exhibited a significant decrease in TPH2 cell density. Intriguingly, TPH2 cell density in the MnR was the only measure found to be different between male and female animals. More work is needed to comprehensively understand sex differences expressed in the raphe nuclei.

Overall, our data indicate that TPH2 availability is sensitive to perinatal WSD, with the DRdl and MnR exhibiting the most long-lasting effects even after post-natal diet intervention (switching onto the CTR diet). Given that the TPH2 neurons in the DRdl are the largest, this reduction could have important implications for the downstream brain regions and behaviors. Combined with our previous findings (94), these data indicate that WSD-induced changes in the density of TPH2 neurons can restrict serotonin delivery to target brain regions and contribute to dysregulated physiological and behavioral stress response. This conclusion is supported by evidence from murine models that indicate TPH2 abundance is associated with anxiety-like behaviors and is particularly sensitive to early life perturbations (206-208).

Evidence from a rodent model demonstrated that a maternal inflammatory insult produced the same phenotype of reduced TPH2 cell number in adult offspring as well as decreased serotonergic availability in target brain regions (209) supporting our hypothesis of WSD-induced inflammation being an underlying mechanism for the changes in the serotonergic system. These results are consistent with our evidence from our nonhuman primate model where we have previously shown that elevated maternal inflammatory response mediates the influence of WSD on offspring behavioral response (26). Our present results suggest that these changes could be alleviated if nutritional balance is restored before adulthood.

We predicted that the compensatory changes in VGLUT3 expression may coincide with TPH2 disturbances, but no dietary effect reached significance in any measure examined. These results are consistent with a study in VGLUT3 knockout mice where VGLUT3 deletion did not modify TPH2 level or serotonin levels (187). This study did however find that somatic VGLUT3 regulated basal neuronal activity of serotonergic neurons by facilitating glutamate-dependent serotonin reuptake. Whether the differences in VGLUT3 expression between DR regions contribute to nuclei-specific basal activity rates has not been examined.

Our study was limited by a small sample size and a large number of factors (i.e., maternal diet, post-weaning diet, sex and possibly differences in maternal metabolic state) which, in combination with mostly nonparametric distribution of measurements, limited our statistical analyses and power. Additionally, another limitation was not having a group where animals experienced a maternal CTR diet and were switched to a WSD post-weaning. Addition of this group could help determine whether a post-weaning WSD independently influenced certain subnuclei, or whether it was the combination of a pre- and post-weaning WSD that was associated with differences in TPH2 neuron characteristics. Future investigation will pursue consideration of maternal metabolic state covariates (e.g., maternal age and pre-pregnancy obesity) that have been shown in previous work to significantly impact offspring serotonergic and behavioral outcomes. Follow-up experiments will attempt to both apply and validate conclusions drawn in this analysis to inform future DR subnuclei groupings.

In summary, the juvenile Japanese macaque dorsal raphe reflects similar complexity and heterogeneity to the adult macaque and human DR. Our examination reveals that VGLUT3 is broadly co-expressed in TPH2 neurons in the DR of nonhuman primates. Differential VGLUT3 expression in juvenile macaques mirrors patterns seen in rodents, where VGLUT3 participates in serotonergic transmission to cortical and limbic areas and modulates behavioral response. Importantly, maternal WSD and continued WSD consumption post-weaning decreased TPH2 availability and resulted in nuclei-specific alterations in TPH2 protein expression in the primate DR. Additionally, the observed subnuclei-specific effects may impact serotonergic innervation of certain projection locations in the forebrain and could provide insight into how WSD exposure may program offspring risk for anxiety and stress responses.

IV. MATERNAL WESTERN-STYLE DIET AND ADIPOSITY ELICIT TRANSIENT AND PERSISTENT EFFECTS ON MICROGLIA AND MORPHOLOGY IN THE AMYGDALA OF NONHUMAN PRIMATE OFFSPRING

4.1 Introduction

Microglia are the main immunocompetent cell of the central nervous system. These cells perform a variety of different functions throughout prenatal and postnatal neurodevelopment. During prenatal development these functions include synaptic pruning (54), phagocytosis of neural progenitor cells (50), and refining network connectivity (122). Importantly, the early postnatal period remains a critical window for microglial synaptic pruning with the ability to shape long-term brain outcomes (210). Postnatally, microglia transition into more typical tissue-resident macrophage functionality, performing tasks such as surveying their local environment, phagocytosing damaged or dying cells, and fighting off pathogens (211, 212). Research seeking to understand the long-lasting effects of maternal environmental challenges on offspring brain development have connected microglia disruption during pre-and early postnatal periods with neurodevelopmental disorders such as schizophrenia (212, 213), autism spectrum disorder (214), and attention-deficit hyperactivity disorder (123). In a study using a rodent model of maternal immune activation, it was demonstrated that microglia maintain a complex inflammatory phenotype later in life as a direct result of the increased inflammatory environment the fetus experienced in gestation (215, 216). This long lasting effect on microglia has been translated across many different mediums of maternal challenges during pregnancy including stress (217), pollutants (218), diet, and metabolic state (77, 219). Previous work by our group in the same non-human primate model, showed that microglia quantity was increased in the amygdala of offspring born to obese mothers consuming a WSD (106) (**Chapter 2**). That previous work, similar to other studies, was limited in scope by only examining changes in microglial quantity. In this study we more comprehensively explored the impact of maternal WSD and obesity on offspring microglia through measuring both quantity and morphology.

During gestation the close relationship of the fetus with the maternal circulation has large influences on the functional state and morphology of fetal microglia (220). Consumption of a Western-Style diet (WSD) and the resulting increase in adiposity during pregnancy has been shown to shift fetal microglia to a more proinflammatory state in a murine model of maternal

obesity (221). Much of the work studying microglia in fetal animals of maternal WSD utilizes rodent models and whole brain homogenates to compare differences. Work studying maternal WSD's impact on microglia in primates is relatively understudied. Additionally, since microglia are known to display region-specific morphology and functional states (143), examination of these cells in specific brain regions is of importance. In this study we focus on the amygdala, a brain region typically involved in threat detection and navigating potentially dangerous stimuli. Dysregulation of the amygdala has been implicated in the disease progression of neurodevelopmental disorders and mood disorders such as anxiety (120, 222-224). Previous work by our lab has suggested maternal WSD and adiposity are associated with increases in the prevalence of anxiety-like behaviors in offspring (26, 94, 95).

The goal of this study was to understand if maternal diet and metabolic state influence offspring microglia measures in the amygdala during gestation. Additionally, this study explored if these perturbations persisted into adolescence. We hypothesized that fetal offspring from mothers consuming a WSD would display a higher microglia density as well as a less complex, more ameboid morphology compared to control animals. Additionally, we predicted WSD adolescent animals at 3 years old would display persistent increases in microglial quantity and ameboid morphology.

4.2 Methods

4.2.1 Animals

All animal procedures were in accordance with National Institutes of Health guidelines on the ethical use of animals and were approved by the Oregon National Primate Research Center (ONPRC) Institutional Animal Care and Use Committee. The present study utilized an established preclinical NHP model (Macaca fuscata) of maternal overnutrition which has been previously described in Chapter 2 of this dissertation.

4.2.2 Measurement of Maternal Adiposity

Maternal pre-pregnant levels of adiposity was measured as previously described in Chapter 2.1 Briefly, prior to pregnancy, 122 female animals underwent dual-energy X-ray absorptiometry scans to determine body composition. The mean ± standard error of pre-pregnancy adiposity for each diet group is as follows: CTR = 19.96 ± 1.15% body fat; WSD = 27.51 ± 1.42% body fat (Table 2.1).

4.2.3 Tissue Collection and Immunohistochemistry Methodology

A fluorescent immunohistochemistry (IHC) experiment was performed to quantify microglial cell density and morphology in the right amygdala of fetal and 3-year-old adolescent animals. Tissue was obtained from the Obese Resource tissue bank.

Fetal brain tissue was collected as previously described (112). Briefly, at gestational day 130, fetal offspring were collected through cesarian section and taken directly for necropsy. The cesarian section procedure was performed by ONPRC Veterinarian staff and adhered to American Veterinary Medical Association Guidelines on C-section in Animals and ONPRC standard operating procedures and guidelines. Fetal brain tissue was then collected and fixed in 4% paraformaldehyde.

At 38.35 ± 0.90 months 3-year-old animals were euthanized, and brain tissue was collected. Euthanasia was performed by ONPRC Necropsy staff and adhered to American Veterinary Medical Association Guidelines on Euthanasia in Animals and ONPRC standard operating procedures and guidelines.

Sixteen fetal and 3-year-old animals balanced for offspring sex (8 females) were included in this study. Diet manipulation involved long-term maternal consumption of a control (CTR) or Western Style diet (WSD) throughout pregnancy and breast feeding. For 36-month offspring all animals were weaned onto CTR diets around 6-7 months. Standard IHC methodology was used for tissue from both timepoints. Briefly, 35 μm thick temporal lobe tissue sections containing the amygdala were washed in a KPBS solution. Sections were blocked for 1 hour in 2% Normal Donkey Serum (NDS; Jackson ImmunoResearch Cat #017-000-121), 0.4% Triton-X100 (Fischer Bioreagents Cat# BP151-500) KPBS solution. Following blocking, sections were transferred to a primary antibody solution (2% NDS in KPBS) containing 1:1500 rabbit anti-IBA-1 (Wako FujiFilm Cat# 019-19471 Lot# PTE0555). 36-month tissue included an additional primary antibody of 1:100 mouse anti-Acetylcholinesterase (Abcam Cat# ab2803 Lot# GR3242309-4) which was used for identification of amygdala subregions. Sections were incubated at room temperature for 2 hours before being transferred to 4°C where they remained for 22 hours.

After primary incubation, sections were removed from 4°C and washed in KPBS. Tissue was then transferred to a secondary antibody solution (2% NDS in KPBS) containing 1:1000 donkey anti-rabbit Alexa 488 (ThermoFisher Cat# A21206) and 1:1000 donkey anti-mouse Alexa 555

(ThermoFisher Cat# A31570). Sections were incubated for 2 hours at room temperature. After secondary incubation, sections were again washed in KPBS. Finally, tissue sections were mounted onto gelatin-subbed slides, coverslipped using Prolong Gold Antifade (ThermoFisher Cat# P36930) and stored at 4°C until imaging.

4.2.4 Image Acquisition

Fetal Tissue

Z-stacks of the right amygdala were acquired using a Nikon Ti2 microscope partnered with the Yokogawa CSU-W1 Spinning Disk using a Plan Apo l 20x magnification 0.75 NA objective. Each stack was 665.6 μm by 665.6 μm, with 27 frames separated by 0.9 μm to acquire information through the entire volume of each region of interest. Five sections, representing the whole rostral to caudal aspect of the right amygdala, from each animal were analyzed. To obtain a representative selection, 5 images of the amygdala were randomly acquired from each section from using a semi-automated macro with the NIS-Elements JOBS software. Briefly, using a Plan Fluor 4x magnification 0.13 NA objective, a large overview image of the amygdala was collected. There, an experimenter manually outlined the boundary of the amygdala region using gross anatomical structures as described in a non-human primate atlas (132). Five random, 20x magnification, images were then collected within the drawn boundary of the amygdala for analysis (**Figure 4.1**).

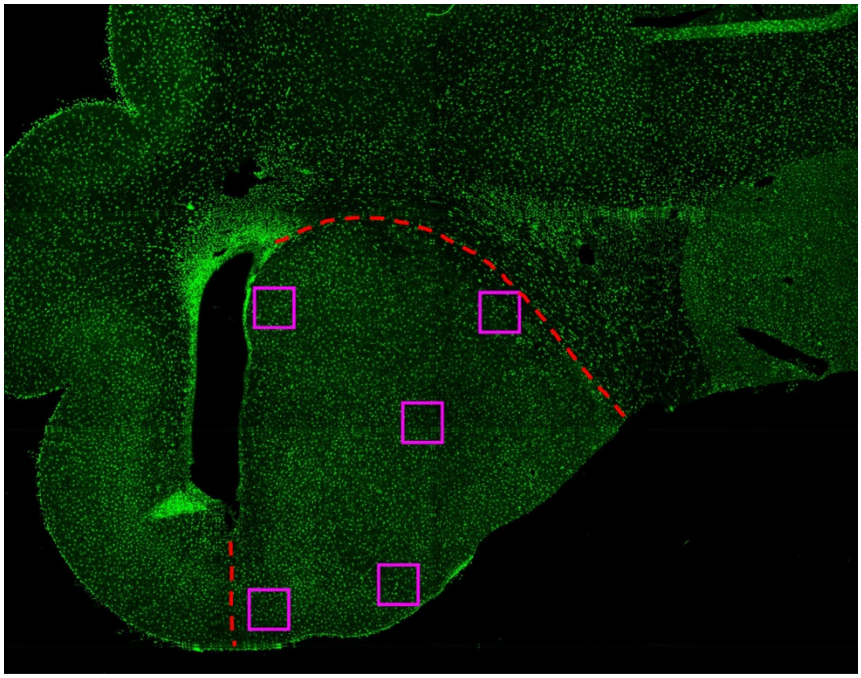

Figure 4.1. Representative image of fetal amygdala stained for IBA1 at 4x magnification. Dashed lines indicate approximate location of amygdala region based on reference of the non-human primate atlas (132). Twelve images were stitched together to create the overview image shown here. Magenta boxes indicate representative locations of 20x magnification images that were randomly selected for analysis.

36-Month Tissue

Image acquisition in 36month old animals was conducted similarly to previously described methodology in Chapter 2.2.3.1. Briefly, 45 Z-stacks of the right amygdala were acquired using a Leica SPE point scanning confocal with an HC Fluotar L 25x magnification 0.95 N.A. W VISIR objective. Each stack was 293.91 µm by 293.91 µm, separated by 0.57 µm to acquire information through the entire volume of each region of interest. Seven sections, spanning the rostral to caudal aspect of the right amygdala, from each animal were analyzed. To examine specific subregions of the amygdala, boundaries of each region were determined using an AChE stain with a 5x objective (**Figure 2.1**), referencing an adolescent non-human primate atlas (132). To have a representative count for each subregion, three images were acquired and averaged for each subregion per section.

4.2.5 Image Analysis

Morphological analysis was performed on 3D images using Imaris 10.0 software (Bitplane, Zurich, Switzerland). All images were processed and analyzed by an experimenter blinded to animal diet and sex. Microglial cells were 3D reconstructed using the Imaris "Surfaces" creation tool. While, the software automatically recreated microglial cells, the expert manually verified and removed any false positive objects before final morphometric statistics were collected. The morphometric parameters of interest that were exported and analyzed in detail included number, surface area, and volume (Figure 4.2).

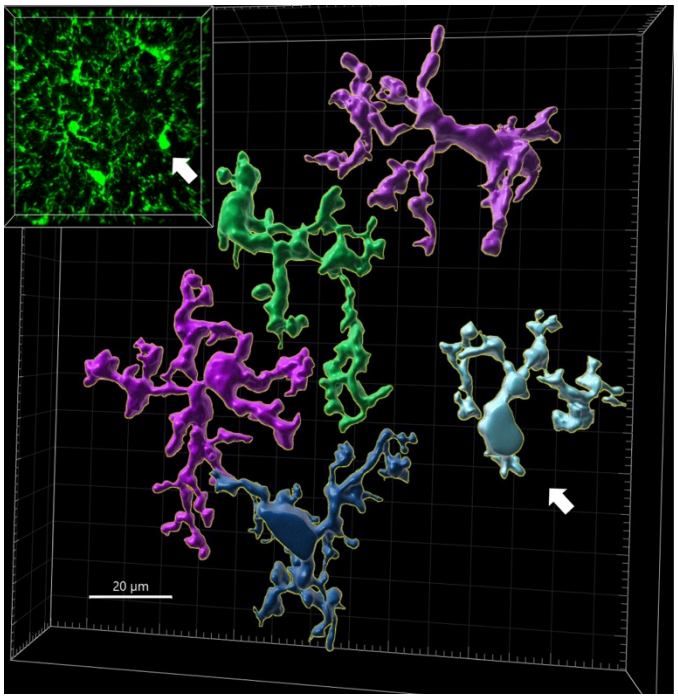

Figure 4.2. Representative image of 3D reconstruction of microglial cells.

4.2.6 Data analysis/Statistics

Data were analyzed using a structural equation modeling (SEM) framework (134) using Mplus 7.4 (135), which was previously described in more detail in Chapter 2.2.4. Briefly, the robust maximum likelihood estimator was used which accommodates non-normally distributed data through adjusting standard errors with the Huber-White sandwich estimator. The non-independence of outcomes in offspring (i.e. offspring who share the same mother) was handled using the Mplus "cluster" command. Missing data were estimated using the well-established full information maximum likelihood method (138).

4.2.7 Hypothesis testing

As mentioned previously in Chapter 2.2.4.3, SEM allows for the simultaneous estimation of complex relationships between maternal diet, metabolic state, offspring sex and offspring microglial outcome measures. In this study, model estimation proceeded as follows. First, the influence of maternal WSD and adiposity on offspring microglial quantity in the amygdala. Specifically, offspring microglial count was regressed on maternal adiposity, maternal WSD, and

offspring sex (Example can be found in Figure 4.3 A). Additionally, maternal adiposity was regressed on WSD. Second, offspring microglia morphology was considered in the same manner microglial count was previously. Specifically, offspring microglial surface area to volume ratio was regressed on maternal adiposity, maternal WSD, and offspring sex (Example can be found in Figure 4.3 A). Fetal and 3-year-old offspring microglial measures were considered in separate models. The statistical significance of indirect effects was tested using the model indirect command.

4.3 Results

4.3.1 Offspring microglia quantity during prenatal development was associated with maternal adiposity while maternal diet appears to influence microglial quantity at a postnatal 3-year timepoint.

Results from the model used to test the influence of maternal diet, pre-pregnant adiposity, and offspring sex on fetal microglia quantity in the amygdala are presented in **Figure 4.3A.** Recent research has suggested that microglia may display sex dependent phenotypes in density, morphology, and transcriptomes during development and into adulthood (225-228), so offspring sex was included in each of the models for this study. It was found that maternal diet had no significant direct effect on microglial quantity in fetal offspring ($\beta_{\text{Diet} \rightarrow \text{offspring microglia counts}} = -0.417$, SE = 0.268, p=0.120) (**Figure 4.3A/B**), when accounting for the effects of maternal adiposity and offspring sex. However, there was evidence for a significant indirect effect of maternal WSD on microglia number via maternal WSD's effect on maternal adiposity ($\beta_{\text{indirect WSD} \rightarrow \text{pre-pregnant adiposity} \rightarrow \text{offspring microglia counts}} = -0.195$, SE = 0.068, p<0.01). Specifically, maternal WSD was associated with increased pre-pregnant adiposity ($\beta = 0.391$, SE = 0.081, p<0.01) compared to CTR animals, which in turn was associated with reduced microglial cell counts in the amygdala ($\beta = -0.499$, SE = 0.162, p<0.01) (**Figure 4.3C**). There was no effect of offspring sex detected in this model (**Figure 4.3D**).

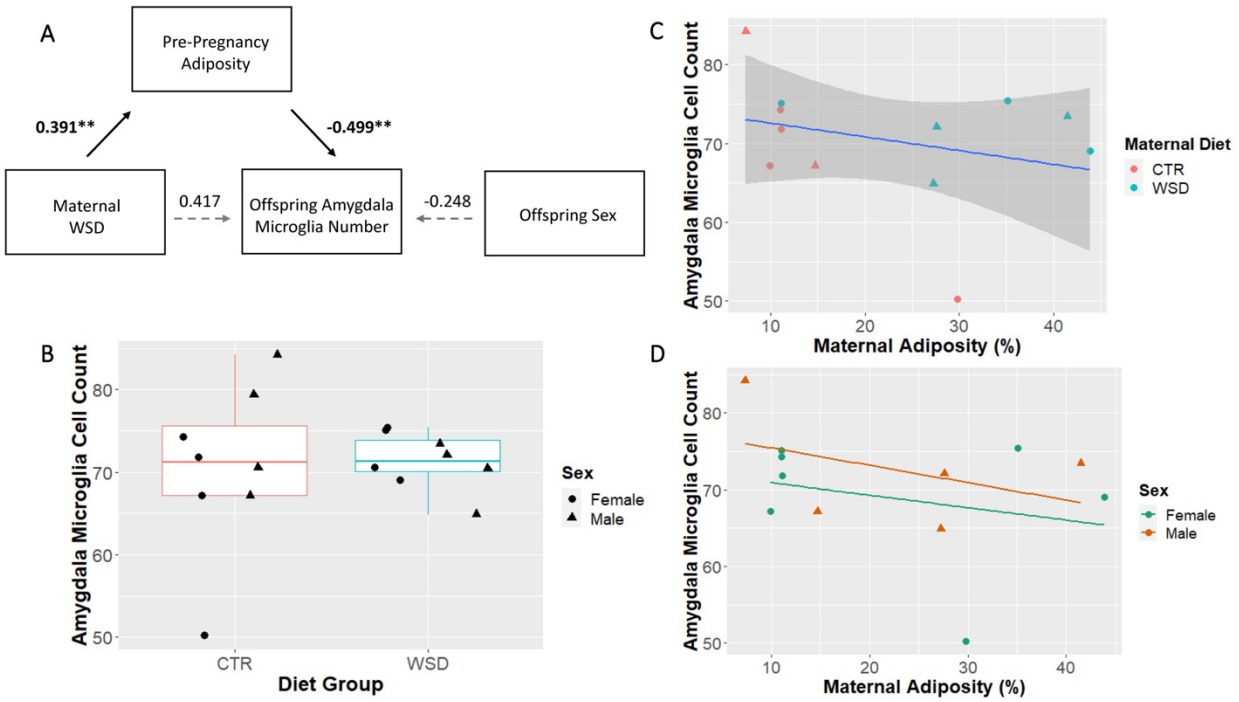

Figure 4.3. The relationship between maternal diet and adiposity with microglia counts in the prenatal amygdala. Maternal adiposity but not diet nor offspring sex significantly predict microglial quantity in the amygdala of fetal offspring. A) The path analysis model including maternal metabolic state measures and fetal offspring microglia counts appear to show a significant indirect mediated effect of maternal diet through maternal adiposity. Solid black lines indicate significant direct effects (* = $p<0.05$, ** = $p<0.01$). B) Box plots with boxes indicating 1st-3rd quartiles and the median expressed as a horizontal bold line. C) The relationship between maternal adiposity and microglial counts in the fetal amygdala. D) Visualization of the relationship of offspring sex with maternal adiposity and microglial number in the fetal amygdala.

To test if the effects of maternal diet and adiposity resulted in long-term impacts on offspring microglial quantity, models similar to fetal models described above were run in 3-year-old, adolescent animals. Results from the model used to test the relationship between maternal WSD, pre-pregnant adiposity, and offspring sex on microglia quantity in 36-month-old animals are reported in **Figure 4.4A**. Here, it was found that maternal WSD had a direct effect on offspring microglial quantity in the amygdala, with maternal WSD animals having significantly more microglia than control animals ($\beta_{\text{Diet} \rightarrow \text{offspring microglia counts}} = 0.509$, SE = 0.187, $p<0.01$) (**Figure 4.4A/B**). This effect remained when controlling for the effect of maternal adiposity and offspring sex. At this timepoint, we did not detect any indirect effect of maternal WSD on offspring microglia through maternal adiposity ($\beta_{\text{indirect WSD} \rightarrow \text{pre-pregnant adiposity} \rightarrow \text{offspring microglia counts}}$

= -0.039, SE = 0.072, p=0.589) (**Figure 4.4A/C**). Similar to the fetal timepoint, a sex effect was not detected in microglial quantity in the amygdala of 36-month animals ($\beta_{\text{Sex} \rightarrow \text{offspring microglia counts}}$ = 0.173, SE = 0.210, p=0.431).

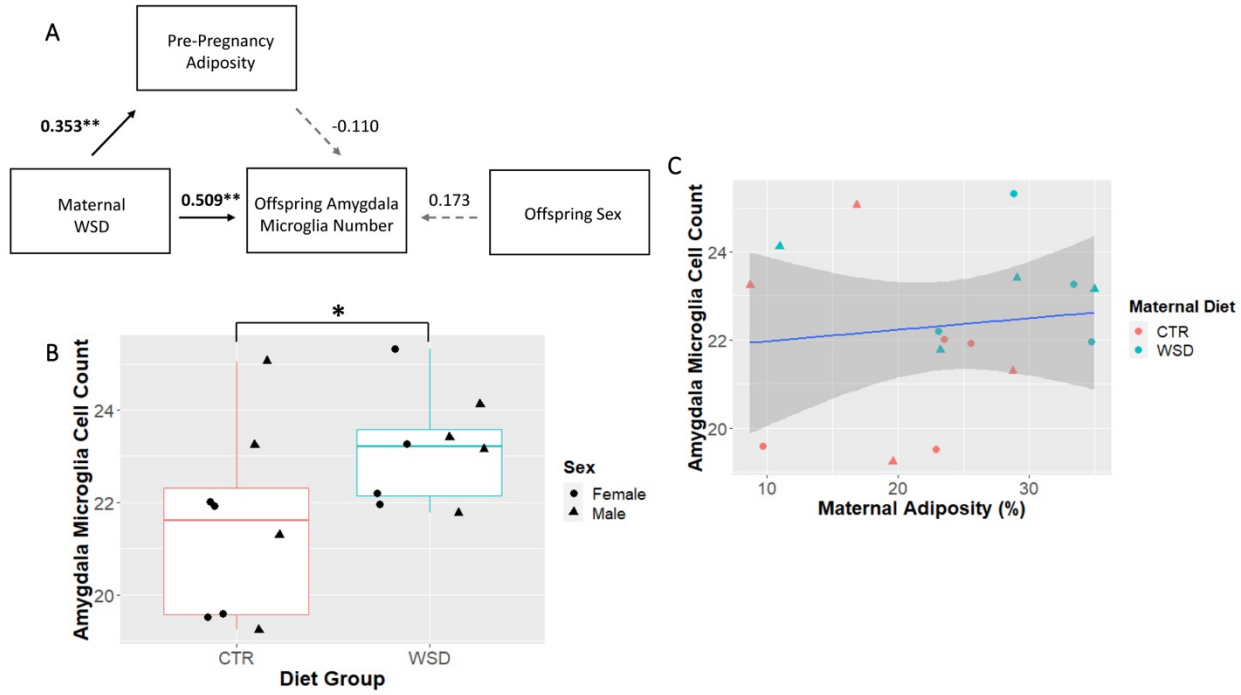

Figure 4.4. The relationship between maternal diet and adiposity with microglia counts in the amygdala of 3-year-old offspring. A) The path analysis model including maternal metabolic state measures appeared to show a significant direct effect of maternal diet on microglia counts in 3-year-old offspring. Solid black lines indicate significant direct effects (* = p<0.05, ** = p<0.01). B) Box plots with boxes indicating 1st-3rd quartiles and the median expressed as a horizontal bold line. C) The relationship between maternal adiposity and microglial number in the amygdala of 3-year-old offspring.

4.3.2 Offspring microglia morphology during prenatal development was associated with maternal adiposity and offspring sex while no difference was seen in the postnatal 3-year timepoint.

In addition to microglial quantity, other aspects of the microglial phenotype, such as morphology, are important to understand the functional state of the cell type. To examine microglial morphology in this study we utilized the ratio of surface area to volume of microglial cells. A higher surface area to volume ratio would suggest a more ramified cell morphology

while a lower ratio would be indicative of a more amoeboid-like morphology. The results from the model used to test the influence maternal diet, adiposity prior to pregnancy, and offspring sex on microglial morphology at a fetal timepoint are reported in **Figure 4.5**. It was found that maternal adiposity had a significant effect on microglial morphology with increased levels of pre-pregnant adiposity being associated with a higher microglial surface area to volume ratio in the fetal offspring amygdala ($\beta_{\text{pre-pregnant adiposity} \rightarrow \text{offspring microglia morphology}} = 0.454$, SE = 0.232, p=0.05) (**Figure 4.5A/C**). Additionally, a significant effect of offspring sex was detected in this model, with male offspring displaying more ameboid microglia compared to female offspring ($\beta_{\text{Sex} \rightarrow \text{offspring microglia morphology}} = 0.411$, SE = 0.184, p<0.05) (**Figure 4.5A/D**).

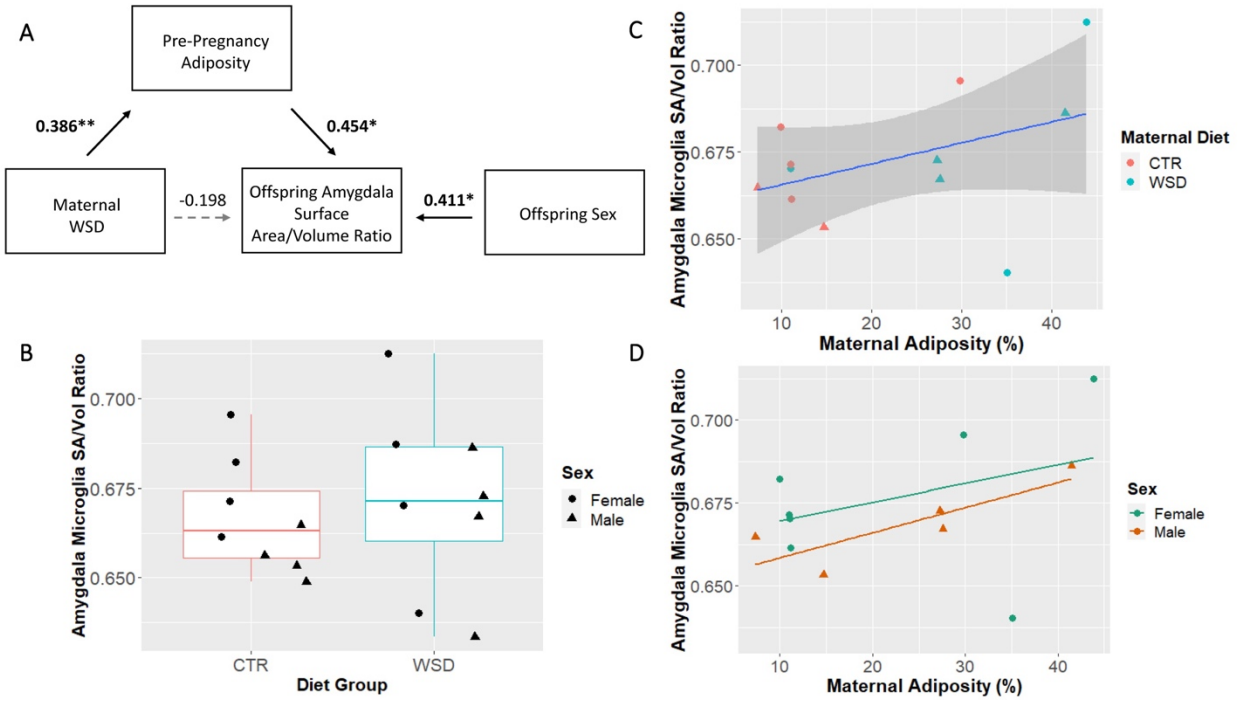

Figure 4.5. The relationship between maternal diet and adiposity with microglia morphology in the prenatal amygdala. A) A path analysis model including maternal metabolic state measures and fetal offspring microglia morphology appeared to show a significant indirect mediated effect of maternal diet through maternal adiposity. Solid black lines indicate significant direct effects (* = p<0.05, ** = p<0.01). B) Box plots with boxes indicating 1st-3rd quartiles and the median expressed as a horizontal bold line. C) Relationship between maternal adiposity and microglial morphology in the fetal amygdala. D) Visualization of the relationship of offspring sex with maternal adiposity and microglial morphology in the fetal amygdala.

To examine if the influences of maternal diet and metabolic state on offspring microglia morphology during gestation persist into adolescence, we examined similar surface area to volume measure in 3-year-old animals. The results from the model used to test the influence of maternal diet, adiposity, and offspring sex on microglial morphology in 3-year-old animals are reported in **Figure 4.6**. It was found that microglia morphology was not significantly influenced by any of the variables tested **Figure 4.6A**. The effect of maternal adiposity on offspring microglia morphology displayed a slight trend indicating more maternal adiposity was associated with a lower surface area to volume ratio ($\beta_{\text{pre-pregnant adiposity} \rightarrow \text{offspring microglia counts}} = -0.533$, SE = 0.295, p=0.061), however this result was not statistically significant (**Figure 4.6A/C**).

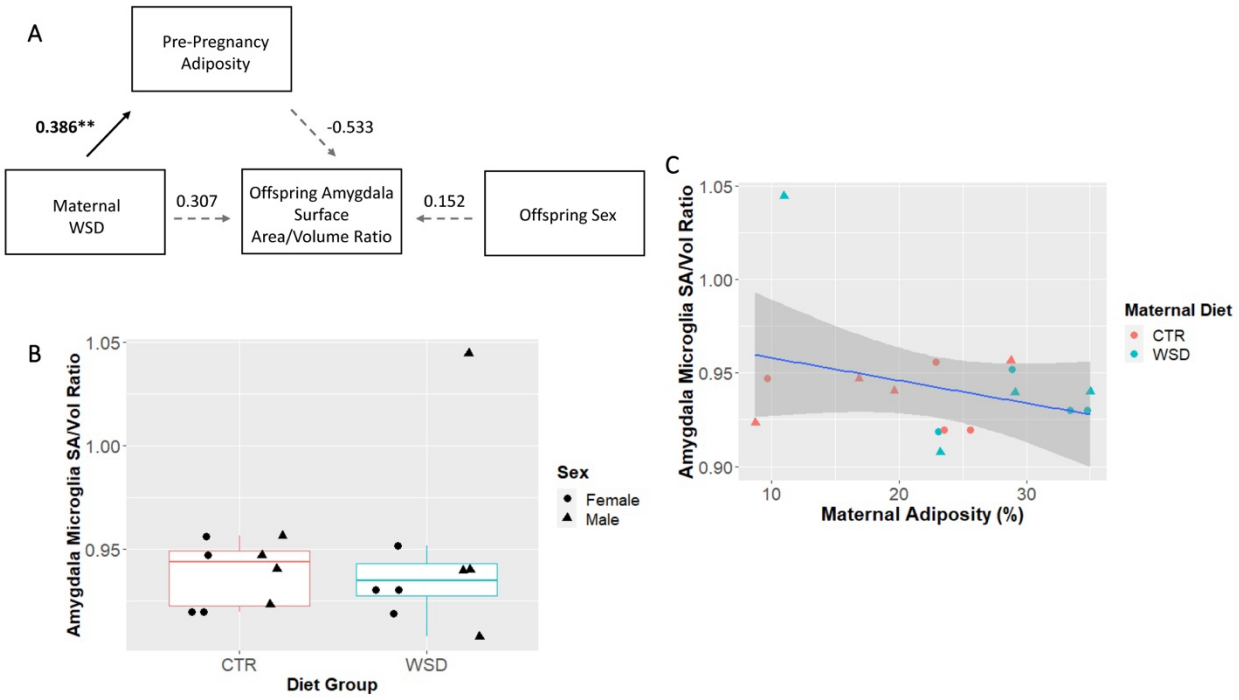

Figure 4.6. The relationship between maternal diet and adiposity with microglia morphology in the amygdala of 3-year-old animals. A) A path analysis model including maternal metabolic state measures appear to show a significant direct effect of maternal diet on microglia morphology and no association with any predictor variables. Solid black lines indicate significant direct effects (* = $p<0.05$, ** = $p<0.01$). B) Box plots with boxes indicating 1st-3rd quartiles and the median expressed as a horizontal bold line. C) The relationship between maternal adiposity and microglial morphology in the 3-year-old amygdala. D) Visualization of the relationship of offspring sex with maternal adiposity and microglial morphology in the 3-year-old amygdala.

In summary, these results suggest that during prenatal development offspring microglial quantity is reduced while their morphology is more ramified in the amygdala because of increased levels of maternal adiposity. However, postnatally, maternal WSD exposure resulted in increased quantity of microglial in 3-year-old offspring compared to controls while no influence of maternal diet nor adiposity was observed in microglia morphology (Table 4.1).

4.4 Discussion

Maternal consumption of a WSD has been associated with neurobehavioral deficits in offspring. Previously work from our lab has connected increases in maternal circulating inflammatory factors with increases in aberrant anxiety-like behavior in offspring. These findings suggest maternal nutrition and metabolic state may be working through an inflammatory mechanism. However, the precise mechanisms by which maternal metabolic state influences the developing offspring brain and behavior have yet to be fully understood. In this study, we aimed to expand our understanding of how the fetal neuroimmune system may be impacted by maternal diet and metabolic state during gestation and if these effects persisted into adolescence. We predicted that offspring from maternal WSD animals would display increased number of microglia with more ameboid morphology, suggestive of an "activated" state, compared to controls. Additionally, we predicted this effect would be mediated through increases in maternal adiposity, which has been associated with alterations in circulating inflammatory factors.

While no direct diet effects were observed, we found that higher levels of maternal adiposity were associated with reduced number and more ramified microglia in the amygdala of fetal WSD animals when compared to controls. Further, we detected that male offspring were particularly impacted by maternal adiposity levels, displaying more ramified morphology compared to females. These findings are counter to what we predicted to observe since microglia have been shown to proliferate and transition into a more ameboid morphology in response to inflammatory signals (229). Maintaining a reduced quantity and more ramified morphology of microglia may be indicative of reduced microglia function. While a puzzling result, our findings do find some support in the research examining functional outcomes after manipulation of microglial functions during development. Research here has found that microglial function is a key component in neurotypical brain development (54, 230), and that under active microglial function is associated with increased repetitive behaviors as well as impaired social behavior (55, 231). Other work has shown that depletion of microglia during gestation is associated with many

deficits in brain development including improper positioning of interneurons in the cortical plate and defective shaping of important axonal tracts (232).

Interestingly when we looked at persistent effects on microglial quantity and morphology in 3-year-old offspring we found that maternal diet was strongly associated with increased number of microglia in the amygdala. However, we did not detect any differences in morphology when compared to controls. Additionally, levels of maternal adiposity did not appear to influence microglial outcomes at this older timepoint.

The specific effects of maternal diet and adiposity appear to be important based on the timepoint observed. It appears that maternal adiposity is more influential during gestational development, while the specific effects of WSD are observed to persist through to older timepoints in development. While not fully understood, this may suggest that the early postnatal period is a highly critical window for eliciting long-term persistent effects on offspring microglia in the amygdala. Research suggests that the early postnatal time period is when microglia perform a majority of their synaptic pruning functions (233) and that reduced microglial function is sufficient to induce significant neuronal cell death in the cortex (234). One important aspect that may influence brain development is nutrition received through lactation. Evidence from our group has shown that breast milk from WSD dams contained lower levels of the essential polyunsaturated fatty acids eicosapentaenoic acid (EPA) and docosahexaenoic acid (DHA) as well as lower levels of total protein than CTR dams (170). These fatty acids have been shown to influence microglial functioning, with reduced levels of EPA and DHA being associated with increased phagocytosis of synapses by microglia (76). In addition to breast milk, maternal behavior and care of the newborn is critical for proper neurodevelopment. Evidence shows reduced quality of maternal care of newborn mice is associated with increased anxiety-like behaviors and reduced social interactions with peers (235).

One key aspect that would extend this study and provide a more comprehensive understanding of the function of microglial cells in these WSD fetal offspring is gene transcription data. A growing body of research is emerging that suggests proliferation rates and morphology of microglia does not provide the full picture of function in the cells. In fact, gene transcription and proteins that are released in response to stimuli are necessary to classify microglia functional states (236).

In summary, this study provides support for a neuroinflammatory mechanism underlying the effect of maternal diet and adiposity on offspring neural and behavioral outcomes. The consequence of these alterations in microglia during fetal and postnatal development on neural architecture remains to be fully elucidated. The serotonin system appears to be a particularly susceptible circuitry that is known to be involved in anxiety and social behaviors our laboratory has described previously. Microglial alterations may influence the development of this important regulatory neurotransmitter system that would result in behavioral abnormalities in offspring.

Table 4.1. Summary Table of Results from Microglia in Fetal and 3yo Animals

Timepoint	Microglia			
	Count		Morphology	
	Diet	Adiposity	Diet	Adiposity
Fetal	-	↓	-	↑*
3yo	↑	-	-	-

Note: CTR control Diet; WSD Western-style Diet. *Indicates a sex effect. – indicates no significant differences.

V. INCREASED ADIPOSITY DUE TO MATERNAL WESTERN-STYLE DIET CONSUMPTION SHAPES SEROTONIN INNERVATION OF THE AMGYDALA AND ANXIETY BEHAVIOR IN ADOLESCENT NONHUMAN PRIMATE OFFSPRING

5.1 Introduction

Maternal obesity and consumption of a Western-style diet (WSD) has been extensively shown, in both humans and animal models, to be associated with behavioral deficits in offspring. In humans, children born to people classified as obese display a higher risk of developing neuropsychiatric disorders. This increased risk in humans is supported by evidence in animal models, where offspring of mothers consuming a WSD or high-fat diet or display similar behavioral deficits including increased risk for anxiety-like behaviors, disruptive, high-energy outbursts, and even reduced social initiation between peers (25, 26, 94, 95, 237). While these behaviors involve many different brain regions (238, 239), the amygdala is a key structure in this network. Lesion studies that result in ablation of amygdala function in humans, nonhuman primates, and rodents demonstrate an inability to detect fearful stimuli, less anxiety-like behaviors (240) as well as more affiliative contact with peers (241, 242). Moreover, when the amygdala is electrically stimulated in humans, subjects describe more feelings of fear and anxiety (240). These results suggest the amygdala functions as a protective "break" on interaction with objects, peers, or other possibly threatening stimuli in the environment (120). Attempting to study the precise role the amygdala plays in complex social and emotional behaviors displayed by humans requires employing animal models that approach this level of behavioral sophistication. Since they live in highly organized and stable social groups, non-human primates are uniquely situated as an ideal animal model to allow study of the mechanistic role the amygdala may play in social behavior and psychopathologies such as anxiety (120).

In addition to the amygdala, anxiety-like behaviors have been associated with the dysregulation of the central serotonin system. One of the most common and effective treatments for people suffering from anxiety disorders is prescription of selective serotonin reuptake inhibitors (SSRIs) (243, 244). The precise relationship between levels of central serotonin and anxiety remains a highly debated field of study. Evidence for both increased and decreased innervation of serotonin axons in the forebrain have been connected to anxiety in animal models

(245). Importantly, the primate amygdala is typically heavily innervated by serotonergic projections originating from the dorsal raphe (99). Studies focusing specifically on the serotonergic system within the amygdala provide evidence for an association between dysregulation of this neurotransmitter system in the amygdala and anxiety/fear. For example, Studies in both humans and non-human primates with genetic variations in the serotonin transporter gene (SLC6A4), which result in reduced expression of the serotonin transporter (5HTT), demonstrated increased fear and anxiety behaviors as well as greater amygdala neuronal activity (246-248).

Finally, there is evidence suggesting the central serotonin system is vulnerable to maternal insults during gestational development. In a rodent model of maternal infection, offspring serotonergic neurodevelopment was disrupted. This resulted in reduced axonal outgrowth and innervation of serotonin neurons to forebrain regions such as the prefrontal cortex (92, 94). These effects were suggested to work through an inflammatory mechanism disrupting placental output of serotonin. Previous work by our group has consistently demonstrated a connection between maternal western-style diet, adiposity, and inflammation, and neurobehavioral dysregulation in offspring (26, 95, 105, 109, 112). Specially, in work performed previously by our group, it was found that animals born to mothers consuming a WSD displayed increased rates of anxiety-like behavior. Further, this previous work also detected a sex effect with females displaying increased anxiety at younger timepoints with males also displaying increased anxiety by 11-months of age (94, 95). Additionally, our group has demonstrated that the central serotonergic system is perturbed in the raphe nuclei at fetal and 13-month timepoints. At both timepoints, maternal consumption of a WSD appeared to result in a reduction in both TPH2 mRNA and TPH2+ cells, which are the main serotonin producing cells of the central nervous system (94, 95, 106). The purpose of this study is to determine if perturbations to the serotonergic system due to maternal diet and metabolic state are observed in the forebrain structures, such as the amygdala, which is known to be associated with anxiety behaviors. Further, we sought to determine if these perturbations occurred prenatally and persisted to adolescence. We hypothesized that maternal Western-style diet's effect on adiposity will increase offspring anxiety-like behaviors through a reduction in serotonin innervation in the amygdala. Further, we hypothesize that this reduction in amygdala serotonin occurs during prenatal development and is driven by an increased maternal inflammatory environment.

5.2 Methods

5.2.1 Animals

All animal procedures were in accordance with National Institutes of Health guidelines on the ethical use of animals and were approved by the Oregon National Primate Research Center (ONPRC) Institutional Animal Care and Use Committee. The present study utilized an established preclinical NHP model (M*acaca fuscata*) of maternal overnutrition which has been previously described in Chapter 4 of this dissertation (Table 5.1).

5.2.2 Measurement of Maternal Adiposity

Prepregnant maternal adiposity measures were collected as previously described in Chapter 4.2.2.

5.2.3 Offspring Behavior Assessment

Assessment of anxiety behaviors in 11-month-old animals has been previously described in detail (26, 94) and was adapted slightly to 34-month-old animals. Briefly, 34-month-old juveniles were transferred from their social groups to the behavioral testing suite where they were then placed in a testing cage and the transporter left the room. All tests occurred between 0900 and 1200 and were videotaped through a one-way mirror.

The assessment started with a 10-minute acclimation period followed by a 2-minute control period, where the animal was alone in the behavior suite. Following acclimation, an unfamiliar human female entered for three separate epochs interluded by 2-minute control periods, presenting potentially threatening social stimuli. The first 2-minute epochs involved the human intruder presenting a facial profile, the second, prolonged eye contact, and finally prolonged eye contact with an offer of an apple slice (a familiar food). After the human intruder test, the animal underwent a novel object test including two segments with different unfamiliar objects placed in front of the testing cage and left for the animal to freely interact with. The first segment included presenting a potentially threating, toy bobble head that had large eyes facing the animal for 5 minutes. After 5 minutes the toy was replaced with a knot rope toy hanging from the cage for 2 minutes. Finally, the rope toy was removed and a seaweed food snack was placed in the tray in front of the cage for 2 more minutes. After the novel object test the assessment ended, and the animal was returned to their social group. Only behavior data from collected

during the human intruder test and while the bobble head toy was present was used in analysis. Using video recordings of the behavior assessment, behaviors were scored using continuous sampling methods with The Observer CT, Version 12 (Noldus Information Technology, Leesburg, VA, USA) by experiments blinded to diet group and sex of the animal. Due to many behaviors displaying infrequent expression throughout the testing period, behaviors were categorized into related groups, combined using the summed z-score to create four distinct behavior composites as well as an overall total anxiety behavior composite (26).

Table 5.1. Animal Numbers for Adolescent Procedures

Offspring Measures	N (per diet group)	N (per sex)
Immunohistochemistry	16 (CTR = 8, WSD = 8)	F = 8, M = 8
34-month Behavior measures	51 (CTR = 24, WSD = 27)	F = 26, M = 25

Note: CTR control Diet; WSD Western-style Diet.

5.2.4 Tissue Collection and Immunohistochemistry Methodology

Tissue collection and IHC methods followed the exact same procedures as described in Chapter 4.2.3. The only difference that occurred in this study was sections were transferred to a primary antibody solution (2% NDS in KPBS) containing 1:500 rat anti-5-HT (Novus Biologicals Cat# NB100-65037).

5.2.5 Image Acquisition

All images in both fetal and 3-year-old animals were collected as previously described in Chapter 4.2.4.

5.2.6 Image Analysis

Morphological analysis was performed on 3D images using Imaris 10.0 software (Bitplane, Zurich, Switzerland). All images were processed and analyzed by an experimenter blinded to animal diet and sex.

5.2.7 Data analysis/Statistics

Data were analyzed using a structural equation modeling (SEM) framework (134) using *Mplus* 7.4 (135), in the same methodology described in Chapter 4.2.6.

5.2.8 Hypothesis testing

Similar to Chapter 4.2.6, SEM was utilized for the simultaneous estimation of the relationship between maternal diet, metabolic state, offspring sex and offspring serotonin or behaviors measures. In this study, model estimation proceeded as follows. First, the influence of maternal WSD and adiposity on offspring serotonin innervation in the amygdala. Specifically, offspring serotonin was regressed on maternal adiposity, maternal WSD and offspring sex (Example can be found in **Figure 5.1**). Additionally, maternal adiposity was regressed on WSD. Fetal and 3-year-old offspring serotonin innervation levels were considered in separate models. The statistical significance of indirect effects was tested using the *model indirect* command. Second, in a similar model scheme just described, offspring anxiety behavior in 3-year-old animals was included in the model in place of the 5-HT innervation outcome measure.

Lastly, in 3-year-old offspring, serotonin innervation level in the amygdala was added as a serial mediator of the effect of WSD and adiposity on offspring anxiety behaviors. Specifically, offspring anxiety behavior was regressed on offspring 5-HT innervation in the amygdala, which was in turn regressed on maternal WSD and adiposity.

5.3 Results

5.3.1 Reduced serotonin innervation of the amygdala was associated with maternal adiposity in 3-year-old animals but not during prenatal development.

Results from the model to test the influence of maternal diet, adiposity, and offspring sex on fetal offspring serotonin (5-HT) innervation in the amygdala are presented in **Figure 5.1.** Results from this model suggested that there is no effect of any maternal predictor variable on offspring 5-HT innervation of the amygdala at the fetal timepoint. We did not detect a significant

direct effect of maternal diet on offspring 5-HT ($\beta_{Diet \rightarrow offspring\ serotonin} = 0.127$, SE = 0.242, p=0.120) (**Figure 5.1A/B**). Additionally, neither maternal adiposity ($\beta_{Adiposity \rightarrow offspring\ serotonin} = 0.05$, SE = 0.266, p=0.850) nor offspring sex ($\beta_{Sex \rightarrow offspring\ microglia\ counts} = 0.181$, SE = 0.242, p=0.455) were detected to have a significant influence on fetal 5-HT innervation in the amygdala (**Figure 5.1A/C**).

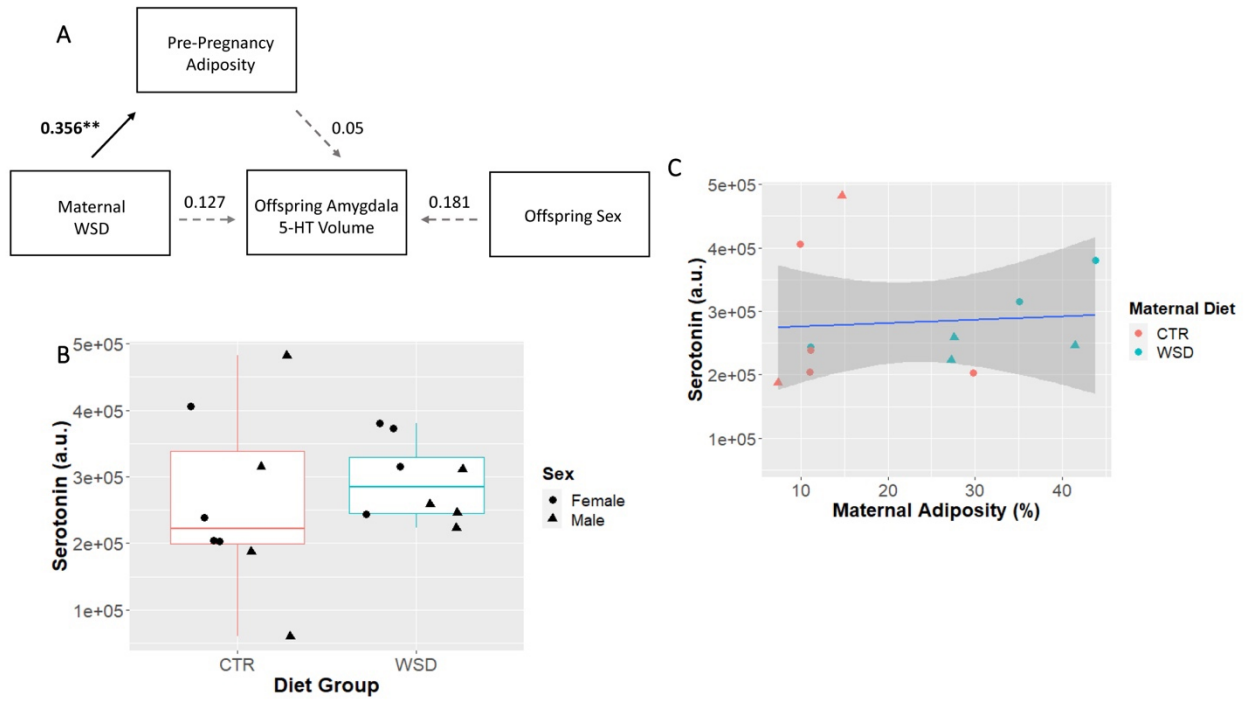

Figure 5.1. Maternal diet and adiposity did not significantly predict 5-HT innervation in the amygdala of fetal offspring. A) The path analysis model including maternal metabolic state measures and fetal offspring 5-HT innervation levels appeared to show no association with any predictor variables. Solid black lines indicate significant direct effects (* = p<0.05, ** = p<0.01). B) Box plots with boxes indicate 1st-3rd quartiles and the median expressed as a horizontal bold line. C) Relationship between maternal adiposity and Serotonin in the fetal amygdala.

There is substantial evidence of considerable postnatal development of both the central serotonin system and the amygdala are vulnerable to early life stressors (31, 92, 249). These findings led us to examine the effect of maternal diet and metabolic state on long term outcomes in the serotonin system's development in the offspring amygdala. The results of the model testing this relationship measured in 3-year-old animals are reported in **Figure 5.2**. It was found that there was no significant direct effect of maternal WSD on serotonin innervation at 3-years ($\beta_{Diet \rightarrow Offspring\ Serotonin} = 0.153$, SE = 0.211, p=0.470) (**Figure 5.2A/B)**. However, maternal

adiposity appeared to have a significant direct effect when controlling for maternal diet and offspring sex ($\beta_{Adiposity \rightarrow Offspring\ Serotonin} = -0.482$, SE = 0.239, $p<0.05$) (**Figure 5.2 A/C**). Additionally, a significant sex effect was detected suggesting male offspring were significantly more impacted than their female counterparts and drive the overall reduction in 5-HT observed previously ($\beta_{Sex \rightarrow Offspring\ Serotonin} = -0.402$, SE = 0.190, $p<0.05$) (**Figure 5.2 A/D**).

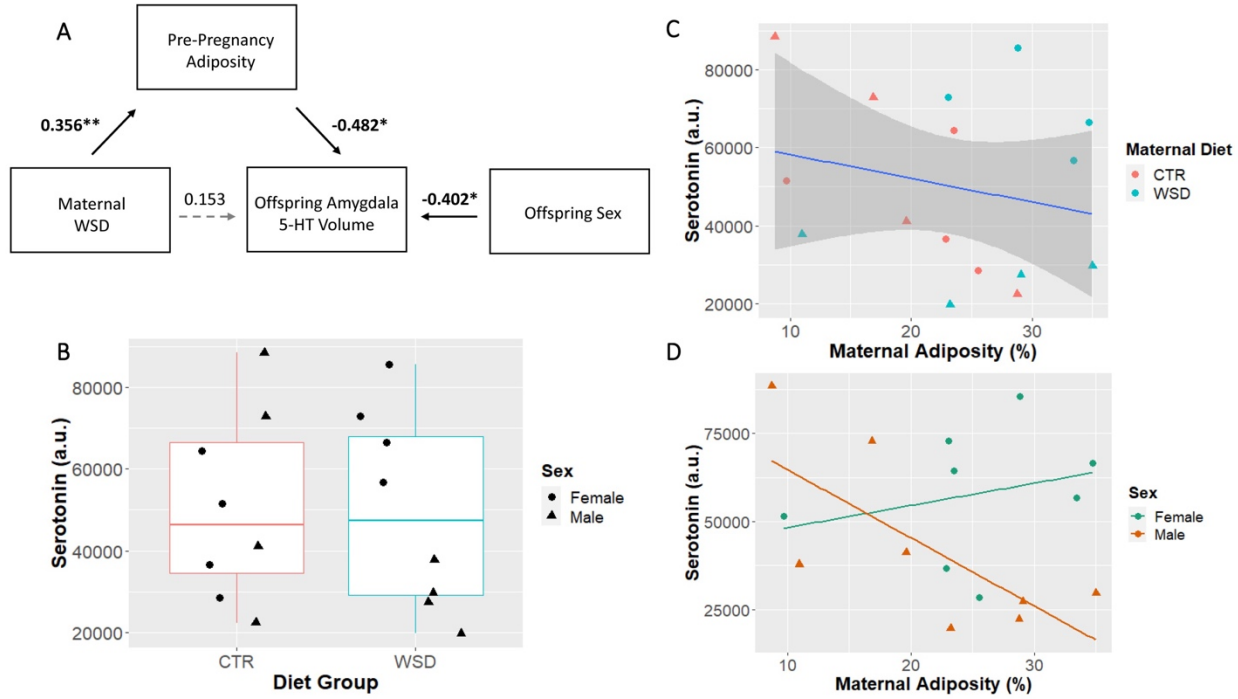

Figure 5.2. Maternal adiposity and offspring sex but not maternal diet significantly predicted 5-HT innervation in the amygdala of 3-year-old offspring. A) The path analysis model including maternal metabolic state measures appeared to show a significant indirect mediated effect of maternal diet through adiposity on 5-HT innervation levels in 3-year-old offspring. Solid black lines indicate significant direct effects (* = $p<0.05$, ** = $p<0.01$). B) Box plots with boxes indicating 1st-3rd quartiles and the median expressed as a horizontal bold line. C) Relationship between maternal adiposity and Serotonin in the 3-year-old amygdala. D) Visualization of the relationship of offspring sex with maternal adiposity and serotonin in the 3-year-old amygdala.

5.3.1 Increases in maternal adiposity was associated with increases in anxiety-like behaviors in 3-year-old animals, which appeared to be associated with the observed reduction in serotonin in the amygdala.

Previous work by our group demonstrated that maternal WSD is associated with an increased anxiety-like behaviors in infant and juvenile offspring (26, 94, 95). Additionally, this previous work suggested that offspring sex may influence the risk for increased anxiety behavior with females displaying increased anxiety at earlier ages (95). These findings led us to test if these behavioral perturbations persisted at an older age. Offspring anxiety behavior was increased as a result of maternal adiposity. Results from the model examining the influence of maternal diet, adiposity, and offspring sex on 3-year-old offspring anxiety behaviors are presented in **Figure 5.3.** It was found that there was no significant direct effect of maternal WSD

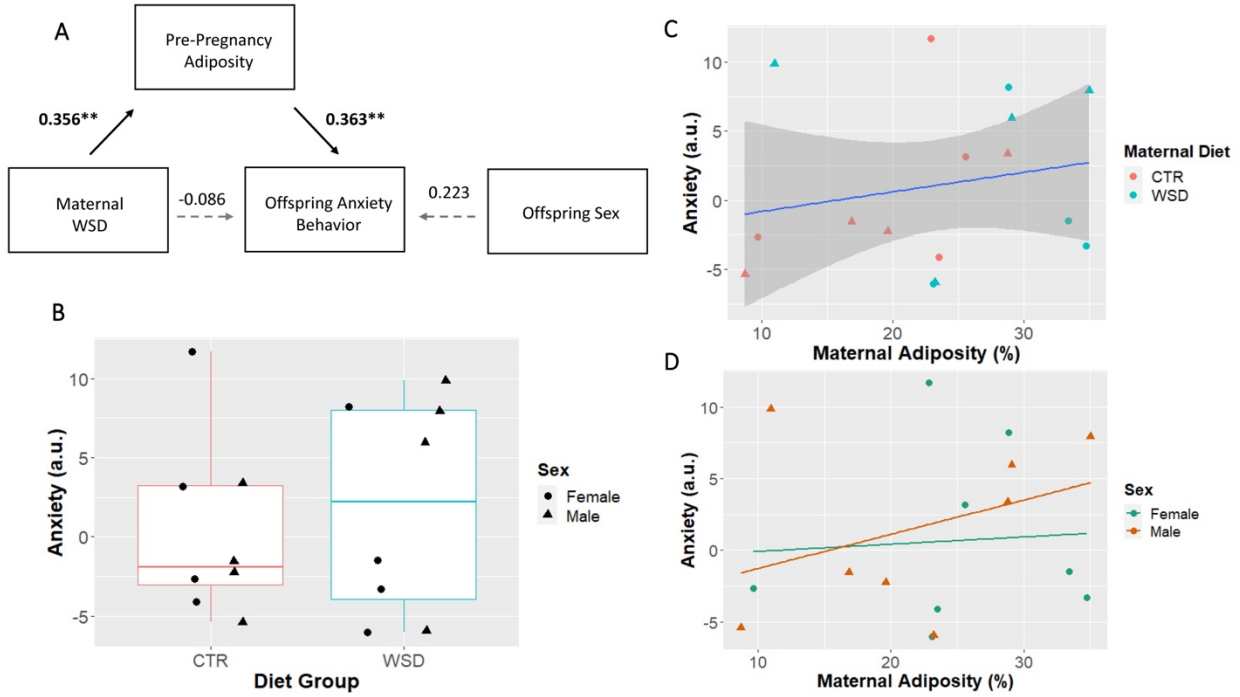

Figure 5.3. Maternal adiposity but not diet nor offspring sex significantly predicted anxiety-like behaviors in 3-year-old offspring. A) The path analysis model including maternal metabolic state measures and offspring anxiety behaviors appeared to show a significant indirect mediated effect of maternal diet through adiposity on anxiety-like behaviors in 3-year-old offspring. Solid black lines indicate significant direct effects (* = $p<0.05$, ** = $p<0.01$). B) Box plots with boxes indicating 1st-3rd quartiles and the median expressed as a horizontal bold line. C) The relationship between maternal adiposity and serotonin in the amygdala of 3-year-oldoffspring. D) Visualization of the relationship of offspring sex with maternal adiposity and serotonin in the 3-year-old amygdala.

on anxiety-like behaviors ($\beta_{\text{Diet} \rightarrow \text{Offspring Anxiety}}$ = -0.086, SE = 0.120, p=0.473) (**Figure 5.3A/B)**. However, maternal adiposity appeared to have a significant direct effect when maternal diet and offspring sex were controlled for ($\beta_{\text{Adiposity} \rightarrow \text{Offspring Serotonin}}$ = 0.363, SE = 0.135, p<0.01), where increased levels of maternal adiposity was associated with increased anxiety-like behaviors in offspring (**Figure 5.3 A/C**). In this model no significant effect of offspring sex on anxiety-like behaviors was detected ($\beta_{\text{Sex} \rightarrow \text{offspring microglia counts}}$ = 0.223, SE = 0.123, p=0.07) (**Figure 5.3 A/D**).

Serotonin, and specifically serotonin innervation within the amygdala, is known to be related anxiety-like behavior (246, 248). This led us to examine if the reduction in amygdala 5-HT we detected in 3-year-old animals mediated the increase in anxiety-like behaviors we observed. The results from the model testing this relationship are described in **Figure 5.4**. In this full serial mediation model, we detect a significant direct effect of offspring anxiety behavior on offspring amygdala 5-HT innervation ($\beta_{\text{Offspring Serotonin} \rightarrow \text{Offspring Anxiety}}$ = -0.486, SE = 0.129, p<0.01), where increases in serotonergic innervation of the amygdala was associated with reduce anxiety-like behaviors in 3-year-old offspring (**Figure 5.4A/B**). Consistent with the findings reported above, it was found that there was no significant direct effect of maternal WSD on anxiety-like behaviors ($\beta_{\text{Diet} \rightarrow \text{Offspring Anxiety}}$ = 0.044, SE = 0.133, p=0.741) or 5-HT innervation in the amygdala ($\beta_{\text{Diet} \rightarrow \text{Offspring Serotonin}}$ = 0.222, SE = 0.186, p=0.232). Similarly, this path model suggested that maternal WSD acts through increasing maternal adiposity to reduce serotonergic innervation in the amygdala, which in turn was associated with increased anxiety-like behaviors in offspring (**Figure 5.4A**).

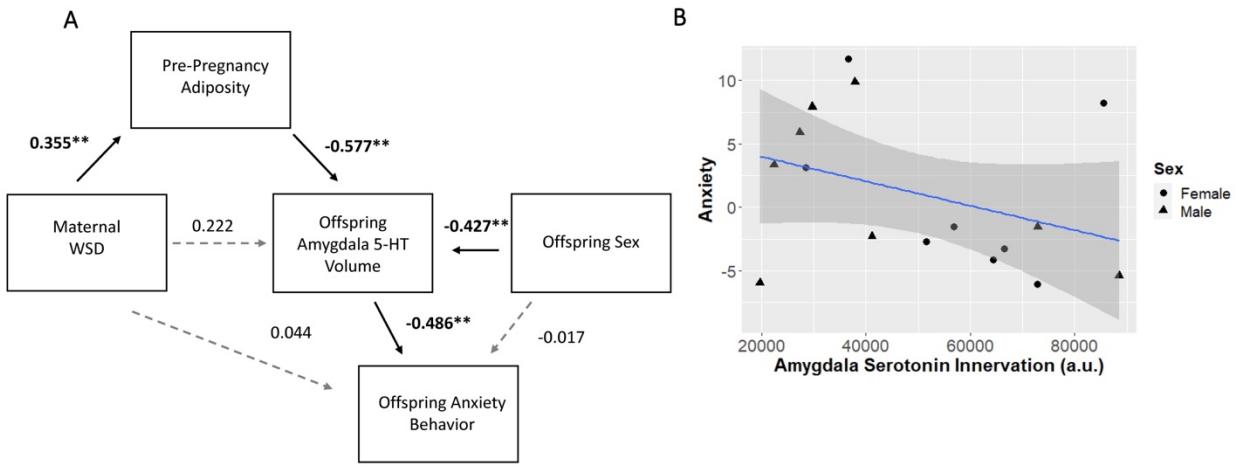

Figure 5.4. Maternal diet and metabolic state work influence offspring anxiety behavior outcomes by impacting 5-HT innervation of the offspring amygdala. A) The full path analysis model testing serial mediation of maternal metabolic state measures to offspring behavior indicated a significant serial mediation effect where the influence of maternal WSD on offspring behavior was mediated by maternal adiposity and offspring amygdala 5-HT innervation in 3-year-old offspring. Solid black lines indicate significant direct effects (* = $p<0.05$, ** = $p<0.01$). B) Visualization of the relationship between the level of 5-HT innervation in the 3-year-old offspring amygdala with offspring anxiety-like behaviors.

5.4 Discussion

Dysfunction of the serotonergic system is thought to play a central role in the underlying mechanisms associated with anxiety disorders (245). Further, the amygdala is a brain structure heavily innervated by serotonergic axons (99, 103, 182) and is well supported to be involved in emotional regulation of fear, anxiety, and social behaviors (97, 120, 240, 250). Previous work from our laboratory has demonstrated that maternal WSD and obesity are associated with perturbations to the central serotonergic system and increased anxiety behavior in non-human primates (94, 95, 106). However, the relationships between maternal nutrition, offspring anxiety behaviors, and serotonergic innervation of forebrain areas, such as the amygdala, have yet to be fully realized. In this study we provide evidence that maternal WSD reduces serotonergic axonal innervation of the offspring amygdala, which in turn is directly associated with increased anxiety-like behaviors.

We originally hypothesized that maternal WSD would impact central serotonin (5-HT) innervation of the amygdala during prenatal development, and that this would persist into postnatal life. Interestingly, when we examined 5-HT innervation in the fetal amygdala we did not detect any significant differences due to maternal WSD. This result is in partial contrast to previous work from our group in this model which detailed reduced TPH2 mRNA, the rate limiting enzyme in 5-HT synthesis, expression in the raphe nuclei of fetal animals (95). It is important to note that the raphe nuclei are the cluster of regions in the brain stem where serotonergic neuron cell bodies are located and they differentiate very early in gestation (87). From this region, axons of these neurons project and innervate almost every forebrain area. The axonal outgrowth of these 5-HT neurons continues throughout pre- and postnatal brain development. This could possibly explain why we did not detect an effect of maternal WSD on 5-HT innervation in the amygdala as the final innervation architecture may not have been fully established at the fetal timepoint.

However, in line with previous work from our group, the current study suggests that maternal WSD reduced serotonin innervation of the amygdala in 3-year old offspring (94). Specifically, we observed that maternal WSD's effect on 5-HT innervation of the amygdala was mediated by maternal adiposity such that maternal WSD increased maternal adiposity and increased maternal adiposity was associated with reduced 5-HT innervation. In addition, to what was discussed above regarding the developmental timing of axonal outgrowth in the fetal amygdala, this result may also be due to early postnatal effects experienced by the offspring. Early life adversity in children has been associated with nontypical serotonergic functionality later in life (251). As maternal consumption of WSD and obesity have been linked to lower quality maternal care (252), this may be an indirect contributing factor resulting in an overall reduction in 5-HT innervation in the amygdala at 3-years of age. Additionally, research examining how maternal nutrition impacts the nutrient composition of breast milk has indicated a reduced quantity in essential omega-3 fatty acids present in maternal WSD animals (170). Maternal omega-3 fatty acids have been shown to modulate microglial function during development resulting in long lasting behavioral deficits in offspring (76, 77).

Expanding on our groups previous behavioral findings we examined if increased anxiety behaviors due to maternal WSD persisted into adolescence. In the current study, we provide evidence in support of this hypothesis. We observed that the relationship between maternal WSD

and offspring anxiety behavior was mediated by maternal adiposity such that maternal WSD increased maternal adiposity which increased performance of anxiety-like behaviors by offspring. Further, in an attempt to directly connect offspring 5-HT innervation levels in the amygdala with offspring anxiety behavior we included both outcome measures in a full serial mediation model (**Figure 5.4A**). The results from this model suggests a direct effect of reduced 5-HT innervation in the amygdala to increased anxiety behaviors. As noted above the reduction in 5-HT innervation was mediated by increased maternal adiposity. These findings provide some of the clearest support of neuro-mechanisms underlying maternal WSD's association with increased aberrant behavior in offspring.

Some limitations to this study are that the measurement of 5-HT in the amygdala was obtained postmortem through immunohistochemistry. Serotonin can degrade relatively rapidly post-mortem, and this may introduce some confounding limitations in our interpretations. However, all animals and tissue were treated the same so most of the confounds should have been accounted for in the experimental design. Further, simply measuring the quantity of 5-HT innervation does not account for the functional signaling of this circuitry. Considerable research has demonstrated that the relative expression levels of either excitatory (5-HT2A) or inhibitory (5-HT1A) 5-HT receptors are associated with modulating behavioral phenotypes in the organism (240, 248). Additionally, the serotonergic system interacts with a highly intricate network of interneurons that are critical in overall functioning of the amygdala to produce appropriate or inappropriate responses to stimuli (240).

In summary, the current study provides support for reduced 5-HT innervation of the amygdala being a mechanism underlying the association between maternal WSD and increased anxiety behaviors in offspring (Table 5.2). Future research should expand on these findings through studies examining functional changes in the serotonergic system *in vivo*. Additionally, the amygdala maintains strong connections between many other brain regions commonly implicated in behavior abnormalities, such as the prefrontal cortex (253). These functional connections should be further explored as they may provide insight of the broader whole brain functionality and association with regulation of anxiety behaviors in offspring.

Table 5.2. Summary Table of Results from Fetal and 3yo Animals in Chapter 5

Timepoint	Serotonin		Behavior	
	Diet	Adiposity	Diet	Adiposity
Fetal	-	-	n/a	n/a
3yo	-	↓*	-	↑

Note: CTR control Diet; WSD Western-style Diet. *Indicates a sex effect. n/a indicates these measures were not measured. – indicates no significant differences.

VI. DISCUSSION

6.1 Effects of Maternal WSD and Obesity on Offspring Behavior

Epidemiological evidence has connected increased maternal BMI to increased risk of neurodevelopmental disorders including Attention Deficit Hyperactivity Disorder (ADHD) and Autism Spectrum Disorder (ASD) in children. These initial observations warranted research into mechanisms that underly these observed associations. The use of a non-human primate (NHP) model in this dissertation provides strong translatability of any effects observed due to maternal WSD and obesity to humans. Non-human primates demonstrate considerable similarities in physiology that are key in this dissertation. These similarities include pre and postnatal brain developmental timings, trajectories, and anatomical locations; although moderate differences in size and functional connectivity are observed (254). Many NHPs are share a similar prolonged developmental window from birth to adulthood (255). Additionally, NHPs typically live in complex social hierarchies, similar to humans, that require advanced social cognition and behavior to succeed and thrive (256). Importantly, many neurodevelopmental disorders in humans are characterized in part by deficits in typical social interactions of an individual. Further, NHPs display similar characteristics in the metabolic phenotypic progression in obesity, such as insulin resistance, dyslipidemia, and other cardiovascular comorbidities often observed in the metabolic syndrome in humans (257-259).

Previous work examining offspring behavioral outcomes in our NHP model of maternal WSD and obesity supported the findings from human epidemiologic studies. Offspring of maternal WSD animals displayed increased anxiety behaviors at 4 months and 1 year old (26, 94, 95). Here, we expanded on this work and found that increased anxiety behaviors persist to a 3-year-old adolescent age (Chapter 5) (Table 6.1). Importantly, at this adolescent timepoint, maternal WSD's influence on offspring behavior acted indirectly through increases in maternal adiposity levels (**Figure 6.1**).

6.2 The Serotonin System, and the Amygdala

Behaviors such as evaluating and responding to a threat or social interactions require precise and complex coordination across many different brain areas and circuitry pathways. To attempt to peel back the underlying mechanisms of the previously observed behavioral abnormalities in offspring, this dissertation focused on characterizing the impact of maternal WSD and adiposity on the amygdala and serotonergic system (Chapter 5). Both the amygdala and serotonergic system have been implicated as sites of perturbation underlying psychiatric and anxiety related disorders (95, 224, 243, 248, 260). Serotonin performs many key functions during proper neurodevelopment such as guiding neuronal migration, neural precursor proliferation and survival, as well as circuit formation (88). Considering the integral role that 5-HT plays during pre and postnatal neurodevelopment, perturbations to this system during gestation has the potential to elicit long lasting alterations in brain development and function. Further, while serotonin axonal projections are quite ubiquitous throughout the forebrain, the amygdala is particularly densely innervated by this neurotransmitter system (99). To our surprise, we found that maternal WSD and adiposity did not impact serotonergic innervation of the amygdala during a third trimester fetal timepoint. However, maternal WSD was indirectly associated with reductions in 5-HT postnatally at 3 years of age through increases in maternal adiposity levels (Table 6.1, Figure 6.1). This may suggest the early post-natal period is a window where the 5-HT development is particularly susceptible. Factors including nutritional composition of breast milk or quality of maternal care just after birth may elicit effects on the developing 5-HT system. Importantly, we also suggest that the reduction in 5-HT innervation in the amygdala is directly associated with increases in anxiety behaviors in these same animals.

To further characterize the impact of maternal WSD and adiposity on the central serotonergic system we sought to understand if the perturbation in the serotonergic system was region-specific or more global. Therefore, we examined TPH2+ cells in the raphe nuclei, the location of serotonergic neuron cell bodies (Chapter 3). Tryptophan hydroxylase 2 (TPH2) is the rate limiting enzyme involved in serotonin synthesis in the central nervous system and is often used as a biomarker for classifying serotonergic neuron identity. In these studies, we found that consumption of a WSD both pre and postweaning by offspring was necessary to observe a significant reduction in TPH2+ cell number in the raphe nuclei (**Figure 6.1**). Switching to a control diet after weaning appeared to “rescue” the reduction in serotonin producing cells in the raphe. This group did however, trend towards a reduction and this experiment may have been

underpowered to detect an effect in this group. Together these studies suggest maternal WSD and adiposity elicit alterations in the serotonergic system both peripherally and in the brainstem. Further these alterations appear to be associated with increases in anxiety-like behaviors in offspring.

6.3 Involvement of Inflammatory mechanisms resulting from maternal obesity

Alterations in the inflammatory environment during gestation are strongly connected to adverse neurodevelopmental outcomes in offspring (261). Additionally, an increased pro-inflammatory state in mothers has been shown to alter the offspring peripheral immune system (261). An altered inflammatory state has been proposed as a common mechanism underlying aberrant neurobehavioral outcomes in a number of models of maternal environmental stressors such as maternal infection, exposure to pollutants, or stress (218, 231). Consuming a WSD and increased levels of adiposity are associated with a characteristic chronic low-grade inflammatory state within the peripheral circulation (41). During pregnancy, this alteration to the inflammatory state is hypothesized to elicit adverse effects on the developing fetal brain and immune system (157). In fact, previous work by our group in our same model has connected maternal third trimester inflammatory state with alterations in offspring anxiety behavior (26). In the current studies we sought to characterize the influence of maternal WSD, adiposity, and inflammatory state, on offspring peripheral inflammatory states (Chapter 2). Here we suggest that offspring inflammatory markers were indirectly influenced by maternal metabolic state's effect on maternal inflammation. Specifically, maternal chemokines were reduced as a result of increases in adiposity and this reduction was associated with increases in offspring cytokines and decreases in offspring chemokines (**Figure 6.1**). These findings provide further support that the offspring peripheral immune system is perturbed indirectly by maternal WSD and adiposity. Research human studies of maternal obesity have suggested similar results with additional evidence for alterations in circulating immune cells of the offspring (262, 263). Interestingly, while we observed influences on basal levels of circulating immune factors, work by others have suggested offspring immune cells demonstrate a "primed" phenotype with dampened pro-inflammatory responses to immune challenges later in life (263).

Considering our findings from the 5-HT system in combination with the altered maternal and offspring peripheral immune system, the potential mechanism connecting these outcomes

remains unknown. It is possible the altered inflammatory state may influence placental serotonin output of 5-HT during gestation eventually leading to the postnatal effects observed (89, 90). In fact, in a rodent model of maternal immune activation placental, 5-HT production and bioavailability to the fetus was increased due to increased inflammation during gestation (92). Importantly, the increased 5-HT during prenatal development resulted in significant disruption in serotonergic axonal outgrowth in the forebrain of offspring. The protein indoleamine 2, 3-dioxygenase (IDO) is a key enzyme in the tryptophan metabolic pathway which converts tryptophan into kynurenine instead of serotonin. Activity of IDO has been shown to be modulated by inflammatory factors (91). Therefore, the characteristic low-grade inflammatory state associated with maternal WSD and obesity may be modulating the tryptophan metabolic pathway to deliver altered amounts of 5-HT to the developing fetus throughout prenatal development and lead to suppression in 5-HT axonal outgrowth in the offspring forebrain.

6.4 Microglia are impacted across different developmental timepoints by maternal diet and adiposity.

Microglia are the main immunocompetent cell of the central nervous system. They are able to detect and respond to inflammatory signals present in the parenchyma. During development they are highly involved in proper neurodevelopment, performing functions including synaptic pruning (54), phagocytosis of neural progenitor cells (50), and refining network connectivity (122). Microglial have been implicated as a common underlying mechanism of aberrant neurobehavioral development in models of maternal immune activation (226). Here, we sought to characterize the influence of maternal WSD and adiposity on microglia during pre and postnatal development (**Chapters 2 & 4**). As mentioned earlier, examination of microglia was focused in the amygdala region due to its relationship with 5-HT and anxiety behaviors. These studies add to the field by reporting that microglial quantity appear to be reduced and display more ramified morphology during gestation as a result of increased levels of maternal adiposity. However, postnatally, at 1 and 3-years-old microglia display seemingly opposite results in microglial measures (**Figure 6.1**). At 1 year old, decreased quantity of microglia in offspring was associated with maternal WSD and increased quantity of microglial were associated with maternal adiposity. At 3 years old, microglia appear to be significantly increased in WSD offspring but display no differences in morphology (**Table 6.2**). The changing effects on microglial quantity and morphology throughout the three different timepoints

examined is not fully understood. However, these differences may be explained by the temporal distance from maternal influences on these brain macrophages. At the fetal timepoint, it appears that the influence of maternal adiposity levels was the strongest predictor of microglial quantity and morphology. Brain development when offspring are 1 years old, has been influenced by both prenatal and lactation periods. Adiposity continues to play a role in microglial quantity as observed previously in the fetal timepoint. However, now maternal WSD also appears to influence microglia quantity. This may be due to additional exposure to the WSD during the lactation period. Breast milk from mothers consuming the WSD appear to have decreases in essential omega-3 fatty acids (170). Omega-3 fatty acid consumption has been shown to modulate microglial function. Finally, any maternal WSD effects observed at 3 years-old would be due to long term programming effects. Here we observed a persistent increase in microglial quantity due to maternal WSD but no long-term changes in microglia morphology. In contrast, levels of maternal adiposity appear to not have persistent effects on microglia number or morphology. In conclusion, it does appear maternal WSD elicits persistent effects on offspring microglia number while levels of adiposity appear to have a more transient effect in early prenatal development. However, it is possible other factors, such as stress, age, maternal care, that were not measured in this study contribute to the observed alterations in microglial phenotypes throughout development. It would be important for future study these additional factors with more scrutiny to further tease apart specific effects.

6.5 Summary and Conclusions

Overall, the studies conducted in this dissertation add to the field by providing evidence that consumption of a WSD and obesity during pregnancy is associated with persistent increases in offspring anxiety-like behaviors that are directly linked to reductions in serotonin innervation of the amygdala. Further, we provide support that these alterations are possibly due to an inflammatory mechanism acting through microglia function during development. The findings reported here should inform future intervention studies in pregnant people. Alterations or supplementations to diet during pregnancy may be protective to offspring neurodevelopment. Support for these future directions are seen in follow up studies by our group which have suggested omega-3 fatty acid supplementation during pregnancy in humans may ameliorate the adverse effects of maternal obesity on offspring behavior (171).

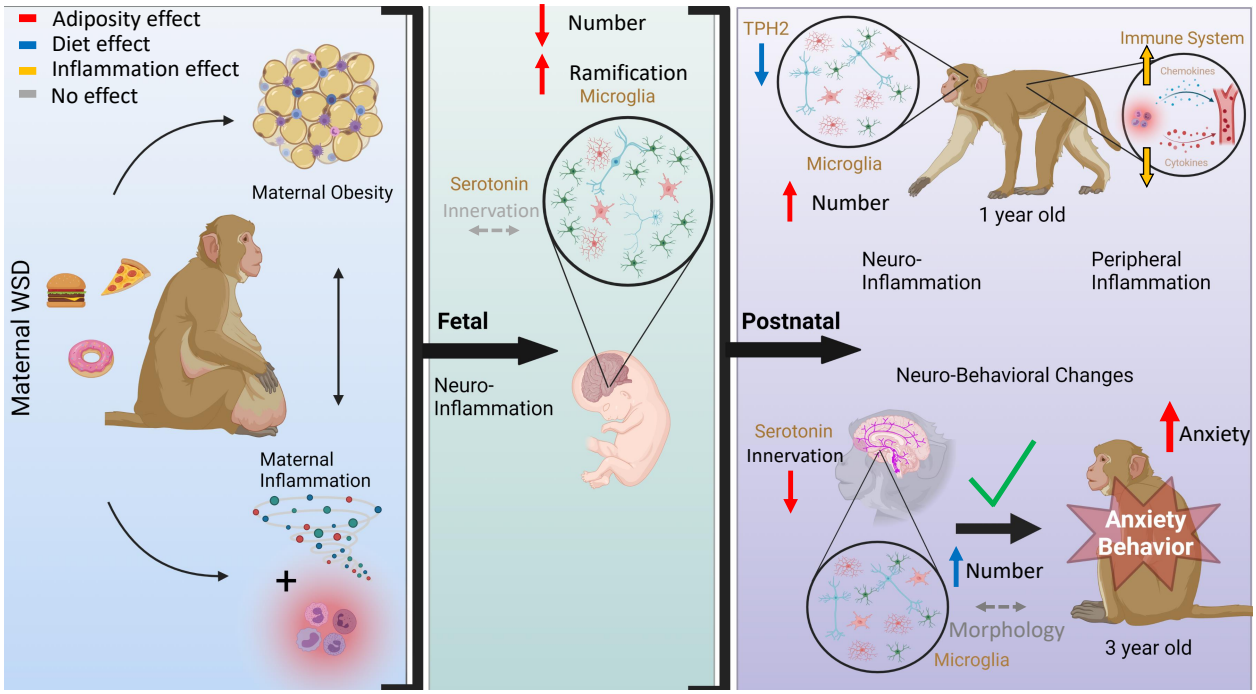

Figure 6.1. Conceptual figure describing the results observed in this dissertation. Red arrows indicate unique effects of maternal adiposity on offspring outcomes. Blue arrows indicate unique effects of maternal western-style diet on offspring outcomes. Yellow arrows indicate unique effects of maternal inflammatory state on offspring outcomes. Dashed gray arrows indicate when maternal measures had no effect on offspring outcomes.

Table 6.1. Summary Table of Results of Maternal WSD and Adiposity on Offspring Serotonin and Anxiety Behavior Measures at Different Timepoints

	Serotonin				Anxiety Behavior	
Brain region	Raphe Nuclei		Amygdala			
Timepoint	Diet	Adiposity	Diet	Adiposity	Diet	Adiposity
Fetal	n/a	n/a	-	-	n/a	n/a
13mo	↓	n/a	n/a	n/a	n/a	n/a
3yo	n/a	n/a	-	↓*	-	↑

Note. CTR control Diet; WSD Western-style Diet. *Indicates a sex effect. n/a indicates this metric was not measured at the timepoint. – Indicates no significant difference detected.

Table 6.2 Summary Table of Results of Maternal WSD and Adiposity on Offspring Microglial Measures at Different Timepoints

Timepoint	Microglia			
	Count		Morphology	
	Diet	Adiposity	Diet	Adiposity
Fetal	-	↓	-	↑*
1yo	↓	↑	n/a	n/a
3yo	↑	-	-	-

Note. CTR control Diet; WSD Western-style Diet. *Indicates a sex effect. n/a indicates this metric was not measured at this timepoint. – Indicates no significant difference detected.

APPENDIX A: SUPPLEMENTAL MATERIALS
CHAPTER 2 SUPPLEMENTARY TABLES

Table S2.1. Concentrations of Inflammatory Markers

Protein	Maternal			Offspring		
	% below the LLOQ	Average concentration (pg/mL)	*SE*	% below the LLOQ	Average Concentration (pg/mL)	*SE*
MCP-1	0.00%	188.30	6.86	0.00%	281.57	10.44
Eotaxin (CCL11)	0.00%	171.98	13.30	0.00%	135.89	11.66
RANTES (CCL2)	0.00%	410.52	30.82	0.00%	680.40	46.64
I-TAC (CXCL11)	0.00%	693.38	40.11	0.00%	936.78	47.45
MDC (CCL22)	3.25%	368.99	37.80	0.00%	709.73	51.96
IL-1RA	0.00%	212.33	16.30	2.15%	156.9	17.09
MIF (GIF)	7.32%	329.93	42.23	0.00%	469.11	52.55
IFNγ	0.00%	29.62	7.56	0.00%	15.41	1.98
IL-1β	4.07%	12.02	0.86	11.83%	10.00	.79
IL-12	0.00%	386.25	63.68	0.00%	1199.27	69.56
IL-6#	11.38%	8.39	0.72	45.16%	N/A	N/A
TNFα#	8.13%	35.18	8.18	34.41%	N/A	N/A
IP-10 (CXCL10)^	13.01%	N/A	N/A	2.15%	17.08	1.28
IL-2ǂ	47.15%	N/A	N/A	51.61%	N/A	N/A
IL-15 ǂ	28.46%	N/A	N/A	54.84%	N/A	N/A
IL-17ǂ	46.34%	N/A	N/A	20.43%	N/A	N/A
Not Included in Latent Variable Formation						
MIP-1b#	1.63%	36.36	5.22	15.05%	N/A	N/A
MIP-1aǂ	36.59%	N/A	N/A	31.18%	N/A	N/A
IL-8ǂ	41.46%	N/A	N/A	16.13%	N/A	N/A
DISCARDED by LLOQ						
IL-4	81.30%			90.32%		
IL-5	70.73%			90.32%		
IL-10	88.62%			78.49%		
MIG	64.23%			78.49%		

Note: Standardized factor loadings above 0.3 with p-values <0.05 are considered adequate. #categorical in offspring only, ^categorical in maternal only, ǂcategorical in both. Inflammatory markers that had <LLOQ values for greater than 55% of subjects were discarded.

Table S2.3 Latent Variable Creation for Inflammatory Markers

	Offspring				Maternal			
Protein	Chemokines		Cytokines		Chemokines		Pro-inflammatory Cytokines	
	Standardized factor loading	*p*	Standardized factor loading	*p*	Standardized factor loading	*p*	Standardized factor loading	*p*
MCP-1	0.788	0.000			0.796	0.000		
Eotaxin (CCL11)	0.380	0.001			0.636	0.000		
RANTES (CCL2)	0.309	0.008			0.499	0.000		
I-TAC (CXCL11)	0.696	0.000			0.668	0.000		
MDC (CCL22)	0.388	0.000			0.519	0.000		
IP-10 (CXCL10)	0.492	0.000			0.535	0.000		
IL-12							0.593	0.000
MIF (GIF)			0.478	0.000			0.345	0.001
TNFα			0.329	0.003			0.706	0.000
IFNγ			0.540	0.000			0.804	0.000
IL-1β			0.740	0.000			0.697	0.000
IL-2			0.586	0.000				
IL-6			0.356	0.000				
IL-15			0.767	0.000				
IL-17			0.406	0.000				
IL-1RA			0.554	0.000				

Note: Standardized factor loadings above 0.3 with p-values <0.05 are considered adequate

Table S2.2 Results of Models Relating Maternal Metabolic State and Offspring Microglial Counts in Amygdala Subregions

	Total			Lateral			Basolateral-dorsal			Basolateral-intermediate		
Direct Effects	β(SE)	*p*	95% CI of β	β(SE)	*p*	95% CI of β	β(SE)	*p*	95% CI of β	β(SE)	*p*	95% CI of β
Maternal WSD → Amygdala region	-.443(.292)	.129	-.925, .038	**-.554(.207)**	**.007**	**-.336, .196**	**-.483(.226)**	**.033**	**-.855, -.111**	-.368(.252)	.144	-.782, .046
Pre-Pregnancy Adiposity → Amygdala region	.433(.269)	.100	.000, .886	**.628(.166)**	**.001**	**.354, .901**	**.471(.215)**	**.029**	**.117, .824**	**.521(.206)**	**.011**	**.182, .860**
Gestation Length → Amygdala region	.114(.092)	.215	-.037, .264	**.164(.077)**	**.034**	**.036, .291**	**.226(.080)**	**.005**	**.095, .358**	.138(.096)	.153	-.021, .297
Indirect Effect Paths												
Maternal WSD → Pre-Pregnancy Adiposity → Amygdala region	.155(.107)	.145	-.020, .331	**.219(.094)**	**.016**	**.069, .369**	.166(.091)	.068	.016, .315	**.183(.094)**	**.050**	**.029, .336**

Note: WSD = Western Style Diet; Bold numbers indicate significance at $p<0.05$

Table S2.4. Maternal Obesity and Maternal and Offspring Diet Effects on Individual Offspring Cytokine Levels

Offspring Cytokine	Maternal Obesity regression		Maternal WSD regression		Offspring WSD regression	
	β(SE)	*p*	β(SE)	*p*	β(SE)	*p*
MCP-1	0.098(0.100)	0.327	-0.032(0.106)	0.766	-0.062(0.114)	0.587
EOTAXIN (CCL11)	-0.003(0.110)	0.982	**-0.209(0.100)**	**0.037**	-0.077(0.100)	0.443
RANTES (CCL2)	-0.066(0.127)	0.604	-0.078(0.099)	0.430	-0.086(0.093)	0.358
I-TAC (CXCL11)	-0.156(0.107)	0.146	-0.072(0.104)	0.489	0.028(0.112)	0.801
MDC (CCL22)	0.029(0.127)	0.819	-0.108(0.092)	0.241	0.076(0.102)	0.455
IL-1RA	0.074(0.137)	0.588	-0.095(0.097)	0.327	-0.083(0.112)	0.459
MIF (GIF)	**-0.288(0.115)**	**0.012**	-0.048(0.103)	0.639	0.118(0.107)	0.271
IFNγ	0.165(0.100)	0.099	-0.086(0.103)	0.400	**-0.273(0.091)**	**0.003**
IL-1β	0.001(0.110)	0.996	-0.042(0.105)	0.684	-0.101(0.107)	0.349
IL-12	0.159(0.103)	0.122	0.165(0.094)	0.081	-0.171(0.103)	0.096
IL-6^	0.029(0.124)	0.814	0.100(0.103)	0.333	0.030(0.104)	0.769
TNFα^	0.004(0.108)	0.967	-0.022(0.104)	0.829	-0.011(0.097)	0.912
IP-10 (CXCL10)	**-0.239(0.115)**	**0.037**	-0.052(0.112)	0.645	-0.093(0.102)	0.363
IL-2^	0.212(0.122)	0.082	-0.006(0.104)	0.957	-0.141(0.102)	0.166
IL-15^	-0.117(0.125)	0.349	0.027(0.104)	0.796	-0.051(0.103)	0.796
IL-17^	0.099(0.109)	0.364	-0.063(0.102)	0.541	**-0.219(0.096)**	**0.022**
MIP-1b^	0.077(0.112)	0.494	-0.131(0.099)	0.188	-0.097(0.104)	0.350
MIP-1a^	0.015(0.121)	0.902	0.088(0.105)	0.401	0.145(0.099)	0.144
IL-8^	0.023(0.102)	0.819	0.005(0.104)	0.960	-0.162(0.096)	0.092

Note: WSD = Western Style Diet; Bold numbers indicate significance at $p<0.05$; ^categorical variables

CHAPTER 3 SUPPLEMENTARY FIGURES

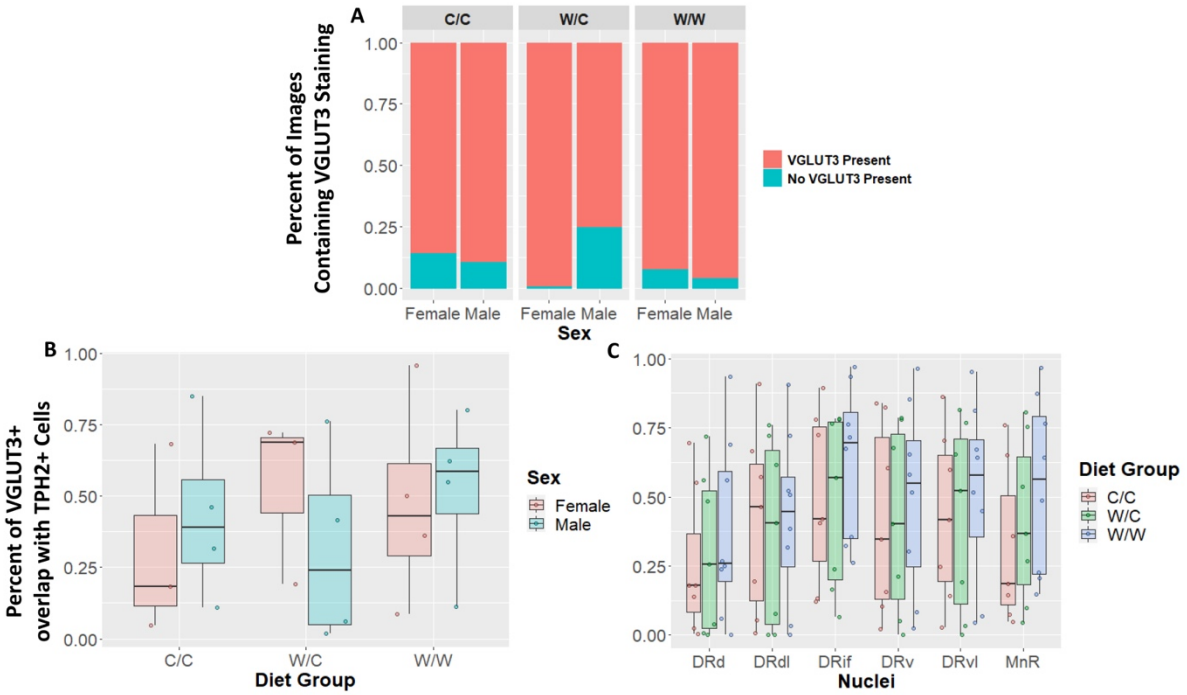

Supplementary Figure 3.1. Proportion of VGLUT3+/TPH2+ cells does not appear to be impacted by maternal WSD. Data in B and C are expressed as box plots with boxes indicating the 1st to 3rd quartile range and the median expressed as the horizontal bold line.

A) No significant diet or sex main effects were found when comparing the percentage of images that either contained some VGLUT3 staining or no staining at all.
B) Proportion of VGLUT3+/TPH2+ cells was not significantly impacted by perinatal diet.
C) Proportion of VGLUT3+/TPH2+ cells in specific subregions were not uniquely impacted by perinatal diet.
Abbreviations: DRd: dorsal nucleus of the Dorsal Raphe; DRdl: dorsolateral nucleus of the Dorsal Raphe DRv: ventral nucleus of the Dorsal Raphe; DRvl: ventrolateral nucleus of the Dorsal Raphe MnR: Median Raphe nucleus

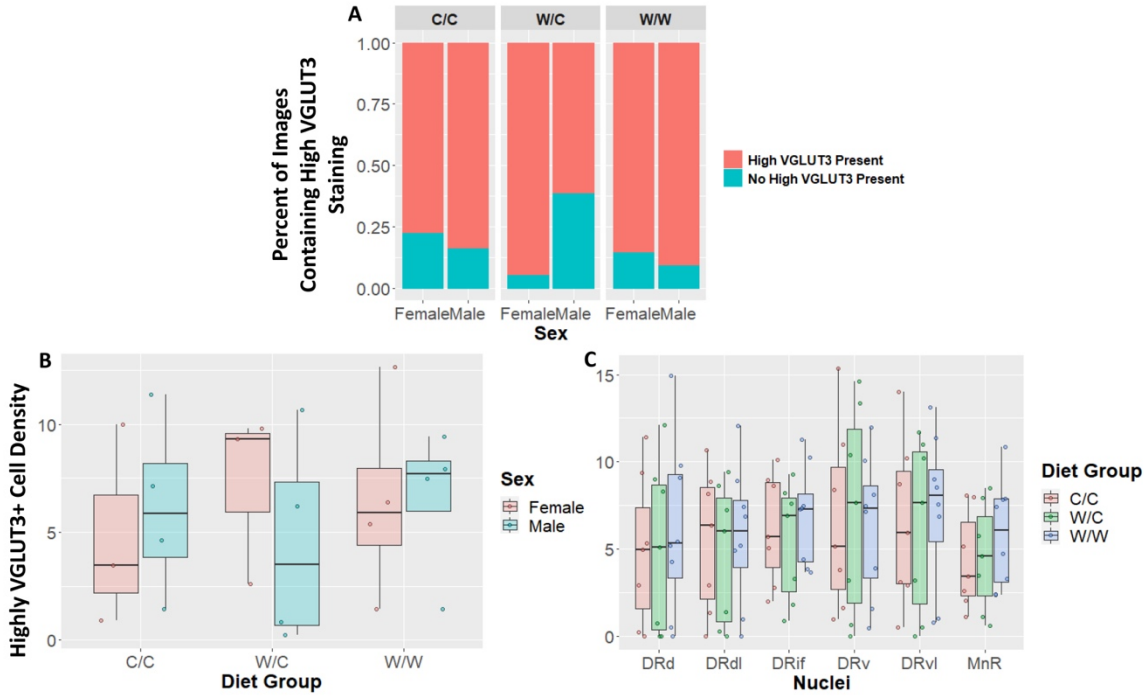

Supplementary Figure 3.2. Cell density of highly VGLUT3+ cells does not appear to be impacted by maternal WSD. Data in B and C are expressed as box plots with boxes indicating the 1st to 3rd quartile range and the median expressed as the horizontal bold line.

A) No significant diet or sex main effects were found when comparing the percentage of images that either contained some highly VGLUT3+ stained cells or no highly VGLUT3+ stained cells at all.
B) Cell density of highly VGLUT3+ cells was not significantly impacted by perinatal diet.
C) Cell density of highly VGLUT3+ cells in specific subregions were not uniquely impacted by perinatal diet.
Abbreviations: DRd: dorsal nucleus of the Dorsal Raphe; DRdl: dorsolateral nucleus of the Dorsal Raphe DRv: ventral nucleus of the Dorsal Raphe; DRvl: ventrolateral nucleus of the Dorsal Raphe MnR: Median Raphe nucleus

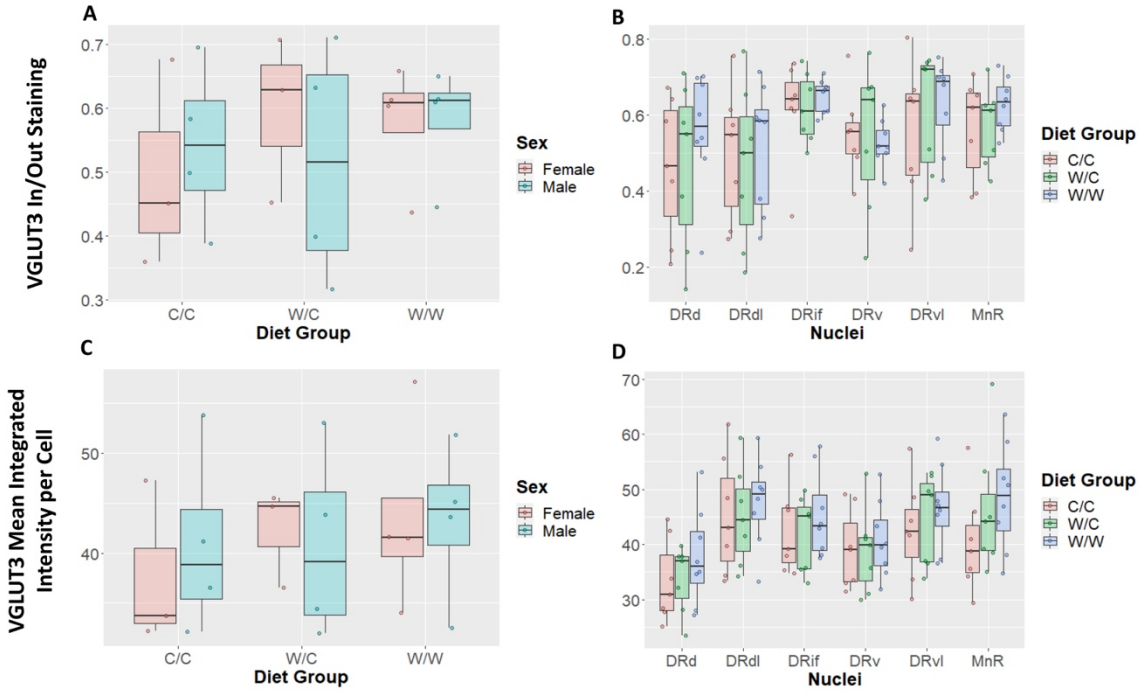

Supplementary Figure 3.3. WSD does not appear to influence other raphe VGLUT3+ cell outcomes. Data are expressed as box plots with boxes indicating the 1st to 3rd quartile range and the median expressed as the horizontal bold line.

A) Ratio of signal that is located either inside or outside of a TPH2+ cell. A ratio of 0.5 indicates VGLUT3 signal is equally likely as not to occur within a TPH2+ cell. Ratios above 0.5 indicate a highly likelihood VGLUT3 signal will be located inside a TPH2+ cell. VGLUT3 In/Out ratio staining was not found to be significantly impacted by perinatal exposure to WSD.
B) VGLUT3 In/Out ratio staining was not found to be significantly different in any specific subregions.
C) VGLUT3 average cell integrated intensity was not found to be significantly different between diet groups.
D) VGLUT3 average cell integrated intensity was not found to be significantly different in any specific subregions.
Abbreviations: DRd: dorsal nucleus of the Dorsal Raphe; DRdl: dorsolateral nucleus of the Dorsal Raphe DRv: ventral nucleus of the Dorsal Raphe; DRvl: ventrolateral nucleus of the Dorsal Raphe; MnR: Median Raphe nucleus

REFERENCES CITED

1. de Boo HA, Harding JE (2006): The developmental origins of adult disease (Barker) hypothesis. *Aust N Z J Obstet Gynaecol*. 46:4-14.

2. Roseboom T, de Rooij S, Painter R (2006): The Dutch famine and its long-term consequences for adult health. *Early Hum Dev*. 82:485-491.

3. Marques AH, O'Connor TG, Roth C, Susser E, Bjørke-Monsen AL (2013): The influence of maternal prenatal and early childhood nutrition and maternal prenatal stress on offspring immune system development and neurodevelopmental disorders. *Front Neurosci*. 7:120.

4. Rosenberg MD (2018): Baby brains reflect maternal inflammation. *Nat Neurosci*. 21:651-653.

5. Mednick SA, Machon RA, Huttunen MO, Bonett D (1988): Adult schizophrenia following prenatal exposure to an influenza epidemic. *Arch Gen Psychiatry*. 45:189-192.

6. (CDC) CfDCaP BRFSS Prevalence & Trends Data. 2021 ed. Atlanta, Georgia: U.S. Department of Health and Human Services, Centers for Disease Control and Prevention.

7. Ward ZJ, Bleich SN, Cradock AL, Barrett JL, Giles CM, Flax C, et al. (2019): Projected U.S. State-Level Prevalence of Adult Obesity and Severe Obesity. *N Engl J Med*. 381:2440-2450.

8. Wallin A, Larsson SC (2011): Body mass index and risk of multiple myeloma: a meta-analysis of prospective studies. *Eur J Cancer*. 47:1606-1615.

9. Campbell PT, Newton CC, Freedman ND, Koshiol J, Alavanja MC, Beane Freeman LE, et al. (2016): Body Mass Index, Waist Circumference, Diabetes, and Risk of Liver Cancer for U.S. Adults. *Cancer Res*. 76:6076-6083.

10. Schnurr TM, Jakupović H, Carrasquilla GD, Ängquist L, Grarup N, Sørensen TIA, et al. (2020): Obesity, unfavourable lifestyle and genetic risk of type 2 diabetes: a case-cohort study. *Diabetologia*. 63:1324-1332.

11. Ades PA, Savage PD (2017): Obesity in coronary heart disease: An unaddressed behavioral risk factor. *Prev Med*. 104:117-119.

12. Hammond RA, Levine R (2010): The economic impact of obesity in the United States. *Diabetes Metab Syndr Obes*. 3:285-295.

13. Wang YC, McPherson K, Marsh T, Gortmaker SL, Brown M (2011): Health and economic burden of the projected obesity trends in the USA and the UK. *Lancet*. 378:815-825.

14. Driscoll AK, Gregory ECW (2020): Increases in Prepregnancy Obesity: United States, 2016-2019. *NCHS Data Brief*.1-8.

15. Godfrey KM, Reynolds RM, Prescott SL, Nyirenda M, Jaddoe VW, Eriksson JG, et al. (2017): Influence of maternal obesity on the long-term health of offspring. *Lancet Diabetes Endocrinol*. 5:53-64.

16. Drake AJ, Reynolds RM (2010): Impact of maternal obesity on offspring obesity and cardiometabolic disease risk. *Reproduction*. 140:387-398.

17. Edlow AG (2017): Maternal obesity and neurodevelopmental and psychiatric disorders in offspring. *Prenat Diagn*. 37:95-110.

18. Contu L, Hawkes CA (2017): A Review of the Impact of Maternal Obesity on the Cognitive Function and Mental Health of the Offspring. *Int J Mol Sci*. 18.

19. Rodriguez A (2010): Maternal pre-pregnancy obesity and risk for inattention and negative emotionality in children. *J Child Psychol Psychiatry*. 51:134-143.

20. Krakowiak P, Walker CK, Bremer AA, Baker AS, Ozonoff S, Hansen RL, et al. (2012): Maternal metabolic conditions and risk for autism and other neurodevelopmental disorders. *Pediatrics*. 129:e1121-1128.

21. Rakhra V, Galappaththy SL, Bulchandani S, Cabandugama PK (2020): Obesity and the Western Diet: How We Got Here. *Mo Med*. 117:536-538.

22. Elsakr JM, Zhao SK, Ricciardi V, Dean TA, Takahashi DL, Sullivan E, et al. (2021): Western-style diet consumption impairs maternal insulin sensitivity and glucose metabolism during pregnancy in a Japanese macaque model. *Sci Rep*. 11:12977.

23. Elsakr JM, Dunn JC, Tennant K, Zhao SK, Kroeten K, Pasek RC, et al. (2019): Maternal Western-style diet affects offspring islet composition and function in a non-human primate model of maternal over-nutrition. *Mol Metab*. 25:73-82.

24. Jones HN, Woollett LA, Barbour N, Prasad PD, Powell TL, Jansson T (2009): High-fat diet before and during pregnancy causes marked up-regulation of placental nutrient transport and fetal overgrowth in C57/BL6 mice. *FASEB J*. 23:271-278.

25. DeCapo M, Thompson JR, Dunn G, Sullivan EL (2019): Perinatal Nutrition and Programmed Risk for Neuropsychiatric Disorders: A Focus on Animal Models. *Biol Psychiatry*. 85:122-134.

26. Thompson JR, Gustafsson HC, DeCapo M, Takahashi DL, Bagley JL, Dean TA, et al. (2018): Maternal Diet, Metabolic State, and Inflammatory Response Exert Unique and Long-Lasting Influences on Offspring Behavior in Non-Human Primates. *Front Endocrinol (Lausanne)*. 9:161.

27. Speight A, Davey WG, McKenna E, Voigt JW (2017): Exposure to a maternal cafeteria diet changes open-field behaviour in the developing offspring. *Int J Dev Neurosci*. 57:34-40.

28. Giriko C, Andreoli CA, Mennitti LV, Hosoume LF, Souto ToS, Silva AV, et al. (2013): Delayed physical and neurobehavioral development and increased aggressive and depression-like behaviors in the rat offspring of dams fed a high-fat diet. *Int J Dev Neurosci*. 31:731-739.

29. Ribeiro ACAF, Batista TH, Veronesi VB, Giusti-Paiva A, Vilela FC (2018): Cafeteria diet during the gestation period programs developmental and behavioral courses in the offspring. *Int J Dev Neurosci*. 68:45-52.

30. Wright T, Langley-Evans SC, Voigt JP (2011): The impact of maternal cafeteria diet on anxiety-related behaviour and exploration in the offspring. *Physiol Behav*. 103:164-172.

31. Janthakhin Y, Rincel M, Costa AM, Darnaudéry M, Ferreira G (2017): Maternal high-fat diet leads to hippocampal and amygdala dendritic remodeling in adult male offspring. *Psychoneuroendocrinology*. 83:49-57.

32. Rincel M, Lépinay AL, Janthakhin Y, Soudain G, Yvon S, Da Silva S, et al. (2018): Maternal high-fat diet and early life stress differentially modulate spine density and dendritic morphology in the medial prefrontal cortex of juvenile and adult rats. *Brain Struct Funct*. 223:883-895.

33. Hatanaka Y, Wada K, Kabuta T (2016): Maternal high-fat diet leads to persistent synaptic instability in mouse offspring via oxidative stress during lactation. *Neurochem Int*. 97:99-108.

34. Penzes P, Cahill ME, Jones KA, VanLeeuwen JE, Woolfrey KM (2011): Dendritic spine pathology in neuropsychiatric disorders. *Nat Neurosci*. 14:285-293.

35. Banks WA, Kastin AJ, Broadwell RD (1995): Passage of cytokines across the blood-brain barrier. *Neuroimmunomodulation*. 2:241-248.

36. Rustenhoven J, Jansson D, Smyth LC, Dragunow M (2017): Brain Pericytes As Mediators of Neuroinflammation. *Trends Pharmacol Sci*. 38:291-304.

37. Duan L, Zhang XD, Miao WY, Sun YJ, Xiong G, Wu Q, et al. (2018): PDGFRβ Cells Rapidly Relay Inflammatory Signal from the Circulatory System to Neurons via Chemokine CCL2. *Neuron*. 100:183-200.e188.

38. Breit S, Kupferberg A, Rogler G, Hasler G (2018): Vagus Nerve as Modulator of the Brain-Gut Axis in Psychiatric and Inflammatory Disorders. *Front Psychiatry*. 9:44.

39. Ransohoff RM, Kivisäkk P, Kidd G (2003): Three or more routes for leukocyte migration into the central nervous system. *Nat Rev Immunol*. 3:569-581.

40. McBride DA, Kerr MD, Dorn NC, Ogbonna DA, Santos EC, Shah NJ (2021): Triggers, Timescales, and Treatments for Cytokine-Mediated Tissue Damage. *Euro Med J Innov*. 5:52-62.

41. de Heredia FP, Gómez-Martínez S, Marcos A (2012): Obesity, inflammation and the immune system. *Proc Nutr Soc*. 71:332-338.

42. Rowitch DH, Kriegstein AR (2010): Developmental genetics of vertebrate glial-cell specification. *Nature*. 468:214-222.

43. Gregg C, Weiss S (2005): CNTF/LIF/gp130 receptor complex signaling maintains a VZ precursor differentiation gradient in the developing ventral forebrain. *Development*. 132:565-578.

44. Adachi T, Takanaga H, Kunimoto M, Asou H (2005): Influence of LIF and BMP-2 on differentiation and development of glial cells in primary cultures of embryonic rat cerebral hemisphere. *J Neurosci Res*. 79:608-615.

45. Stolp HB, Turnquist C, Dziegielewska KM, Saunders NR, Anthony DC, Molnár Z (2011): Reduced ventricular proliferation in the foetal cortex following maternal inflammation in the mouse. *Brain*. 134:3236-3248.

46. Falk S, Wurdak H, Ittner LM, Ille F, Sumara G, Schmid MT, et al. (2008): Brain area-specific effect of TGF-beta signaling on Wnt-dependent neural stem cell expansion. *Cell Stem Cell*. 2:472-483.

47. Kasai M, Satoh K, Akiyama T (2005): Wnt signaling regulates the sequential onset of neurogenesis and gliogenesis via induction of BMPs. *Genes Cells*. 10:777-783.

48. Ginhoux F, Greter M, Leboeuf M, Nandi S, See P, Gokhan S, et al. (2010): Fate mapping analysis reveals that adult microglia derive from primitive macrophages. *Science*. 330:841-845.

49. Andjelkovic AV, Nikolic B, Pachter JS, Zecevic N (1998): Macrophages/microglial cells in human central nervous system during development: an immunohistochemical study. *Brain Res*. 814:13-25.

50. Cunningham CL, Martinez-Cerdeno V, Noctor SC (2013): Microglia regulate the number of neural precursor cells in the developing cerebral cortex. *J Neurosci*. 33:4216-4233.

51. Aarum J, Sandberg K, Haeberlein SL, Persson MA (2003): Migration and differentiation of neural precursor cells can be directed by microglia. *Proc Natl Acad Sci U S A*. 100:15983-15988.

52. Nakanishi M, Niidome T, Matsuda S, Akaike A, Kihara T, Sugimoto H (2007): Microglia-derived interleukin-6 and leukaemia inhibitory factor promote astrocytic differentiation of neural stem/progenitor cells. *Eur J Neurosci*. 25:649-658.

53. Roumier A, Pascual O, Bechade C, Wakselman S, Poncer JC, Real E, et al. (2008): Prenatal activation of microglia induces delayed impairment of glutamatergic synaptic function. *PLoS One*. 3:e2595.

54. Paolicelli RC, Bolasco G, Pagani F, Maggi L, Scianni M, Panzanelli P, et al. (2011): Synaptic pruning by microglia is necessary for normal brain development. *Science*. 333:1456-1458.

55. Zhan Y, Paolicelli RC, Sforazzini F, Weinhard L, Bolasco G, Pagani F, et al. (2014): Deficient neuron-microglia signaling results in impaired functional brain connectivity and social behavior. *Nat Neurosci*. 17:400-406.

56. Estes ML, McAllister AK (2016): Maternal immune activation: Implications for neuropsychiatric disorders. *Science*. 353:772-777.

57. Weisberg SP, McCann D, Desai M, Rosenbaum M, Leibel RL, Ferrante AW (2003): Obesity is associated with macrophage accumulation in adipose tissue. *J Clin Invest*. 112:1796-1808.

58. Cinti S, Mitchell G, Barbatelli G, Murano I, Ceresi E, Faloia E, et al. (2005): Adipocyte death defines macrophage localization and function in adipose tissue of obese mice and humans. *J Lipid Res*. 46:2347-2355.

59. Coats BR, Schoenfelt KQ, Barbosa-Lorenzi VC, Peris E, Cui C, Hoffman A, et al. (2017): Metabolically Activated Adipose Tissue Macrophages Perform Detrimental and Beneficial Functions during Diet-Induced Obesity. *Cell Rep*. 20:3149-3161.

60. Verboven K, Wouters K, Gaens K, Hansen D, Bijnen M, Wetzels S, et al. (2018): Abdominal subcutaneous and visceral adipocyte size, lipolysis and inflammation relate to insulin resistance in male obese humans. *Sci Rep*. 8:4677.

61. Tran HQ, Bretin A, Adeshirlarijaney A, Yeoh BS, Vijay-Kumar M, Zou J, et al. (2020): "Western Diet"-Induced Adipose Inflammation Requires a Complex Gut Microbiota. *Cell Mol Gastroenterol Hepatol*. 9:313-333.

62. Huang EY, Devkota S, Moscoso D, Chang EB, Leone VA (2013): The role of diet in triggering human inflammatory disorders in the modern age. *Microbes Infect*. 15:765-774.

63. Padin AC, Hébert JR, Woody A, Wilson SJ, Shivappa N, Belury MA, et al. (2019): A proinflammatory diet is associated with inflammatory gene expression among healthy, non-obese adults: Can social ties protect against the risks? *Brain Behav Immun*. 82:36-44.

64. Fritsche KL (2015): The science of fatty acids and inflammation. *Adv Nutr*. 6:293S-301S.

65. Wiese DM, Horst SN, Brown CT, Allaman MM, Hodges ME, Slaughter JC, et al. (2016): Serum Fatty Acids Are Correlated with Inflammatory Cytokines in Ulcerative Colitis. *PLoS One*. 11:e0156387.

66. Rocha DMUP, Lopes LL, da Silva A, Oliveira LL, Bressan J, Hermsdorff HHM (2017): Orange juice modulates proinflammatory cytokines after high-fat saturated meal consumption. *Food Funct*. 8:4396-4403.

67. van Dijk SJ, Feskens EJ, Bos MB, Hoelen DW, Heijligenberg R, Bromhaar MG, et al. (2009): A saturated fatty acid-rich diet induces an obesity-linked proinflammatory gene expression profile in adipose tissue of subjects at risk of metabolic syndrome. *Am J Clin Nutr*. 90:1656-1664.

68. Rocha DM, Caldas AP, Oliveira LL, Bressan J, Hermsdorff HH (2016): Saturated fatty acids trigger TLR4-mediated inflammatory response. *Atherosclerosis*. 244:211-215.

69. Milanski M, Degasperi G, Coope A, Morari J, Denis R, Cintra DE, et al. (2009): Saturated fatty acids produce an inflammatory response predominantly through the activation of TLR4 signaling in hypothalamus: implications for the pathogenesis of obesity. *J Neurosci*. 29:359-370.

70. Das UN (2021): Essential Fatty Acids and Their Metabolites in the Pathobiology of Inflammation and Its Resolution. *Biomolecules*. 11.

71. Crawford MA, Broadhurst CL, Guest M, Nagar A, Wang Y, Ghebremeskel K, et al. (2013): A quantum theory for the irreplaceable role of docosahexaenoic acid in neural cell signalling throughout evolution. *Prostaglandins Leukot Essent Fatty Acids*. 88:5-13.

72. Calder PC (2017): Omega-3 fatty acids and inflammatory processes: from molecules to man. *Biochem Soc Trans*. 45:1105-1115.

73. Yates CM, Calder PC, Ed Rainger G (2014): Pharmacology and therapeutics of omega-3 polyunsaturated fatty acids in chronic inflammatory disease. *Pharmacol Ther*. 141:272-282.

74. Sastry PS (1985): Lipids of nervous tissue: composition and metabolism. *Prog Lipid Res*. 24:69-176.

75. Guixà-González R, Javanainen M, Gómez-Soler M, Cordobilla B, Domingo JC, Sanz F, et al. (2016): Membrane omega-3 fatty acids modulate the oligomerisation kinetics of adenosine A2A and dopamine D2 receptors. *Sci Rep*. 6:19839.

76. Madore C, Leyrolle Q, Morel L, Rossitto M, Greenhalgh AD, Delpech JC, et al. (2020): Essential omega-3 fatty acids tune microglial phagocytosis of synaptic elements in the mouse developing brain. *Nat Commun*. 11:6133.

77. Madore C, Nadjar A, Delpech JC, Sere A, Aubert A, Portal C, et al. (2014): Nutritional n-3 PUFAs deficiency during perinatal periods alters brain innate immune system and neuronal plasticity-associated genes. *Brain Behav Immun*. 41:22-31.

78. Yu JZ, Wang J, Sheridan SD, Perlis RH, Rasenick MM (2021): N-3 polyunsaturated fatty acids promote astrocyte differentiation and neurotrophin production independent of cAMP in patient-derived neural stem cells. *Mol Psychiatry*. 26:4605-4615.

79. Mauerer R, Walczak Y, Langmann T (2009): Comprehensive mRNA profiling of lipid-related genes in microglia and macrophages using taqman arrays. *Methods Mol Biol*. 580:187-201.

80. Chen X, Wu S, Chen C, Xie B, Fang Z, Hu W, et al. (2017): Omega-3 polyunsaturated fatty acid supplementation attenuates microglial-induced inflammation by inhibiting the HMGB1/TLR4/NF-κB pathway following experimental traumatic brain injury. *J Neuroinflammation*. 14:143.

81. Rey C, Nadjar A, Joffre F, Amadieu C, Aubert A, Vaysse C, et al. (2018): Maternal n-3 polyunsaturated fatty acid dietary supply modulates microglia lipid content in the offspring. *Prostaglandins Leukot Essent Fatty Acids*. 133:1-7.

82. Grundy SM, Denke MA (1990): Dietary influences on serum lipids and lipoproteins. *J Lipid Res*. 31:1149-1172.

83. Tall AR, Yvan-Charvet L (2015): Cholesterol, inflammation and innate immunity. *Nat Rev Immunol*. 15:104-116.

84. Moore KJ, Tabas I (2011): Macrophages in the pathogenesis of atherosclerosis. *Cell*. 145:341-355.

85. Zhu X, Owen JS, Wilson MD, Li H, Griffiths GL, Thomas MJ, et al. (2010): Macrophage ABCA1 reduces MyD88-dependent Toll-like receptor trafficking to lipid rafts by reduction of lipid raft cholesterol. *J Lipid Res*. 51:3196-3206.

86. An J, Zhao X, Wang Y, Noriega J, Gewirtz AT, Zou J (2021): Western-style diet impedes colonization and clearance of Citrobacter rodentium. *PLoS Pathog*. 17:e1009497.

87. Deneris E, Gaspar P (2018): Serotonin neuron development: shaping molecular and structural identities. *Wiley Interdiscip Rev Dev Biol*. 7.

88. Daubert EA, Condron BG (2010): Serotonin: a regulator of neuronal morphology and circuitry. *Trends Neurosci*. 33:424-434.

89. Bonnin A, Levitt P (2011): Fetal, maternal, and placental sources of serotonin and new implications for developmental programming of the brain. *Neuroscience*. 197:1-7.

90. Bonnin A, Goeden N, Chen K, Wilson ML, King J, Shih JC, et al. (2011): A transient placental source of serotonin for the fetal forebrain. *Nature*. 472:347-350.

91. Williams M, Zhang Z, Nance E, Drewes JL, Lesniak WG, Singh S, et al. (2017): Maternal Inflammation Results in Altered Tryptophan Metabolism in Rabbit Placenta and Fetal Brain. *Dev Neurosci*. 39:399-412.

92. Goeden N, Velasquez J, Arnold KA, Chan Y, Lund BT, Anderson GM, et al. (2016): Maternal Inflammation Disrupts Fetal Neurodevelopment via Increased Placental Output of Serotonin to the Fetal Brain. *J Neurosci*. 36:6041-6049.

93. Leung S, Lee A (2014): Negative Affect. In: Michalos AC, editor. *Encyclopedia of Quality of Life and Well-Being Research*. Dordrecht: Springer Netherlands, pp 4302-4305.

94. Thompson JR, Valleau JC, Barling AN, Franco JG, DeCapo M, Bagley JL, et al. (2017): Exposure to a High-Fat Diet during Early Development Programs Behavior and Impairs the Central Serotonergic System in Juvenile Non-Human Primates. *Front Endocrinol (Lausanne)*. 8:164.

95. Sullivan EL, Grayson B, Takahashi D, Robertson N, Maier A, Bethea CL, et al. (2010): Chronic consumption of a high-fat diet during pregnancy causes perturbations in the serotonergic system and increased anxiety-like behavior in nonhuman primate offspring. *J Neurosci*. 30:3826-3830.

96. McDonald AJ (1998): Cortical pathways to the mammalian amygdala. *Prog Neurobiol*. 55:257-332.

97. Amaral DG (2003): The amygdala, social behavior, and danger detection. *Ann N Y Acad Sci*. 1000:337-347.

98. Bocchio M, McHugh SB, Bannerman DM, Sharp T, Capogna M (2016): Serotonin, Amygdala and Fear: Assembling the Puzzle. *Front Neural Circuits*. 10:24.

99. Asan E, Steinke M, Lesch KP (2013): Serotonergic innervation of the amygdala: targets, receptors, and implications for stress and anxiety. *Histochem Cell Biol*. 139:785-813.

100. Steinbusch HW (1981): Distribution of serotonin-immunoreactivity in the central nervous system of the rat-cell bodies and terminals. *Neuroscience*. 6:557-618.

101. Jacobs BL, Foote SL, Bloom FE (1978): Differential projections of neurons within the dorsal raphe nucleus of the rat: a horseradish peroxidase (HRP) study. *Brain Res*. 147:149-153.

102. Royer S, Martina M, Paré D (1999): An inhibitory interface gates impulse traffic between the input and output stations of the amygdala. *J Neurosci*. 19:10575-10583.

103. Sengupta A, Bocchio M, Bannerman DM, Sharp T, Capogna M (2017): Control of Amygdala Circuits by 5-HT Neurons via 5-HT and Glutamate Cotransmission. *J Neurosci*. 37:1785-1796.

104. Jenkins TA, Nguyen JC, Polglaze KE, Bertrand PP (2016): Influence of Tryptophan and Serotonin on Mood and Cognition with a Possible Role of the Gut-Brain Axis. *Nutrients*. 8.

105. Dunn GA, Mitchell AJ, Selby M, Fair DA, Gustafsson HC, Sullivan EL (2022): Maternal diet and obesity shape offspring central and peripheral inflammatory outcomes in juvenile non-human primates. *Brain Behav Immun*. 102:224-236.

106. Dunn GA, Thompson JR, Mitchell AJ, Papadakis S, Selby M, Fair D, et al. (2022): Perinatal Western-style diet alters serotonergic neurons in the macaque raphe nuclei. *Front Neurosci*. 16:1067479.

107. NHLBI Obesity Education Initiative Expert Panel on the Identification E, and Treatment of Obesity in Adults (US) (1998): Clinical Guidelines on the Identification, Evaluation, and Treatment of Overweight and Obesity in Adults--The Evidence Report. National Institutes of Health. *Obes Res*. 6 Suppl 2:51S-209S.

108. Gaillard R, Durmuş B, Hofman A, Mackenbach JP, Steegers EA, Jaddoe VW (2013): Risk factors and outcomes of maternal obesity and excessive weight gain during pregnancy. *Obesity (Silver Spring)*. 21:1046-1055.

109. McCurdy CE, Bishop JM, Williams SM, Grayson BE, Smith MS, Friedman JE, et al. (2009): Maternal high-fat diet triggers lipotoxicity in the fetal livers of nonhuman primates. *J Clin Invest*. 119:323-335.

110. Frias AE, Morgan TK, Evans AE, Rasanen J, Oh KY, Thornburg KL, et al. (2011): Maternal high-fat diet disturbs uteroplacental hemodynamics and increases the frequency of stillbirth in a nonhuman primate model of excess nutrition. *Endocrinology*. 152:2456-2464.

111. Nicol LE, Grant WF, Grant WR, Comstock SM, Nguyen ML, Smith MS, et al. (2013): Pancreatic inflammation and increased islet macrophages in insulin-resistant juvenile primates. *J Endocrinol*. 217:207-213.

112. Grayson BE, Levasseur PR, Williams SM, Smith MS, Marks DL, Grove KL (2010): Changes in melanocortin expression and inflammatory pathways in fetal offspring of nonhuman primates fed a high-fat diet. *Endocrinology*. 151:1622-1632.

113. Mehta SH, Kerver JM, Sokol RJ, Keating DP, Paneth N (2014): The association between maternal obesity and neurodevelopmental outcomes of offspring. *J Pediatr*. 165:891-896.

114. Torres-Espinola FJ, Berglund SK, García-Valdés LM, Segura MT, Jerez A, Campos D, et al. (2015): Maternal Obesity, Overweight and Gestational Diabetes Affect the Offspring Neurodevelopment at 6 and 18 Months of Age--A Follow Up from the PREOBE Cohort. *PLoS One*. 10:e0133010.

115. Gustafsson HC, Sullivan EL, Battison EAJ, Holton KF, Graham AM, Karalunas SL, et al. (2020): Evaluation of maternal inflammation as a marker of future offspring ADHD symptoms: A prospective investigation. *Brain, behavior, and immunity*. 89:350-356.

116. Andersen CH, Thomsen PH, Nohr EA, Lemcke S (2018): Maternal body mass index before pregnancy as a risk factor for ADHD and autism in children. *Eur Child Adolesc Psychiatry*. 27:139-148.

117. Rivera HM, Kievit P, Kirigiti MA, Bauman LA, Baquero K, Blundell P, et al. (2015): Maternal high-fat diet and obesity impact palatable food intake and dopamine signaling in nonhuman primate offspring. *Obesity (Silver Spring)*. 23:2157-2164.

118. Glendining KA, Fisher LC, Jasoni CL (2018): Maternal high fat diet alters offspring epigenetic regulators, amygdala glutamatergic profile and anxiety. *Psychoneuroendocrinology*. 96:132-141.

119. Ramirez JSB, Graham AM, Thompson JR, Zhu JY, Sturgeon D, Bagley JL, et al. (2020): Maternal Interleukin-6 Is Associated With Macaque Offspring Amygdala Development and Behavior. *Cereb Cortex*. 30:1573-1585.

120. Amaral DG (2002): The primate amygdala and the neurobiology of social behavior: implications for understanding social anxiety. *Biol Psychiatry*. 51:11-17.

121. LeDoux J (2007): The amygdala. *Curr Biol*. 17:R868-874.

122. Eyo UB, Dailey ME (2013): Microglia: key elements in neural development, plasticity, and pathology. *J Neuroimmune Pharmacol*. 8:494-509.

123. Dunn GA, Nigg JT, Sullivan EL (2019): Neuroinflammation as a risk factor for attention deficit hyperactivity disorder. *Pharmacol Biochem Behav*. 182:22-34.

124. Kim JW, Hong JY, Bae SM (2018): Microglia and Autism Spectrum Disorder: Overview of Current Evidence and Novel Immunomodulatory Treatment Options. *Clin Psychopharmacol Neurosci*. 16:246-252.

125. van der Burg JW, Sen S, Chomitz VR, Seidell JC, Leviton A, Dammann O (2016): The role of systemic inflammation linking maternal BMI to neurodevelopment in children. *Pediatr Res*. 79:3-12.

126. Thorpe HHA, Hamidullah S, Jenkins BW, Khokhar JY (2020): Adolescent neurodevelopment and substance use: Receptor expression and behavioral consequences. *Pharmacol Ther*. 206:107431.

127. Mattison JA, Vaughan KL (2017): An overview of nonhuman primates in aging research. *Exp Gerontol*. 94:41-45.

128. Hyman SL, Levy SE, Myers SM, COUNCIL ON CHILDREN WITH DISABILITIES SECTODABP (2020): Identification, Evaluation, and Management of Children With Autism Spectrum Disorder. *Pediatrics*. 145.

129. Wolraich M, Brown L, Brown RT, DuPaul G, Earls M, Feldman HM, et al. (2011): ADHD: clinical practice guideline for the diagnosis, evaluation, and treatment of attention-deficit/hyperactivity disorder in children and adolescents. *Pediatrics*. 128:1007-1022.

130. Havel PJ, Kievit P, Comuzzie AG, Bremer AA (2017): Use and Importance of Nonhuman Primates in Metabolic Disease Research: Current State of the Field. *ILAR J*. 58:251-268.

131. Ryan AM, Berman RF, Bauman MD (2019): Bridging the species gap in translational research for neurodevelopmental disorders. *Neurobiol Learn Mem*. 165:106950.

132. Paxinos G, Huang X-F, Petrides M, Toga AW (2009): *The Rhesus Monkey Brain in Stereotaxic Coordinates*. Second ed. San Diego, USA: Academic Press.

133. Schneider CA, Rasband WS, Eliceiri KW (2012): NIH Image to ImageJ: 25 years of image analysis. *Nat Methods*. 9:671-675.

134. Schumacker RE, Lomax RG (2004): *A beginner's guide to structural equation modeling.*: psychology press.

135. LK Mén, BO M (1998-2012): Mplus User's Guide. Los Angeles: Muthén & Muthén

136. Bentler PM, Bonnett DG (1980): Significance tests and goodness of fit in the analysis of covariance structures. 88 588-605.

137. Browne MW, Cudeck R (1992): Alternative ways of assessing model fit. *Sociological methods & research*. 21:230-258.

138. Enders CK (2001): A primer on maximum likelihood algorithms available for use with missing data. *Structural Equation Modeling*. 8:128-141.

139. Beal SL (2001): Ways to fit a PK model with some data below the quantification limit. *J Pharmacokinet Pharmacodyn*. 28:481-504.

140. Blaine BE (2018): Winsorizing. *The SAGE Encyclopedia of Educational Research, Measurement, and Evaluation*, pp 1817-1818.

141. Davis EP, Buss C, Muftuler LT, Head K, Hasso A, Wing DA, et al. (2011): Children's Brain Development Benefits from Longer Gestation. *Front Psychol*. 2:1.

142. Espel EV, Glynn LM, Sandman CA, Davis EP (2014): Longer gestation among children born full term influences cognitive and motor development. *PLoS One*. 9:e113758.

143. De Biase LM, Schuebel KE, Fusfeld ZH, Jair K, Hawes IA, Cimbro R, et al. (2017): Local Cues Establish and Maintain Region-Specific Phenotypes of Basal Ganglia Microglia. *Neuron*. 95:341-356.e346.

144. Liu Z, Cheng X, Zhong S, Zhang X, Liu C, Liu F, et al. (2020): Peripheral and Central Nervous System Immune Response Crosstalk in Amyotrophic Lateral Sclerosis. *Front Neurosci*. 14:575.

145. Aye IL, Lager S, Ramirez VI, Gaccioli F, Dudley DJ, Jansson T, et al. (2014): Increasing maternal body mass index is associated with systemic inflammation in the mother and the activation of distinct placental inflammatory pathways. *Biol Reprod*. 90:129.

146. Kershaw EE, Flier JS (2004): Adipose tissue as an endocrine organ. *J Clin Endocrinol Metab*. 89:2548-2556.

147. Rogero MM, Calder PC (2018): Obesity, Inflammation, Toll-Like Receptor 4 and Fatty Acids. *Nutrients*. 10.

148. Kern PA, Ranganathan S, Li C, Wood L, Ranganathan G (2001): Adipose tissue tumor necrosis factor and interleukin-6 expression in human obesity and insulin resistance. *Am J Physiol Endocrinol Metab*. 280:E745-751.

149. Sindhu S, Thomas R, Shihab P, Sriraman D, Behbehani K, Ahmad R (2015): Obesity Is a Positive Modulator of IL-6R and IL-6 Expression in the Subcutaneous Adipose Tissue: Significance for Metabolic Inflammation. *PLoS One*. 10:e0133494.

150. Monteiro R, de Castro PM, Calhau C, Azevedo I (2006): Adipocyte size and liability to cell death. *Obes Surg*. 16:804-806.

151. Engin A (2017): Adipose Tissue Hypoxia in Obesity and Its Impact on Preadipocytes and Macrophages: Hypoxia Hypothesis. *Adv Exp Med Biol*. 960:305-326.

152. Li C, Xu MM, Wang K, Adler AJ, Vella AT, Zhou B (2018): Macrophage polarization and meta-inflammation. *Transl Res*. 191:29-44.

153. Graham C, Chooniedass R, Stefura WP, Becker AB, Sears MR, Turvey SE, et al. (2017): In vivo immune signatures of healthy human pregnancy: Inherently inflammatory or anti-inflammatory? *PLoS One*. 12:e0177813.

154. Ander SE, Diamond MS, Coyne CB (2019): Immune responses at the maternal-fetal interface. *Sci Immunol*. 4.

155. Gillespie SL, Porter K, Christian LM (2016): Adaptation of the inflammatory immune response across pregnancy and postpartum in Black and White women. *J Reprod Immunol*. 114:27-31.

156. Brown AS, Meyer U (2018): Maternal Immune Activation and Neuropsychiatric Illness: A Translational Research Perspective. *Am J Psychiatry*. 175:1073-1083.

157. Davis J, Mire E (2021): Maternal obesity and developmental programming of neuropsychiatric disorders: An inflammatory hypothesis. *Brain Neurosci Adv*. 5:23982128211003484.

158. Erridge C, Samani NJ (2009): Saturated fatty acids do not directly stimulate Toll-like receptor signaling. *Arterioscler Thromb Vasc Biol*. 29:1944-1949.

159. GI L, KG L, NA B, HL K, S R, E E, et al. (2018): Evidence that TLR4 is not a receptor for saturate fatty acids but mediates lipid-induced inflammation by reprogramming macrophage metabolism. *Cell Metabolism*. 27:1096-1110.

160. Softic S, Cohen DE, Kahn CR (2016): Role of Dietary Fructose and Hepatic De Novo Lipogenesis in Fatty Liver Disease. *Dig Dis Sci*. 61:1282-1293.

161. Alkhouri N, Dixon LJ, Feldstein AE (2009): Lipotoxicity in nonalcoholic fatty liver disease: not all lipids are created equal. *Expert Rev Gastroenterol Hepatol*. 3:445-451.

162. Valleau JC, Sullivan EL (2014): The impact of leptin on perinatal development and psychopathology. *J Chem Neuroanat*. 61-62:221-232.

163. Maliqueo M, Cruz G, Espina C, Contreras I, García M, Echiburú B, et al. (2017): Obesity during pregnancy affects sex steroid concentrations depending on fetal gender. *Int J Obes (Lond)*. 41:1636-1645.

164. VanRyzin JW, Marquardt AE, Argue KJ, Vecchiarelli HA, Ashton SE, Arambula SE, et al. (2019): Microglial Phagocytosis of Newborn Cells Is Induced by Endocannabinoids and Sculpts Sex Differences in Juvenile Rat Social Play. *Neuron*. 102:435-449.e436.

165. Spalding KL, Bernard S, Näslund E, Salehpour M, Possnert G, Appelsved L, et al. (2017): Impact of fat mass and distribution on lipid turnover in human adipose tissue. *Nat Commun*. 8:15253.

166. Destaillats F, Joffre C, Acar N, Joffre F, Bezelgues JB, Pasquis B, et al. (2010): Differential effect of maternal diet supplementation with alpha-Linolenic adcid or n-3 long-chain polyunsaturated fatty acids on glial cell phosphatidylethanolamine and phosphatidylserine fatty acid profile in neonate rat brains. *Nutr Metab (Lond)*. 7:2.

167. Bowen RA, Clandinin MT (2005): Maternal dietary 22 : 6n-3 is more effective than 18 : 3n-3 in increasing the 22 : 6n-3 content in phospholipids of glial cells from neonatal rat brain. *Br J Nutr*. 93:601-611.

168. Palmer AC (2011): Nutritionally mediated programming of the developing immune system. *Adv Nutr*. 2:377-395.

169. Mandal M, Donnelly R, Elkabes S, Zhang P, Davini D, David BT, et al. (2013): Maternal immune stimulation during pregnancy shapes the immunological phenotype of offspring. *Brain Behav Immun*. 33:33-45.

170. Grant WF, Gillingham MB, Batra AK, Fewkes NM, Comstock SM, Takahashi D, et al. (2011): Maternal high fat diet is associated with decreased plasma n-3 fatty acids and fetal hepatic apoptosis in nonhuman primates. *PLoS One*. 6:e17261.

171. Gustafsson HC, Holton KF, Anderson AN, Nousen EK, Sullivan CA, Loftis JM, et al. (2019): Increased Maternal Prenatal Adiposity, Inflammation, and Lower Omega-3 Fatty Acid Levels Influence Child Negative Affect. *Front Neurosci*. 13:1035.

172. Kraus C, Castrén E, Kasper S, Lanzenberger R (2017): Serotonin and neuroplasticity - Links between molecular, functional and structural pathophysiology in depression. *Neurosci Biobehav Rev*. 77:317-326.

173. Bacqué-Cazenave J, Bharatiya R, Barrière G, Delbecque JP, Bouguiyoud N, Di Giovanni G, et al. (2020): Serotonin in Animal Cognition and Behavior. *Int J Mol Sci*. 21.

174. Sinopoli VM, Burton CL, Kronenberg S, Arnold PD (2017): A review of the role of serotonin system genes in obsessive-compulsive disorder. *Neurosci Biobehav Rev*. 80:372-381.

175. Ciranna L (2006): Serotonin as a modulator of glutamate- and GABA-mediated neurotransmission: implications in physiological functions and in pathology. *Curr Neuropharmacol*. 4:101-114.

176. Rivera HM, Christiansen KJ, Sullivan EL (2015): The role of maternal obesity in the risk of neuropsychiatric disorders. *Front Neurosci*. 9:194.

177. Gawlińska K, Gawliński D, Filip M, Przegaliński E (2021): Maternal feeding patterns affect the offspring's brain: focus on serotonin 5-HT. *Pharmacol Rep*. 73:1170-1178.

178. Okaty BW, Commons KG, Dymecki SM (2019): Embracing diversity in the 5-HT neuronal system. *Nat Rev Neurosci*. 20:397-424.

179. Alonso A, Merchán P, Sandoval JE, Sánchez-Arrones L, Garcia-Cazorla A, Artuch R, et al. (2013): Development of the serotonergic cells in murine raphe nuclei and their relations with rhombomeric domains. *Brain Struct Funct*. 218:1229-1277.

180. Calizo LH, Akanwa A, Ma X, Pan YZ, Lemos JC, Craige C, et al. (2011): Raphe serotonin neurons are not homogenous: electrophysiological, morphological and neurochemical evidence. *Neuropharmacology*. 61:524-543.

181. Okaty BW, Freret ME, Rood BD, Brust RD, Hennessy ML, deBairos D, et al. (2015): Multi-Scale Molecular Deconstruction of the Serotonin Neuron System. *Neuron*. 88:774-791.

182. Ren J, Friedmann D, Xiong J, Liu CD, Ferguson BR, Weerakkody T, et al. (2018): Anatomically Defined and Functionally Distinct Dorsal Raphe Serotonin Sub-systems. *Cell*. 175:472-487.e420.

183. Ren J, Isakova A, Friedmann D, Zeng J, Grutzner SM, Pun A, et al. (2019): Single-cell transcriptomes and whole-brain projections of serotonin neurons in the mouse dorsal and median raphe nuclei. *Elife*. 8.

184. Fernandez SP, Cauli B, Cabezas C, Muzerelle A, Poncer JC, Gaspar P (2016): Multiscale single-cell analysis reveals unique phenotypes of raphe 5-HT neurons projecting to the forebrain. *Brain Struct Funct*. 221:4007-4025.

185. Vigneault É, Poirel O, Riad M, Prud'homme J, Dumas S, Turecki G, et al. (2015): Distribution of vesicular glutamate transporters in the human brain. *Front Neuroanat*. 9:23.

186. Hioki H, Nakamura H, Ma YF, Konno M, Hayakawa T, Nakamura KC, et al. (2010): Vesicular glutamate transporter 3-expressing nonserotonergic projection neurons constitute a subregion in the rat midbrain raphe nuclei. *J Comp Neurol*. 518:668-686.

187. Amilhon B, Lepicard E, Renoir T, Mongeau R, Popa D, Poirel O, et al. (2010): VGLUT3 (vesicular glutamate transporter type 3) contribution to the regulation of serotonergic transmission and anxiety. *J Neurosci*. 30:2198-2210.

188. Prouty EW, Chandler DJ, Waterhouse BD (2017): Neurochemical differences between target-specific populations of rat dorsal raphe projection neurons. *Brain Res*. 1675:28-40.

189. Sengupta A, Holmes A (2019): A Discrete Dorsal Raphe to Basal Amygdala 5-HT Circuit Calibrates Aversive Memory. *Neuron*. 103:489-505.e487.

190. Baker KG, Halliday GM, Törk I (1990): Cytoarchitecture of the human dorsal raphe nucleus. *J Comp Neurol*. 301:147-161.

191. Bethea CL, Reddy AP (2012): The effect of long-term ovariectomy on midbrain stress systems in free ranging macaques. *Brain Res*. 1488:24-37.

192. Schindelin J, Arganda-Carreras I, Frise E, Kaynig V, Longair M, Pietzsch T, et al. (2012): Fiji: an open-source platform for biological-image analysis. *Nat Methods*. 9:676-682.

193. Rueden CT, Schindelin J, Hiner MC, DeZonia BE, Walter AE, Arena ET, et al. (2017): ImageJ2: ImageJ for the next generation of scientific image data. *BMC Bioinformatics*. 18:529.

194. Carpenter AE, Jones TR, Lamprecht MR, Clarke C, Kang IH, Friman O, et al. (2006): CellProfiler: image analysis software for identifying and quantifying cell phenotypes. *Genome Biol*. 7:R100.

195. Team RC (2021): R: A Language and Environment for Statistical Computing.: R Foundation for Statistical Computing.

196. Wickham H, Averick M, Bryan J, Change W, D'Agostino L, Francois R, et al. (2019): Welcome to the tidyverse. *Journal of Open Source Software*. 4:1686.

197. Kuznetsova A, Brockhoff PB, Christensen RHB (2017): lmerTest Package: Tests in Linear Mixed Effects Models. *Journal of Statistical Software*. 82:1-26.

198. Haugas M, Tikker L, Achim K, Salminen M, Partanen J (2016): Gata2 and Gata3 regulate the differentiation of serotonergic and glutamatergic neuron subtypes of the dorsal raphe. *Development*. 143:4495-4508.

199. Sanchez RL, Reddy AP, Centeno ML, Henderson JA, Bethea CL (2005): A second tryptophan hydroxylase isoform, TPH-2 mRNA, is increased by ovarian steroids in the raphe region of macaques. *Brain Res Mol Brain Res*. 135:194-203.

200. Wilson MA, Molliver ME (1991): The organization of serotonergic projections to cerebral cortex in primates: retrograde transport studies. *Neuroscience*. 44:555-570.

201. Hale MW, Lowry CA (2011): Functional topography of midbrain and pontine serotonergic systems: implications for synaptic regulation of serotonergic circuits. *Psychopharmacology (Berl)*. 213:243-264.

202. Waselus M, Valentino RJ, Van Bockstaele EJ (2011): Collateralized dorsal raphe nucleus projections: a mechanism for the integration of diverse functions during stress. *J Chem Neuroanat*. 41:266-280.

203. Commons KG (2020): Dorsal raphe organization. *J Chem Neuroanat*. 110:101868.

204. Gras C, Herzog E, Bellenchi GC, Bernard V, Ravassard P, Pohl M, et al. (2002): A third vesicular glutamate transporter expressed by cholinergic and serotoninergic neurons. *J Neurosci*. 22:5442-5451.

205. Huang KW, Ochandarena NE, Philson AC, Hyun M, Birnbaum JE, Cicconet M, et al. (2019): Molecular and anatomical organization of the dorsal raphe nucleus. *Elife*. 8.

206. Donner NC, Kubala KH, Hassell JE, Lieb MW, Nguyen KT, Heinze JD, et al. (2018): Two models of inescapable stress increase tph2 mRNA expression in the anxiety-related dorsomedial part of the dorsal raphe nucleus. *Neurobiol Stress*. 8:68-81.

207. Gardner KL, Hale MW, Oldfield S, Lightman SL, Plotsky PM, Lowry CA (2009): Adverse experience during early life and adulthood interact to elevate tph2 mRNA expression in serotonergic neurons within the dorsal raphe nucleus. *Neuroscience*. 163:991-1001.

208. Donner NC, Johnson PL, Fitz SD, Kellen KE, Shekhar A, Lowry CA (2012): Elevated tph2 mRNA expression in a rat model of chronic anxiety. *Depress Anxiety*. 29:307-319.

209. Hsueh PT, Wang HH, Liu CL, Ni WF, Chen YL, Liu JK (2017): Expression of cerebral serotonin related to anxiety-like behaviors in C57BL/6 offspring induced by repeated subcutaneous prenatal exposure to low-dose lipopolysaccharide. *PLoS One*. 12:e0179970.

210. Schafer DP, Lehrman EK, Kautzman AG, Koyama R, Mardinly AR, Yamasaki R, et al. (2012): Microglia sculpt postnatal neural circuits in an activity and complement-dependent manner. *Neuron*. 74:691-705.

211. Li Q, Barres BA (2018): Microglia and macrophages in brain homeostasis and disease. *Nat Rev Immunol*. 18:225-242.

212. Matcovitch-Natan O, Winter DR, Giladi A, Vargas Aguilar S, Spinrad A, Sarrazin S, et al. (2016): Microglia development follows a stepwise program to regulate brain homeostasis. *Science*. 353:aad8670.

213. Sekar A, Bialas AR, de Rivera H, Davis A, Hammond TR, Kamitaki N, et al. (2016): Schizophrenia risk from complex variation of complement component 4. *Nature*. 530:177-183.

214. Koyama R, Ikegaya Y (2015): Microglia in the pathogenesis of autism spectrum disorders. *Neuroscience Research*. 100:1-5.

215. Mattei D, Ivanov A, Ferrai C, Jordan P, Guneykaya D, Buonfiglioli A, et al. (2017): Maternal immune activation results in complex microglial transcriptome signature in the adult offspring that is reversed by minocycline treatment. *Transl Psychiatry*. 7:e1120.

216. Schaafsma W, Basterra LB, Jacobs S, Brouwer N, Meerlo P, Schaafsma A, et al. (2017): Maternal inflammation induces immune activation of fetal microglia and leads to disrupted microglia immune responses, behavior, and learning performance in adulthood. *Neurobiol Dis*. 106:291-300.

217. Diz-Chaves Y, Pernía O, Carrero P, Garcia-Segura LM (2012): Prenatal stress causes alterations in the morphology of microglia and the inflammatory response of the hippocampus of adult female mice. *J Neuroinflammation*. 9:71.

218. Bolton JL, Huff NC, Smith SH, Mason SN, Foster WM, Auten RL, et al. (2013): Maternal stress and effects of prenatal air pollution on offspring mental health outcomes in mice. *Environ Health Perspect*. 121:1075-1082.

219. Terasaki LS, Schwarz JM (2016): Effects of Moderate Prenatal Alcohol Exposure during Early Gestation in Rats on Inflammation across the Maternal-Fetal-Immune Interface and Later-Life Immune Function in the Offspring. *J Neuroimmune Pharmacol*. 11:680-692.

220. Ozaki K, Kato D, Ikegami A, Hashimoto A, Sugio S, Guo Z, et al. (2020): Maternal immune activation induces sustained changes in fetal microglia motility. *Sci Rep*. 10:21378.

221. Edlow AG, Glass RM, Smith CJ, Tran PK, James K, Bilbo S (2019): Placental Macrophages: A Window Into Fetal Microglial Function in Maternal Obesity. *Int J Dev Neurosci*. 77:60-68.

222. Schumann CM, Bauman MD, Amaral DG (2011): Abnormal structure or function of the amygdala is a common component of neurodevelopmental disorders. *Neuropsychologia*. 49:745-759.

223. Avino TA, Barger N, Vargas MV, Carlson EL, Amaral DG, Bauman MD, et al. (2018): Neuron numbers increase in the human amygdala from birth to adulthood, but not in autism. *Proc Natl Acad Sci U S A*. 115:3710-3715.

224. Gina LF, Andrew MN, Jamie LS, Michael JW (2012): The Role of the Amygdala in Anxiety Disorders. In: Barbara F, editor. *The Amygdala*. Rijeka: IntechOpen, pp Ch. 3.

225. Bordt EA, Ceasrine AM, Bilbo SD (2020): Microglia and sexual differentiation of the developing brain: A focus on ontogeny and intrinsic factors. *Glia*. 68:1085-1099.

226. Hanamsagar R, Bilbo SD (2016): Sex differences in neurodevelopmental and neurodegenerative disorders: Focus on microglial function and neuroinflammation during development. *J Steroid Biochem Mol Biol*. 160:127-133.

227. Villa A, Gelosa P, Castiglioni L, Cimino M, Rizzi N, Pepe G, et al. (2018): Sex-Specific Features of Microglia from Adult Mice. *Cell Rep*. 23:3501-3511.

228. Guneykaya D, Ivanov A, Hernandez DP, Haage V, Wojtas B, Meyer N, et al. (2018): Transcriptional and Translational Differences of Microglia from Male and Female Brains. *Cell Rep*. 24:2773-2783.e2776.

229. Morrison H, Young K, Qureshi M, Rowe RK, Lifshitz J (2017): Quantitative microglia analyses reveal diverse morphologic responses in the rat cortex after diffuse brain injury. *Sci Rep*. 7:13211.

230. Paolicelli RC, Ferretti MT (2017): Function and Dysfunction of Microglia during Brain Development: Consequences for Synapses and Neural Circuits. *Frontiers in Synaptic Neuroscience*. 9.

231. Block CL, Eroglu O, Mague SD, Smith CJ, Ceasrine AM, Sriworarat C, et al. (2022): Prenatal environmental stressors impair postnatal microglia function and adult behavior in males. *Cell Rep*. 40:111161.

232. Squarzoni P, Oller G, Hoeffel G, Pont-Lezica L, Rostaing P, Low D, et al. (2014): Microglia modulate wiring of the embryonic forebrain. *Cell Rep*. 8:1271-1279.

233. Parkhurst CN, Yang G, Ninan I, Savas JN, Yates JR, Lafaille JJ, et al. (2013): Microglia promote learning-dependent synapse formation through brain-derived neurotrophic factor. *Cell*. 155:1596-1609.

234. Ueno M, Fujita Y, Tanaka T, Nakamura Y, Kikuta J, Ishii M, et al. (2013): Layer V cortical neurons require microglial support for survival during postnatal development. *Nat Neurosci*. 16:543-551.

235. Starr-Phillips EJ, Beery AK (2014): Natural variation in maternal care shapes adult social behavior in rats. *Dev Psychobiol*. 56:1017-1026.

236. Dubbelaar ML, Kracht L, Eggen BJL, Boddeke EWGM (2018): The Kaleidoscope of Microglial Phenotypes. *Front Immunol*. 9:1753.

237. Mitchell AJ, Khambadkone SG, Dunn G, Bagley J, Tamashiro KLK, Fair D, et al. (2022): Maternal Western-style diet reduces social engagement and increases idiosyncratic behavior in Japanese macaque offspring. *Brain Behav Immun*. 105:109-121.

238. Craske MG, Stein MB (2016): Anxiety. *Lancet*. 388:3048-3059.

239. Tovote P, Fadok JP, Lüthi A (2015): Neuronal circuits for fear and anxiety. *Nat Rev Neurosci*. 16:317-331.

240. Janak PH, Tye KM (2015): From circuits to behaviour in the amygdala. *Nature*. 517:284-292.

241. Emery NJ, Capitanio JP, Mason WA, Machado CJ, Mendoza SP, Amaral DG (2001): The effects of bilateral lesions of the amygdala on dyadic social interactions in rhesus monkeys (Macaca mulatta). *Behav Neurosci*. 115:515-544.

242. Machado CJ, Emery NJ, Capitanio JP, Mason WA, Mendoza SP, Amaral DG (2008): Bilateral neurotoxic amygdala lesions in rhesus monkeys (Macaca mulatta): consistent pattern of behavior across different social contexts. *Behav Neurosci*. 122:251-266.

243. Stefánsdóttir Í, Ivarsson T, Skarphedinsson G (2022): Efficacy and safety of serotonin reuptake inhibitors (SSRI) and serotonin noradrenaline reuptake inhibitors (SNRI) for children and adolescents with anxiety disorders: a systematic review and meta-analysis. *Nord J Psychiatry*.1-10.

244. Wehry AM, Beesdo-Baum K, Hennelly MM, Connolly SD, Strawn JR (2015): Assessment and treatment of anxiety disorders in children and adolescents. *Curr Psychiatry Rep*. 17:52.

245. Gordon JA, Hen R (2004): The serotonergic system and anxiety. *Neuromolecular Med*. 5:27-40.

246. Hariri AR, Mattay VS, Tessitore A, Kolachana B, Fera F, Goldman D, et al. (2002): Serotonin transporter genetic variation and the response of the human amygdala. *Science*. 297:400-403.

247. Reimold M, Batra A, Knobel A, Smolka MN, Zimmer A, Mann K, et al. (2008): Anxiety is associated with reduced central serotonin transporter availability in unmedicated patients with unipolar major depression: a [11C]DASB PET study. *Mol Psychiatry*. 13:606-613, 557.

248. Quah SKL, McIver L, Roberts AC, Santangelo AM (2020): Trait Anxiety Mediated by Amygdala Serotonin Transporter in the Common Marmoset. *J Neurosci*. 40:4739-4749.

249. Li Y, Missig G, Finger BC, Landino SM, Alexander AJ, Mokler EL, et al. (2018): Maternal and Early Postnatal Immune Activation Produce Dissociable Effects on Neurotransmission in mPFC–Amygdala Circuits. *The Journal of Neuroscience*. 38:3358.

250. Marcinkiewcz CA, Mazzone CM, D'Agostino G, Halladay LR, Hardaway JA, DiBerto JF, et al. (2016): Serotonin engages an anxiety and fear-promoting circuit in the extended amygdala. *Nature*. 537:97-101.

251. Malave L, van Dijk MT, Anacker C (2022): Early life adversity shapes neural circuit function during sensitive postnatal developmental periods. *Translational Psychiatry*. 12:306.

252. Connor KL, Vickers MH, Beltrand J, Meaney MJ, Sloboda DM (2012): Nature, nurture or nutrition? Impact of maternal nutrition on maternal care, offspring development and reproductive function. *J Physiol*. 590:2167-2180.

253. Liu WZ, Zhang WH, Zheng ZH, Zou JX, Liu XX, Huang SH, et al. (2020): Identification of a prefrontal cortex-to-amygdala pathway for chronic stress-induced anxiety. *Nat Commun*. 11:2221.

254. Orban GA, Van Essen D, Vanduffel W (2004): Comparative mapping of higher visual areas in monkeys and humans. *Trends Cogn Sci*. 8:315-324.

255. Nelson EE, Winslow JT (2009): Non-human primates: model animals for developmental psychopathology. *Neuropsychopharmacology*. 34:90-105.

256. Balasubramaniam KN, Beisner BA, Berman CM, De Marco A, Duboscq J, Koirala S, et al. (2018): The influence of phylogeny, social style, and sociodemographic factors on macaque social network structure. *Am J Primatol*. 80.

257. Hansen BC (2013): Nonhuman primate advances in nutrition research. *Am J Clin Nutr*. 98:264-265.

258. Harwood HJ, Listrani P, Wagner JD (2012): Nonhuman primates and other animal models in diabetes research. *J Diabetes Sci Technol*. 6:503-514.

259. Stouffer RL, Woodruff TK (2017): Nonhuman Primates: A Vital Model for Basic and Applied Research on Female Reproduction, Prenatal Development, and Women's Health. *ILAR J*. 58:281-294.

260. Winter C, Reutiman TJ, Folsom TD, Sohr R, Wolf RJ, Juckel G, et al. (2008): Dopamine and serotonin levels following prenatal viral infection in mouse--implications for psychiatric disorders such as schizophrenia and autism. *Eur Neuropsychopharmacol*. 18:712-716.

261. Bilbo SD, Schwarz JM (2012): The immune system and developmental programming of brain and behavior. *Front Neuroendocrinol*. 33:267-286.

262. Sureshchandra S, Chan CN, Robino JJ, Parmelee LK, Nash MJ, Wesolowski SR, et al. (2022): Maternal Western-style diet remodels the transcriptional landscape of fetal hematopoietic stem and progenitor cells in rhesus macaques. *Stem Cell Reports*. 17:2595-2609.

263. Sureshchandra S, Wilson RM, Rais M, Marshall NE, Purnell JQ, Thornburg KL, et al. (2017): Maternal Pregravid Obesity Remodels the DNA Methylation Landscape of Cord Blood Monocytes Disrupting Their Inflammatory Program. *J Immunol*. 199:2729-2744.